Roles of LOFSEP genes in barley inflorescence development

By

Hendrik Nicolaas Johannes Kuijer

Submitted to the University of Adelaide for the degree of doctor of philosophy

November 2019

Contents

Abstract

The grasses contain many of the world's important staple crop species, such as rice, maize, wheat and barley. While the spikelets and florets of grass species are similar, variation in their arrangement leads to diverse inflorescence morphologies. The regulation of inflorescence development in grasses is an important component in reproduction and yield and thus of great interest for fundamental biology as well as crop improvement.

The MADS-box gene family is of central importance in inflorescence development, as described in the ABCDE model of floral organogenesis. Within the MADS-box genes, the *SEPALLATA*, or E-class genes, can be divided into a SEP3 and LOFSEP subclade. In grasses the LOFSEP genes have adopted additional roles outside of the ABCDE model in inflorescence architecture.

Based on expression data, and mutant phenotypes where available, it is likely that the LOFSEP genes *MADS1*, *MADS5* and *MADS34* perform the E-class function for the lemma and palea directly, and indirectly influence the development of the inner floral organs through other MADS-box genes. *MADS34* is expressed the earliest in inflorescence development and plays a role in inflorescence branching. While *MADS1* and *MADS34* seem to act oppositely in spikelet initiation, they appear to act cooperatively in lemma development.

To further the understanding of the role of MADS-box genes in grass inflorescence development, different grass species have to be compared. First 34 MIKCc MADS-box genes were identified in barley and found to be very conserved based on comparison to homologs in other grasses and the low numbers of SNPs. To broaden available data for grasses and get specific data for barley a detailed expression profiling experiment for all MIKCc MADS-box genes was performed in barley.

The ABCDE-class genes were generally found to be expressed at the time and place predicted by applying the ABCDE model to barley, and collected into co-expression sets related to the sequential formation of the floral organs, confirming the general applicability of the model for barley. One of the core tenets of the eudicot ABCDE model is the antagonistic nature of A-class and C-class genes, which supress each other's expression, however expression of A-class and C-class genes overlapped significantly in barley florets. This marked deviance from the classic ABCDE model may be indicative that a different approach

to the clear divide between outer and inner floral organs has evolved in grasses, likely involving *HvMADS32*, a MADS-box class unique to grasses.

To focus on the functional analysis of the LOFSEP genes in barley, knockout mutants for *HvMADS1*, *HvMADS5* and *HvMADS34* were generated using a CRISPR/Cas9 system optimised for plants. Homozygous mutants were detected in T0 and confirmed in T1 and T2 generations, while no off-target mutations were found. Editing rates of over 90% were observed, indicating the CRISPR/Cas9 system used here is very effective in barley.

No inflorescence phenotype was observed for *hvmads5* and *hvmads34*, indicating their functions are likely to be covered completely by other genes acting redundantly. Double and triple barley LOFSEP mutants will likely uncover inflorescence phenotypes as observed in rice. In contrast the *hvmads1* mutant has shorter awns, reduced fertility and grain weight and additional tiller formation. These mutants behaved the same in the spring barley Golden Promise and in WI4330, a barley cultivar more recalcitrant to transformation. The additional tillers do not result in higher yield, because fertility and grain weight are reduced. Reduced grain weight could be the result of the smaller photosynthetic contribution from the shorter awns and competition for plant resources by additional tillers during the grain filling phase.

Under high ambient temperature the *hvmads1* mutant has the additional phenotype of a branching inflorescence. The branch-like structures appear at the location of the central spikelets and show that in barley the spikelet is likely to be the first lateral meristem of a transient branch meristem, not a terminal spikelet. The *hvmads1* inflorescence morphology adopts characteristics resembling the rice and maize panicle, and the likely branched inflorescence shape for the last common ancestor barley and rice.

Expression analysis was performed by RNAseq of the early inflorescence at two developmental stages, grown at low and high ambient temperature and comparing the *hvmads1* mutant with the wild type. Expression of several genes, including MADS-box genes, indicated that floret development was delayed in the panicle-like inflorescence of the mutant grown at high ambient temperature. Increased expression of heat shock factors suggests a possible sensitisation to heat and additionally auxin signalling may be slightly altered. Surprisingly *HvMADS34* expression is not significantly increased with the branching phenotype, although the peak expression of *OsMADS34* is in the branch meristems of rice. *HvODDSOC2*, a MADS-box genes from a clade unique to grasses and previously associated

with outgrowth of lateral tissue in the barley inflorescence is correlated with the branching phenotype and may be of regulatory importance.

The genes found to be correlated to the branching phenotype are likely to be predominantly consequences of a developmental change. This leaves the important question of how the combination of the *hvmads1* mutant and high ambient temperature triggers the branching inflorescence morphology. To address this question promoter affinity studies and ChIP-seq experiments are suggested.

The redundancy among the LOFSEP genes in barley can partially be explained by mechanisms such as stabilisation by additional individual functions and stabilisation by developmental error. However, this is not sufficient for *HvMADS34*, which is expressed alone at an early stage of development, where no related genes can provide redundancy, while the *hvmads34* mutant has no visible inflorescence phenotype. Early expression of *HvMADS34* may be vestigial from a time when an ancestor had a branching inflorescence.

When combined these results provide the basics of a generic toolbox for the adaptation of grass inflorescence morphology. Further research building on the branching barley presented here may lead to a higher yielding barley ‘panicle’, which may be translatable to the closely related wheat. Additionally, more research into the adaptations of the ABCDE model in grasses may provide both evolutionary insights and likely additions of complexes like the ‘floral’ quartets beyond the floral organs themselves, strengthening a grass specific model.

Declaration

I certify that this work contains no material which has been accepted for the award of any other degree or diploma in my name, in any university or other tertiary institution and, to the best of my knowledge and belief, contains no material previously published or written by another person, except where due reference has been made in the text. In addition, I certify that no part of this work will, in the future, be used in a submission in my name, for any other degree or diploma in any university or other tertiary institution without the prior approval of the University of Adelaide and where applicable, any partner institution responsible for the joint-award of this degree.

I give consent to this copy of my thesis when deposited in the University Library, being made available for loan and photocopying, subject to the provisions of the Copyright Act 1968.

I also give permission for the digital version of my thesis to be made available on the web, via the University's digital research repository, the Library Search and also through web search engines, unless permission has been granted by the University to restrict access for a period of time.

HNJ Kuijer

7/10/2019

Acknowledgements

I would like to acknowledge my supervisors Professor Dabing Zhang and Professor Rachel Burton. I would like to thank prof. Zhang for giving me the opportunity to work on this project and for stimulating my development into an independent researcher. Thank you Prof. Burton for all your support and advice in both normal and difficult times. My apologies to Prof. McDonald, thank you for your patience with my tardy paperwork. I would also like to thank associate Prof. Ken Chalmers for his support and understanding on many occasions, and Prof. Diane Mathers for her help as independent advisor over the years.

This thesis would not have been possible without the other members of our group. Special thanks goes to Dr. Gang Li for years of wonderful, educational and productive cooperation. Our discussions on the results and experiments have been instrumental in shaping my thoughts as expressed in this thesis. To Dr. Xiujuan, for your help with my many questions at the beginning and the support with *in situ*. To Debbie, my peer, I really enjoyed your company in both the real world and the world of Dungeons and Dragons. To Ann, for being a joy to work with and a good friend. To Carrie, for continuing some of my work, and patiently listening to my rambling speculations. To Yu, Cindy, Zeshan, Shifeng, Wei, Reyhaneh and Hui, for being wonderful colleagues.

Additional thanks go out to Dr. Neil Shirley and Sandy Khor for helping with my big qPCR experiment. To Dr. Rohan Singh for help with barley transformations. To Huiran Liu for processing our RNAseq data. To Dr. Gwen Mayo for help and advice with many microscopy techniques. To Chao Ma for helping with the *in situ* robot, and Prof. Matthew Tucker for letting us use the robot.

The biggest thanks goes to my lovely wife for your unwavering confidence in me; I am so sorry we had to live so far apart this long. To my parents and parents-in-law, thank you for letting me stay in your house and feeding me for as long as I needed. To my brother and sister; now we can finally do that skit where we introduce each other as ‘Doctor’. To my little sister, for introducing me to pokemon.

Chapter 1: The function of *LOFSEP*s in grass inflorescence morphogenesis

1.1 Abstract:

*SEPALLATA*s (*SEP*s) were first described as E-class genes in the ABCDE model, with a function in floral quartets determining floral organ identity in model dicot plants including *Arabidopsis thaliana* and *Antirrhinum majus*. Increasing evidence shows that within the grass family a subset of the *SEP*s, dubbed *LOFSEP* genes, have gained functions earlier in inflorescence development, in addition to the E-class function they share with the SEP3-like genes. The gene duplications, changes of expression patterns and protein interaction partners behind these functions are a driving force behind the diverging inflorescence architecture of grasses.

This review focusses on the function of the *LOFSEP* genes in grasses, drawing on recent studies of *LOFSEP* mutants in rice and other grass plants, expression data from rice, maize, wheat, barley and other grasses, as well as protein interaction studies. The combination of these data is summarised in a speculative model and avenues for further research are indicated. Deciphering the function of the *LOFSEP* genes in grasses with diverse inflorescence architecture will open the toolbox to adapt inflorescence morphology, which is critical for fundamental plant biology as well as crop improvement.

1.2 Introduction

The flowers of plants are not only essential for reproductive success, but also a crucial factor in yield for many crops worldwide. Therefore understanding the development of inflorescences is of fundamental scientific importance but also instrumental in feeding a growing world population over the coming decades.

The grass inflorescence

The grass inflorescence forms through differentiation and growth of several unique meristems. In rice and the maize tassel primary branch meristems form first on the apical meristem after inflorescence initiation. Secondary branches form on the primary branches and

the spikelet meristems arise on both the primary and secondary branches, resulting in a branched inflorescence, a panicle. In wheat and barley the spikelet meristems form directly on the main axis of the inflorescence, resulting in an unbranched inflorescence, the spike (Figure 1A).

The basic unit of grass inflorescence is the spikelet, a modified compact axillary branch. Within the spikelet one or more florets form and the floral organs grow within (Figure 1B). The inner floral organs, or whorl 3 and 4, consist of stamen and carpels in both dicot flowers and monocot florets. Instead of petals, the second whorl floral organs in grasses are lodicules. Lodicules are small flap-like organs that swell during anthesis to open the spikelet for pollination. Apart from having a similar position in flowers and florets, the regulatory mechanisms underlying their development also points to the equivalence of petals and lodicules (Figure 1C; (Ambrose et al., 2000; Cui et al., 2010)). For the lemma and palea the relationship to the sepals is not so clear cut. From a phytomere point of view the lemma is a bract, and therefore could be considered to be outside of the floret, while the palea is either a prophyll, a modified first leaf of the floret, or a fused tepal. However the lemma identity does seem to be ruled by the MADS-box genes of the ABCDE model, so from a regulatory angle it is a moot point: mutants will often have a phenotype that includes the lemma, so the lemma will be considered when discussing the ABCDE model. The lemma and palea are often put in the same box as first whorl organs, but to make progress on understanding these structures better they have to be considered separately, as their origin and regulation are different. Reported differentially expressed genes between the lemma and palea in rice include *RETARDED PALEA1* (*REP1*) (Yuan et al., 2009), *DROOPING LEAF* (*DL*) (Yamaguchi et al., 2004; Wang et al., 2017) and *OsMADS6* (Reinheimer and Kellogg, 2009; Wang et al., 2017).

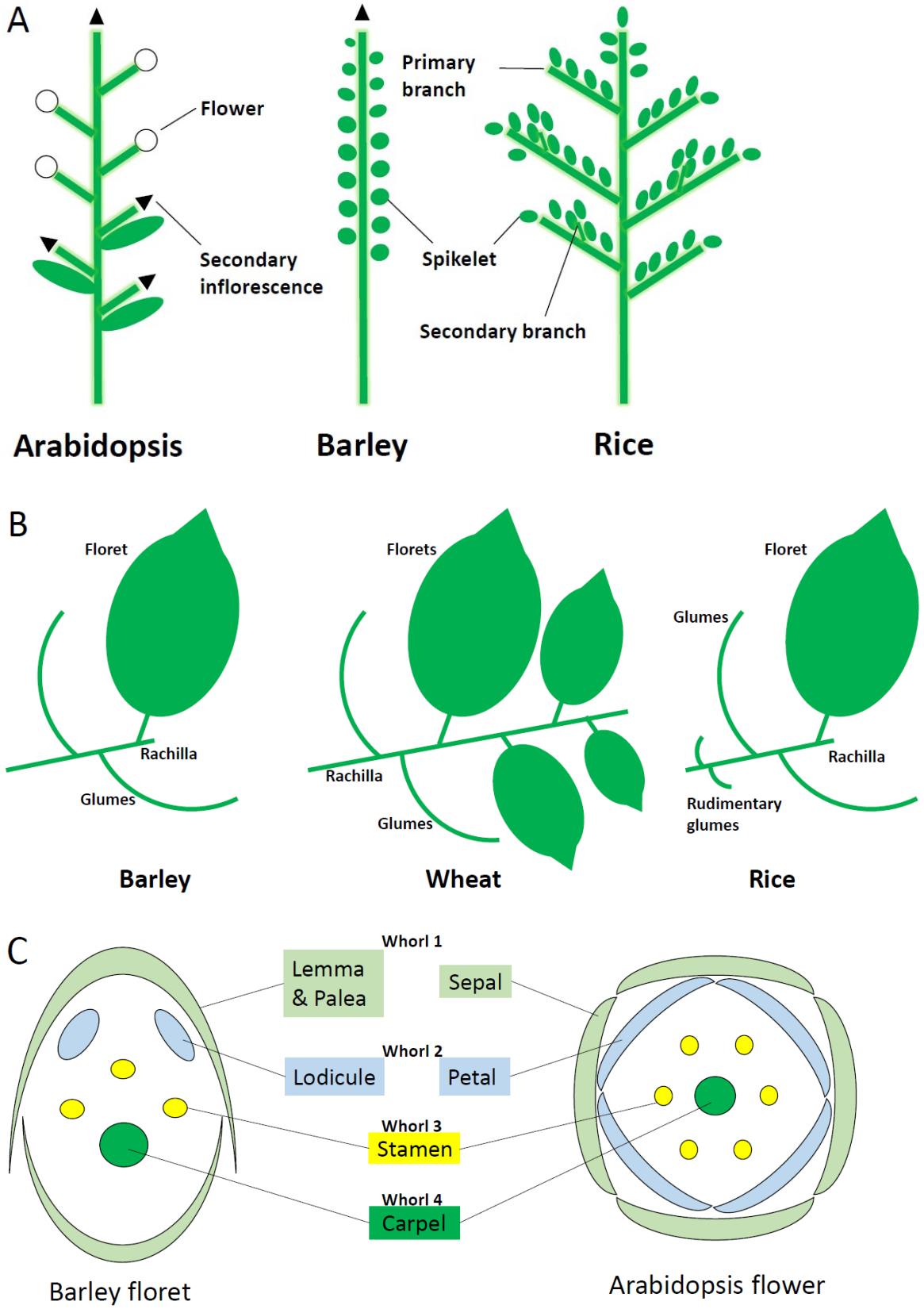

Figure 1: A) Inflorescence architecture of the eudicot model *Arabidopsis* and the grasses barley and rice. The most consistent difference between eudicot and grass inflorescences is the spikelet, a structure only found in grasses. B) Spikelet structure in barley, wheat and rice. C) The *Arabidopsis* flower has four whorls and these can be recognised in the grass floret as well (barley floret shown as an example).

SEPs in the ABCDE model

An important milestone in the study of inflorescence development is the ABC model, presented by Coen and Meyerowitz, which describes the specification of floral organs by overlapping expression of MADS-box transcription factors, and AP2-like genes. The MADS-box family can be divided into classes, where genes within each class or sub-class redundantly perform roughly the same function. Thus, based on mutant phenotypes in *Arabidopsis thaliana* and *Antirrhinum majus*, they posed that the expression of A-class genes in floral organ primordia will lead to development into sepals, A-class and B-class to petals, B-class and C-class to stamen, and C-class alone to carpels (Coen and Meyerowitz, 1991). This model was later refined to include D-class genes which are involved in ovule identity specification (Angenent et al., 1995). The ABCD model was rounded out by the addition of E-class genes, which are essential in all floral whorls for proper floral organ specification (Pelaz et al., 2000). Of all the ABCDE-class genes only *AP2*, which performs an A-class function, is not a MADS-box gene.

Not only are these ABDCE genes co-expressed, there is physical interaction between MADS-box proteins where they form transcription factor complexes of four members: the floral quartet. The members of a floral quartet bind cooperatively to promotors of effector genes, resulting in the specification of floral organ identity. Additionally A-class complexes negatively regulate C-class genes, while C-class complexes suppress A-class expression (Theissen, 2001).

As E-class proteins are involved in all floral quartets, they do not provide the specificity of each complex for a floral organ, but act more like the ‘glue’ protein to facilitate the formation of the quartets (Immink et al., 2009). A quadruple mutant of all four E-class genes in *Arabidopsis* results in homeotic conversion of all floral organs to leaves (Ditta et al., 2004). Therefore, from a more genetic point of view the E-class genes could be seen as an essential factor for flower identity. This idea is reinforced by experiments showing the conversion of leaves into floral organs by ectopic expression of *AtSEP3* in combination with other MADS-box genes (Goto et al., 2001). Combined this shows that Goethe’s prediction that floral organs are modified leaves is essentially correct (Goethe, 1790).

Phylogeny of LOFSEPs

MADS-box genes are named after the first discovered members: **M**CM1 from *Saccharomyces cerevisiae*, **A**GAMOUS from *Arabidopsis thaliana*, **D**EFICIENS from *Antirrhinum majus* and **S**RF from *Homo sapiens.* The large MADS-box gene family of transcription factors can be divided into Type 1 and Type 2 MADS-box genes. Type 1 MADS-box genes have only the conserved DNA binding MADS domain at the beginning of the gene in common. Type 2 MADS-box genes are divided into MIKCc (classic) and MIKC* groups. MIKC MADS-box transcription factors contain the conserved MADS DNA-binding domain, Intervening domain, Keratin-like domain and the C-terminal domain. The MIKC* is a small early side branch of the type 2 MADS-box genes and probably arose initially from a duplication of the keratin-like domain. MIKC* genes are more conserved than MIKCc genes and seem to have an equally conserved function in gametophytes (Kwantes et al., 2012). Within the MIKCc gene family several classes can be distinguished. Many of these classes are associated with the ABC model of floral organogenesis, and are known by both the name of the first described member and the role of the class in the ABC model. For example AGAMOUS/C-class, or APETALA/A-class. The MIKCc genes in A-, B- C- D- and E-classes where A- and E-class genes determine the first whorl organs, A-, B-, and E-class genes determine the second whorl, B-, C-, and E-class genes control the third whorl and C- and E-class genes specify the fourth whorl. D-class genes are involved in a floral quartet that determines ovule development. Individual genes within a class usually act redundantly with each other, so that single mutations often have a subtle or absent phenotype (Coen and Meyerowitz, 1991; Angenent et al., 1995; Pelaz et al., 2000).

The SEPALLATA, or E-class genes, are usually grouped next to the AGL6-class in a phylogenetic tree of the MIKCc genes. Functionally the grouping of AGL6 with SEPALLATA can be supported, since AGL6 has redundancy with SEPs in monocots for establishing floral quartets, although it has other roles in dicots (Dreni and Zhang, 2016). These two classes together are then closest to the duo of A-class and FLC-class genes (Figure 2) (Zahn et al., 2005; Smaczniak et al., 2012; Callens et al., 2018), although alternative phylogenies have been published (Yu et al., 2016).

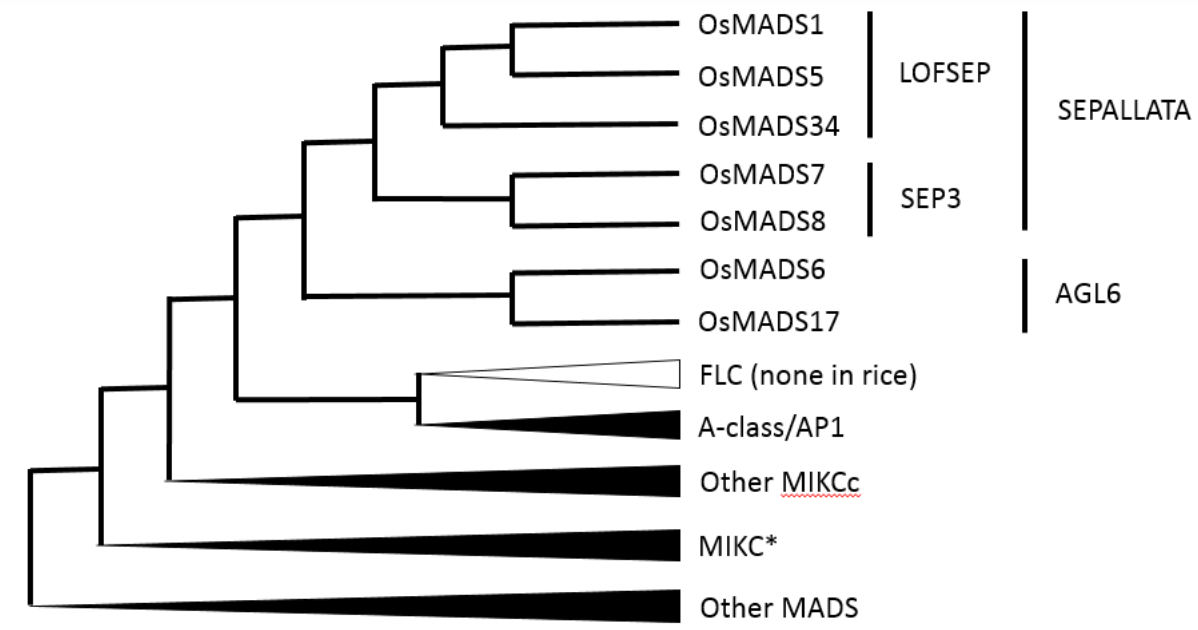

Figure 2: Schematic phylogeny of the rice LOFSEP genes in the context of the MADS-box gene family. *OsMADS1*, *OsMADS5* and *OsMADS34* form the LOFSEP clade, *OsMADS7* and *OsMADS8* the SEP3-like clade and together these are the SEPALLATA. The closely related AGL6 class has two members in rice, *OsMADS6* and *OsMADS17*.

Between the eudicots and grasses, most of the MIKCc type MADS-box classes are conserved (Zahn et al., 2005). Notably missing in the grasses is the FLC-class, which governs vernalisation and flowering time in *Arabidopsis* and other *Brassicaceae* (Becker, 2003). While there are no FLC-class genes in monocots, in some grasses the closely related A-class genes have taken on a role in vernalisation and inflorescence initiation. Unique to grasses is the OsMADS32 class, which contains only one gene, *CHIMAERIC FLORAL ORGANS1* (*CFO1*)/*OsMADS32*, which maintains floral organ identity by supressing expression of *DROOPING LEAF* (*DL,* see below) (Sang et al., 2012). For most of the genes within the classes there is no clear individual homology between eudicots and grasses, indicating that the most recent common ancestor likely had only one member in each class. The B-class genes are an exception to this rule, as AP3- and PI-like subgroups are present in both eudicots and grasses. This is also true for the SEPALLATA, which can be divided into two subclades: the SEP3 clade and the LOFSEP clade. The LOFSEP clade contains among others OsMADS1/LHS1, OsMADS5, OsMADS34, *Petunia* Floral Binding Protein9 (PhFBP9) and *Arabidopsis* SEP1, SEP2 and SEP4, where the underlined letters form the clade acronym (Figure 2) (Malcomber and Kellogg, 2005; Zahn et al., 2005).

The ABCDE model is partially applicable in grasses

The ABCDE model of floral organogenesis can generally be applied to grasses with only minimal adjustments. The A, B, C and D-class genes are expressed in the expected floral whorls, and of the loss-of-function mutants available result in homeotic conversions predicted by the model (reviewed by (Ciaffi et al., 2011; Callens et al., 2018)).

A deviation from the standard ABCDE model is the addition of *DROOPING LEAF* (*DL*), a YABBY family transcription factor, as a necessary factor in carpel identity and floral meristem determinacy in conjunction with *OsMADS3* and *OsMADS13* in rice (Yamaguchi et al., 2004; Li et al., 2011). Carpel and determinacy phenotypes are also observed in mutants of the maize DL co-orthologs *drl1* and *drl2*, and the likely linked locus *indeterminate floral apex1* (*ifa1*) (Laudencia-Chingcuanco and Hake, 2002; Strable et al., 2017). Similarly, the wheat homolog *TaDL* seems to specify carpel identity in wheat florets (Hama et al., 2004; Murai, 2013).

In addition to the A-class role in floral organ specification, A-class genes in temperate grasses have gained a function in vernalisation. *HvMADS14*, also known as *VERNALISATION1* (*HvVRN1*) is induced by vernalisation and accelerates the floral transition (Trevaskis et al., 2007). This is also reflected in an earlier expression in the inflorescence and significant expression in the leaves in both wheat and barley, but not in the leaves of rice (Paolacci et al., 2007; Li and Dubcovsky, 2008; Digel et al., 2015; Feng et al., 2017). A similar dual role in floral induction (but not vernalisation) and inflorescence development was found for the maize homolog ZmM4 (Danilevskaya et al., 2008). In the absence of the FLC-class genes in grasses, it seems that the closest relatives, the A-class genes, have evolved into a similar role.

E-class genes have also acquired additional functions outside of floral organogenesis in grasses. These are described in more detail below.

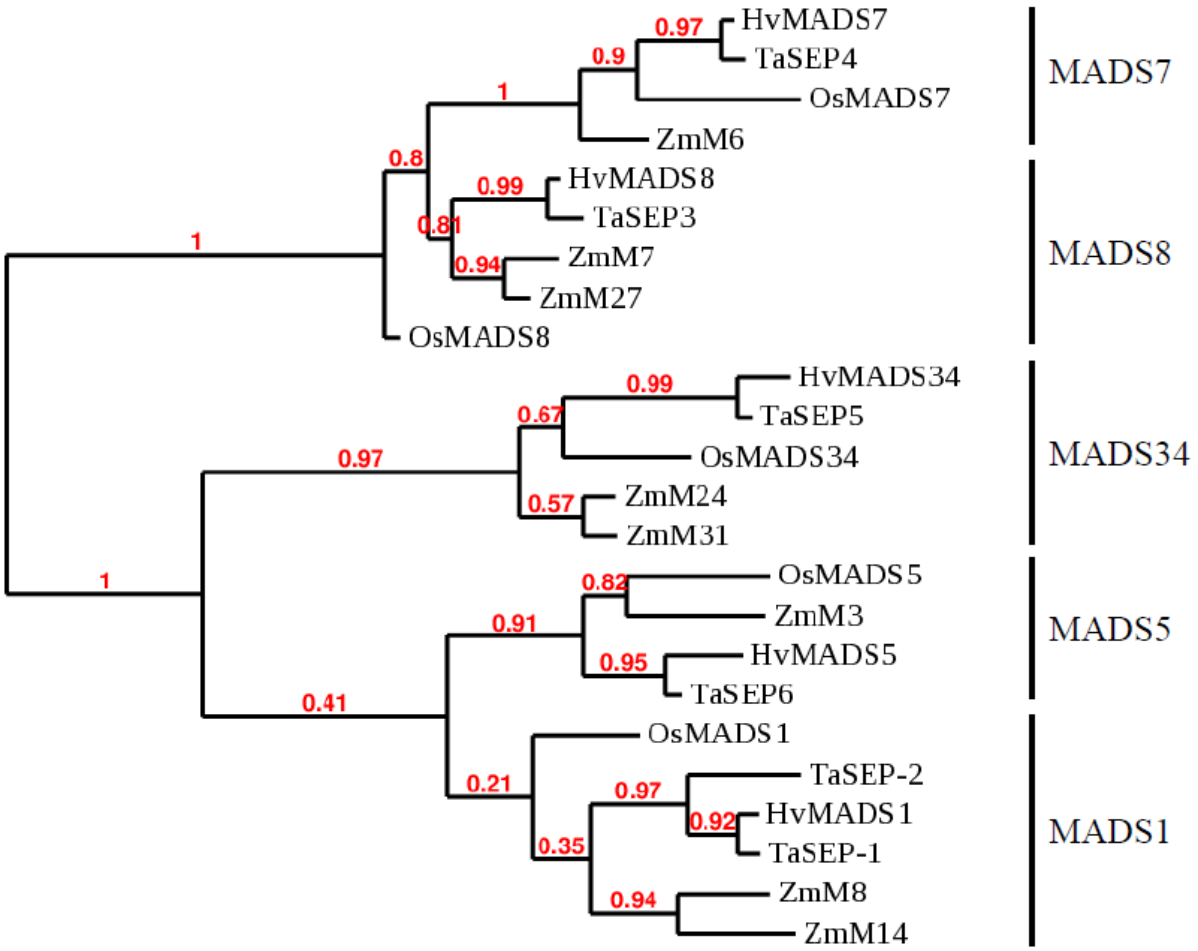

Figure 3: Phylogenetic tree of SEPALLATA genes in rice, maize, wheat and barley. Within the LOFSEP genes MADS1 and MADS5 are most closely related. The preserved grouping into five SEPALLATA genes indicates the last common ancestor probably already had five E-class genes. The maize pairs ZmM7/ZmM27, ZmM24/ZmM31 and ZmM8/ZmM14 are all recent duplications, likely formed in the same whole genome duplication event. Phylogenetic tree created *de novo,* but inspired and verified by part of a very similar published phylogenetic tree (Paolacci et al., 2007).

SEPs in grasses

Rice, maize, wheat and barley each have at least one gene representing each of the five SEP subclasses, suggesting the most recent common ancestor already had five SEP genes (Figure 3; (Paolacci et al., 2007; Ciaffi et al., 2011)). The division into the LOFSEP and SEP3-like clades likely occurred before the extant angiosperms (Zahn et al., 2005). The duplication leading to the split of *MADS34* and *MADS1/5* genes occurred around the base of the monocots, while the more recent division between *MADS1* and *MADS5* happened just before the diversification of the Poaceae. The duplication leading to *MADS7* and *MADS8* likely stems from a genome wide duplication event, before the origin of the Poaceae (Arora et al., 2007; Xu and Kong, 2007).

While in rice and barley there is one gene for each of the five SEP subclasses, maize and wheat have seen subsequent additional duplications. The maize pairs *ZmM7*/*ZmM27*, *ZmM24*/*ZmM31* and *ZmM8*/*ZmM14* are all recent duplications, probably formed in the same whole genome duplication event. *ZmM8* and *ZmM14* are both orthologous to *OsMADS1*, as are *TaSEP-1* and *TaSEP-2*, while ZmM7 and ZmM27 are orthologs of *OsMADS8* and finally *ZmM24* and *ZmM31* are orthologs of *OsMADS34* (Figure 3; (Paolacci et al., 2007; Zhang et al., 2012)). The gene pairs produced by these recent duplications show high sequence identity, and only little subfunctionalisation has been suggested; see below. Strong synteny in the chromosomal positions of all SEP genes has been found between the rice, maize and wheat genomes (Sorrells et al., 2003; Paolacci et al., 2007), making expression changes due to changes in chromosomal region, such as heterochromatic silencing, unlikely.

The SEP3 clade fills the conserved E-class role in grass lodicules, stamen and carpels

In rice the SEP3 clade members are *OsMADS7* and *OsMADS8* (Figure 3). Silencing either of these individually results in only mild phenotypes, while silencing both simultaneously results in severe morphological alterations of the inner floral whorls, indicating close redundancy between them (Cui et al., 2010). Stamen and carpel epidermal cells show characteristics normally found in the palea and lemma, suggesting a partial homeotic conversion. While the simultaneous knockdown of *OsMADS7* and *OsMADS8* showed a significant increase in the expression of the LOFSEP genes *OsMADS1*, *OsMADS5* and *OsMADS34*, this increased expression did not negate the phenotype (Cui et al., 2010). Additionally the lodicules, stamen and carpel still form in the triple mutant of all LOFSEP genes (Wu et al., 2018). This indicates there is significant divergence between the SEP3 and LOFSEP clades in rice, where the SEP3 clade is important for inner floral organ development, and this function is not redundantly covered by the LOFSEP clade.

This function in the inner floral organs is supported by the expression pattern of *OsMADS7* and *OsMADS8* only in the lodicules, stamen and carpel (Cui et al., 2010). This expression pattern is similar in wheat, where *TaSEP-3* and *TaSEP-4* are confined to the lodicule, stamen and carpel as well (Paollacci et al., 2007; Feng et al., 2017). *TaSEP-4* (*WSEP*) expression has been detected in the palea during late floral organ development by *in situ* hybridisation (Shitsukawa et al., 2007). For maize, differential expression of E-class genes in the

inflorescence has not yet been described, but *ZmM6* and *ZmM7* are expressed in both tassels and ears (Zhang et al., 2012). In barley the expression of *HvMADS7* and *HvMADS8* is late in floral development, which suggests the expression pattern may be conserved (Liu et al., 2019). In barley *HvMADS8* (*BM9*) expression in the inflorescence occurs mostly after the awn primordium stage based on real time quantitative PCR data, and is limited to the lodicule, stamen and carpel in mature florets, based on *in situ* hybridisation (Schmitz et al., 2000).

The *AtSEP3* protein has many interaction partners in *Arabidopsis*, including A, B, C, D and E-class proteins, making it a central player in many floral quartets (Immink et al., 2009). In wheat the *TaSEP-4* (WSEP) protein can interact with A-, B-, C- and E-class proteins (Shitsukawa et al., 2007), which is necessary to perform the E-class function.

In conclusion the SEP3 clade in grasses functions like the E-class genes of the ABCDE model for the specification of the lodicules, stamen and carpel.

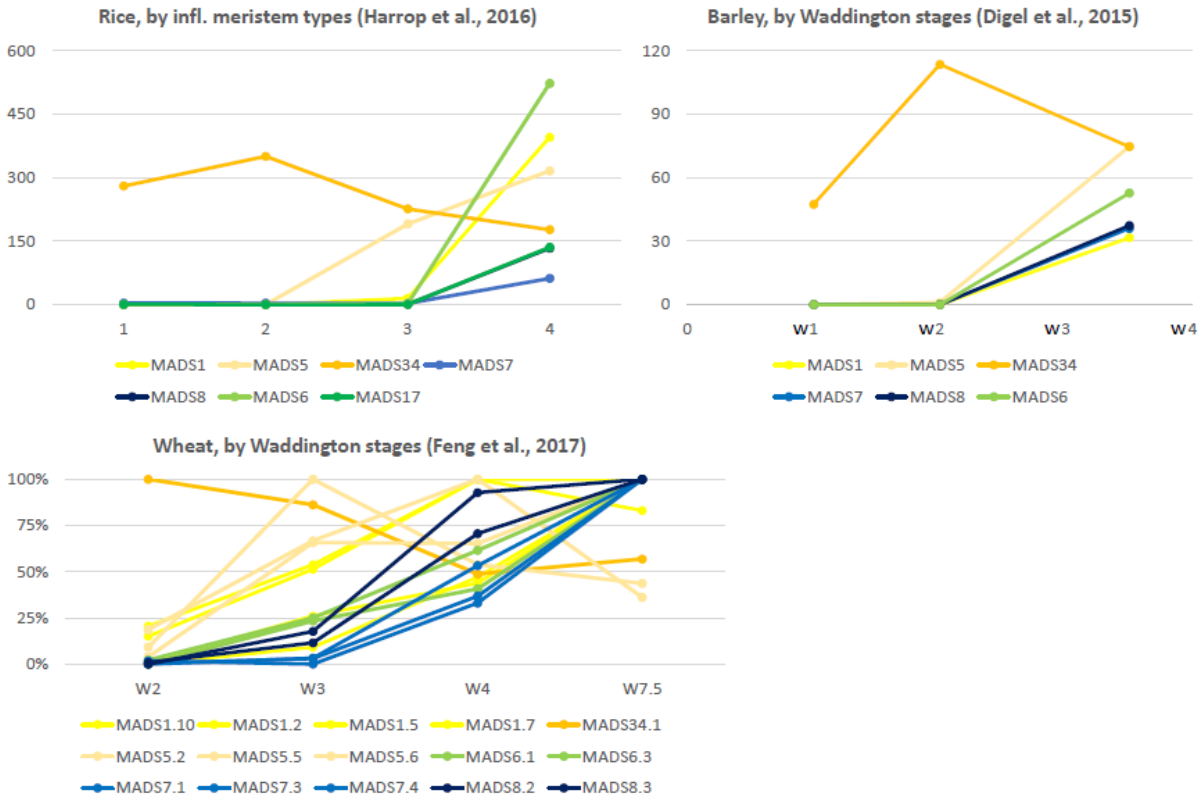

Figure 4: Expression profile of SEPALLATA and AGL6 genes in rice, barley and wheat inflorescence by RNA sequencing. Conserved features include the early expression of MADS34-like genes, followed by the other LOFSEP genes and AGL6-like genes and the late expression of the SEP3 clade. LOFSEP genes in yellow, gold and orange, SEP3 clade genes in blues, and AGL6 like genes in greens.

1.2 The LOFSEP clade has acquired additional functions

Collectively the LOFSEP clade in rice, wheat and barley is expressed earlier in inflorescence development than the SEP3 clade (Figure 4). While still maintaining the E-class function for the lemma and palea, the LOFEP clade is also involved in inflorescence branching, spikelet morphology and floret meristem development and determinacy.

MADS1 functions in the floret meristem, lemma, palea and floral determinacy.

OsMADS1, also known as *LEAFY HULL STERILE1* (*LHS1*), is a member of the LOFSEP clade and has an important role in floret meristem identity, establishing floral organ fate, and floral determinacy. The RNAi knockdown lines of *osmads1* have a leafy glume-like lemma and a leafy palea missing the marginal tissue, as well as glume-like lodicules and stamens and multiple carpels (Prasad et al., 2005; Khanday et al., 2013). In a knockout mutant of *OsMADS1* the lemma, palea and lodicules are transformed into leaf like structures, and the number of inner floral organs is changed (Gao et al., 2010). A similar phenotype is also observed in an epigenetically silenced *osmads1* mutant, although the inner floral organs also seem homeotically affected (Wang et al., 2010). Another observation of the *osmads1* mutant also revealed occasional twin florets, complete absence of the inner floral organs, or completely missing lodicules, stamen and carpel (Wu et al., 2018).

In the double mutant *osmads1 osmads15* the florets revert to plantlets, abandoning its reproductive trajectory for a vegetative fate, indicating MADS1 is important for floral meristem identity (Wang et al., 2010).

OsMADS1 overexpression results in dwarfism and decreased panicle size and branching, and a reduced amount of spikelets. Within the spikelet the sterile lemmas grow out to look much like a normal lemma, including the cell types. The expression of *DL* in the mutant sterile lemmas, normally expressed in the lemma, and lack of expression of *OsMADS6*, which is normally expressed in the palea, confirms the sterile lemmas have assumed lemma identity, not palea identity (Wang et al., 2017) The decreased panicle size and branching may be caused by a faster transition from panicle branch meristem to spikelet/floret meristem.

OsMADS1 is expressed in the spikelet primordium at stage sp4, in the lemma and palea, and weakly in the carpel primordia (Gao et al., 2010). Expression in the carpel primordium is not

uniform, but seems to be concentrated in a polar fashion. In wheat *TaSEP-1* and *TaSEP-2* expression has been found in the stem and leaves but more strongly in the spikelet (Paolacci et al., 2007), while the timing of expression during inflorescence development is similar to *OsMADS1* (Figure 4; (Feng et al., 2017)). Similarly *HvMADS1* expression increases between double ridge and stamen primordium stage, where spikelets, florets and the lemma are initiated (Figure 4; (Digel et al., 2015)). The preserved expression timing suggests the function of *TaSEP-1*, *TaSEP-2* and *HvMADS1* is the similar to the *OsMADS1* function. *ZmM8* and *ZmM14* are expressed in the silks, ears and developing seeds of maize, but only weak expression was found in tassels (Zhang et al., 2012). *ZmM8* and *ZmM14* are mostly expressed in the upper floret meristem of the maize spikelet, suggesting a function in the differential development of the two florets within the maize spikelet (Cacharrón et al., 1999). The position of the *ZmM14* gene in the maize genome may be linked to the *INDETERMINATE FLORAL APEX1* (*IFA1*) locus and because the *ifa1* phenotype shows indeterminate spikelets, florets and gynoecial tissue, this could indicate subfunctionalisation between these two OsMADS1 orthologs (Cacharrón et al., 1999).

OsMADS1 is needed for proper floral organ development in all whorls, but is not expressed in lodicules and stamen, and only weakly in carpels, so some of its function is performed indirectly. In *osmads1* inflorescences several other MADS-box genes are downregulated: B-class genes *OsMADS4* and *OsMADS16*, C-class genes *OsMADS3* and *OsMADS58*, AGL6-like genes *OsMADS6* and *OsMADS17*, and finally the SEP3-like *OsMADS7* and *OsMADS8* (Wu et al., 2018). B-class, C-class and SEP3-like genes are members of the floral quartets of the lodicules, stamen and carpel, so the reduced expression of these genes may explain the phenotype of inner floral organs in the *osmads1* mutant.

MADS5 has no unique functions and shows weak redundancy

MADS5 is the least studied of the LOFSEP genes. The duplication event leading to the split of the *MADS1* and *MADS5* lineages has been mapped to the base of the grass family. Subsequently *MADS5* lost the end of its C-terminal domain by the introduction of a premature stop codon (Christensen and Malcomber, 2012).

The *OsMADS5* mutant has no discernible phenotype, except perhaps an attachment of the lodicules to the lemma (Agrawal et al., 2005; Wu et al., 2018). This is likely to be due to

redundancy in its function with *OsMADS1* and *OsMADS34*, and indeed double and triple mutants show enhanced phenotypes (see below).

OsMADS5 is expressed slightly in the primary and secondary branch meristems of the panicle, but mostly in the developing spikelet, including the sterile lemmas and all floral organs ((Harrop et al., 2016; Wu et al., 2018); Figure 5).

ZmM3 (*ZmMADS5*) is expressed in the ears, developing seeds and tassels of maize, but lacks expression in the silks, while *ZmM6, -7, -8 and -14* are expressed in the silks (Zhang et al., 2012).

TaSEP-6 expression starts later than two other LOFSEP genes *TaSEP-5* and *TaSEP-2*, and aligns more with the SEP3-like *TaSEP-3* and *TaSEP-4* in wheat. In the floral organs however, *TaSEP-6* expression is detected exclusively in the glumes, lemma and palea, along with the other LOFSEP genes (Paollacci et al., 2007). This apparent contradiction is dispelled by newer expression analysis of three MADS5-like genes in wheat that show a general expression around Waddington stage 3, comparable to other LOFSEP gene expression and before the SEP-3 like genes (Figure 4; (Feng et al., 2017))

MADS34 is involved in panicle branching, spikelet morphology and lemma development

OsMADS34/*PANICLE PHYTOMERE2* (*PAP2*) covers the E-function the least well out of all the SEPALLATA in rice, as the quadruple mutant of the other four SEPALLATA genes, *OsMADS1*, *OsMADS5*, *OsMADS7* and *OsMADS8*, leads to the homeotic conversion of all floral organs into leaf-like growths, except for the lemma (Cui et al., 2010). Instead *OsMADS34* has a function earlier in inflorescence development across panicle architecture to spikelet morphogenesis.

The *osmads34* sterile lemmas grow much larger than in the wild type, and have a lemma/palea and leaf like character. While the sterile lemmas normally have only one vascular bundle, the mutants have five to eleven. Also the cell types present in the mutant sterile lemmas are usually found in the lemma, palea or leaves. Together this indicates that *OsMADS34* is essential in the specification of sterile lemmas (Gao et al., 2010; Kobayashi et al., 2010; Wu et al., 2018), or in other words, *OsMADS34* suppresses the outgrowth and differentiation of the sterile lemmas. Outgrowth of some of the rudimentary glumes was

observed in some *OsMADS34* mutants as well, which indicates that the suppression of these lateral outgrowths may be regulated in a similar way by *OsMADS34*, however these similarities are limited, because this phenotype is not always present and is not seen in all mutants of *OsMADS34* (Kobayashi et al., 2010).

OsMADS34 mutants also have an inflorescence architecture phenotype, where there are more primary branches, with fewer secondary branches and spikelets in the panicle (Gao et al., 2010), while Kobayashi et al. observe a similar increase in primary branches, but an increase in secondary branch formation as well as the appearance of tertiary branches and ultimately more spikelets (Kobayashi et al., 2010).

Quantitative RT-PCR shows expression of *OsMADS34* in roots, culms, leaves and the inflorescence (Gao et al., 2010), although the mutant only has a phenotype in the inflorescence, where the expression is strongest. Within the developing inflorescence *OsMADS34* is expressed in the early inflorescence meristem, then highly expressed in the primary and secondary branch meristems and in the early primordia within the spikelet like the glume and sterile lemma primordia, and finally some expression is seen in the early floral organ primordia. ((Gao et al., 2010; Kobayashi et al., 2010; Harrop et al., 2016); Figure 5).

Maize has two MADS34-like genes, *ZmM24* and *ZmM31*, and while this is a relatively recent duplication, their expression pattern has diverged significantly. *ZmM24* is increasingly expressed in the tassel, starting from 0.5cm long and in the ear starting from 2mm long through to pollination. In contrast, *ZmM31* is expressed in the shoot apical meristem during the floral transition up to a tassel length of 0.5cm, and not in the early developmental stages of the ear, except for a relatively modest expression later at 5-10mm ear length (Danilevskaya et al., 2008). The early expression of *ZmM31* in the branching tassel, and lack of early expression in the unbranched ear clearly points to *ZmM31* as the MADS34-like gene in maize that has taken the role in inflorescence branching through subfunctionalisation. With expression starting later, and more consistent throughout floret development, *ZmM24* is likely to be more important in the later E-class function of MADS34 in maize.

In wheat *TaMADS34* (*TaSEP-5*) is highly expressed at the double ridge (DR) stage, in contrast to all other E-class genes and to *TaMADS6* (Figure 4; (Feng et al., 2017)). The same can be observed in barley as well, where *HvMADS34* expression peaks at the DR stage, before the other E-class genes show significant expression (Figure 4; (Digel et al., 2015)). The DR stage is before the start of floral organ meristem formation and since wheat and

barley inflorescences do not branch, the early function of MADS34 in the inflorescence meristem of these cereals is currently unknown.

OsMADS34 has no transcriptional activation activity when assayed in yeast, most likely due to the truncation of the C-terminal domain by an early stop codon (Gao et al., 2010). Therefore all of its functions are likely performed through interactions as a member of protein complexes such as floral quartets. OsMADS34 can form homodimers and heterodimers with the other LOFSEP proteins.

Protein interaction

According to Wu et al. (2018), all of the rice LOFSEP proteins can interact with A-, B-, C-, D- and E-class proteins in a yeast two-hybrid test. Whereas a yeast two-hybrid test by Cui et al. (2010) shows a more selective interaction where OsMADS1 and OsMADS5 do not interact with D-class protein OsMADS13, but the more likely SEP3-like interaction candidates OsMADS7 and OsMADS8 do show strong interaction with OsMADS13. A yeast two-hybrid test by Lim et al. (2000), indicates strong interaction between OsMADS1 and A-class proteins OsMADS14 and OsMADS15, which was confirmed by pulldown assay.

Double and triple mutants reveal redundant LOFSEP functions in rice

The *osmad1 osmads5* double mutant is not significantly different from the *osmads1* single mutant, except for the second whorl phenotype. The *osmads1* reduction in lodicule number in favour of glume-like structures in the second whorl is surprisingly significantly less severe in the double mutant (Wu et al., 2018). Although *OsMADS1* and *OsMADS5* are closely related, they don't seem to have a strong redundancy across functions that are covered by these two genes only.

The *osmads1 osmads34* double mutant phenotype includes elongated, leaf-like sterile lemmas, lemma and palea, extra glume-like organs in the second whorl, and a reduced number of stamen, with an increased number of pistils (Wu et al., 2018). This indicated that *OsMADS1* and *OsMADS34* act partially redundantly in keeping the sterile lemmas supressed and maintaining the floral character of the palea and lemma as opposed to a more leafy appearance.

The *osmads5 osmads34* double mutant phenotype is enhanced compared to the *osmads34* mutant with more leaf-like, longer sterile lemmas, lemma and palea, elongated lodicules and small changes in the number of inner floral organs (Wu et al., 2018). Therefore, while *OsMADS5* and *OsMADS34* act redundantly in the suppression of a leaf phenotype in the sterile lemmas, lemma and palea, their importance is not equal. *OsMADS34* has the more important role, being able to fully cover for the absence of *OsMADS5* in the *osmads5* single mutant. The abnormal numbers of inner floral organs in the *osmads5 osmads34* double mutant does not appear in the single mutants, and is a function of *OsMADS5* and *OsMADS34* that is fully redundant between the two.

The triple mutant *osmads1 osmads5 osmads34* has a severely distorted spikelet phenotype. Sterile lemmas and the lemma and palea grow out to leaf like organs, lodicules grow like glumes, and the inner floral organs are severely reduced. Undifferentiated tissue growth in the centre of the floret indicates that floral determinacy is compromised as well. Additionally the number of leaf-like outer floral organs increases significantly, up to 11 in total (Wu et al., 2018).

When combined these findings reveal the role of *OsMADS34* to be of earliest importance in the spikelet, supressing the bracts and sterile lemmas. *OsMADS1* and *OsMADS34* regulate the outer floral whorl redundantly, with only a minor contribution by *OsMADS5*. The number of outer floral organs is likely to be an outcome of the progression of the floret meristem, where more first whorl organs may be formed when the floret meristem does not progress to producing inner floral organs. Floret meristem organisation is where all three LOFSEP genes show redundancy, since only the triple mutant shows an increased number of outer floral organs (Figure 5, Table 2). While the expression of the LOFSEP genes is predominantly located in the sterile lemma, lemma and palea, the triple mutant has some deleterious effects on the inner floral organs. A possible explanation for this is that while the LOFEP genes are not directly involved in the determination of the inner floral organs, they stimulate the expression of many other MIKCc MADS-box genes. In the triple LOFSEP mutant the expression of *OsMADS7* and *OsMADS8* is reduced, masking the potential lack of direct LOFSEP participation in the specification of the inner floral organs (Wu et al., 2018). *OsMADS5* seems to have a small contrarian effect on some of the inner floral organs where the lodicule phenotype of the *mads1/5* mutant is less severe than the *mads1* phenotype, and the triple mutant has less glume-like second floral whorl organs and less additional pistils compared to the *mads1/34* double mutant. A possible explanation could be that the MADS5

protein can insert itself into a portion of the floral quartets regulating these phenotypes, but makes the quartet non-functional. Therefore it could have a small detrimental effect in the absence of a strong active protein, like MADS1.

1.3 Conclusions and outstanding questions

MADS1 and *MADS34* act in opposition in spikelet transition, but redundantly in lemma identity

MADS1 and *MADS34* show a complex interplay within grass inflorescence development. Established by mutant expression analysis *MADS1* seems to negatively regulate *MADS34* expression, which makes sense for the transition from inflorescence branch meristem, where *MADS34* is dominant, to the spikelet/floret meristem, in which *MADS1* takes over. This is tentatively supported by the overexpression line of *OsMADS1*, where an accelerated transition from branch to spikelet/floret is observed. However, in the lemma *MADS1* and *MADS34* appear to work cooperatively, since the double mutant shows an enhanced phenotype compared to the individual mutants. While the *osmads1/osmads34* double mutant shows an enhanced phenotype of the palea compared to the *osmads1* single mutant, the leaf-like character of the palea when *OsMADS34* is the only E-class gene expressed brings the *MADS34* function in the palea into question. One possible explanation could be that the two E-class proteins present in the palea floral quartet (as predicted by the floral quartet model) are not interchangeable. So while one E-class position in the palea quartet would be redundantly covered by *MADS1* and *MADS34*, the other E-class position can only be filled by another different MADS-box protein, such as *MADS5*, -*7*, and -*8*. Additional interaction studies could reveal how this complex regulation emerges from floral- and perhaps non-floral quartets.

The *MADS1*/*MADS5* function in grasses is likely to be indirect for lodicules, stamen and carpel

The closely related *MADS1* and *MADS5* genes act redundantly for some floral characteristics, as can be seen from mutant studies. However, the expression of *MADS1* and *MADS5* in the floral organs varies greatly between grass species (Christensen and Malcomber, 2012) and yet there is little morphological difference between the floral organs of many grasses. This

leads to the hypothesis that the absence of both *MADS1* and *MADS5* in the floral organs of one or more of the grasses that have been examined, means the *MADS1*/*MADS5* function is either not essential to those floral organs or covered redundantly by other genes. Therefore the absence of both *MADS1* and *MADS5* in the lodicules of sorghum, the stamen of *Avena sativa* and sorghum and the carpel of barley (Christensen and Malcomber, 2012) indicates their function is likely not essential in those three floral whorls, and the E-class function is covered by the SEP3-like SEPALLATA genes *MADS7* and *MADS8*. This indirect effect has already been proposed in rice (see above; (Wu et al., 2018)). In a generic model for grass inflorescence development the effect of *MADS1* and *MADS5* on the lodicule, stamen and carpel identity would thus provisionally be labelled as only indirect through B-class, C-class, and SEP3-like genes. Detailed expression studies in LOFSEP mutants in other grass species can verify whether this inference holds true for grasses in general.

MADS34 regulates branching in panicoid grasses, but has no known function in the non-branching *Triticeae* wheat and barley

MADS34 functions in panicle branching in rice, and likely *ZmM31* performs a similar function in the maize panicle (see above). The early expression of MADS34 in the developing inflorescence is also present in grasses that form a branchless spike, like wheat and barley (Figure 4; (Digel et al., 2015; Harrop et al., 2016; Feng et al., 2017)). The *MADS34* expression peaks around Waddington stage 2, well before the formation of any floral organs, starting with the lemma primordium at W3. This could indicate a transient branch meristem is present in the developing spike of the *Triticeae*, but that it is converted to a spikelet meristem before any outgrowth takes place. Alternatively the early expression of *MADS34* could be merely vestigial, left over from the common ancestor with panicoid grasses that did have a branching inflorescence (Remizowa et al., 2013). And finally, the early expression of *MADS34* could have a new function in *Triticeae* that has no direct relation to inflorescence branching. *MADS34* will be an interesting target for a mutation study in barley and wheat, and since its early expression is well before any of the other E-class genes, the common redundancy among MADS-box genes will not be a complicating factor.

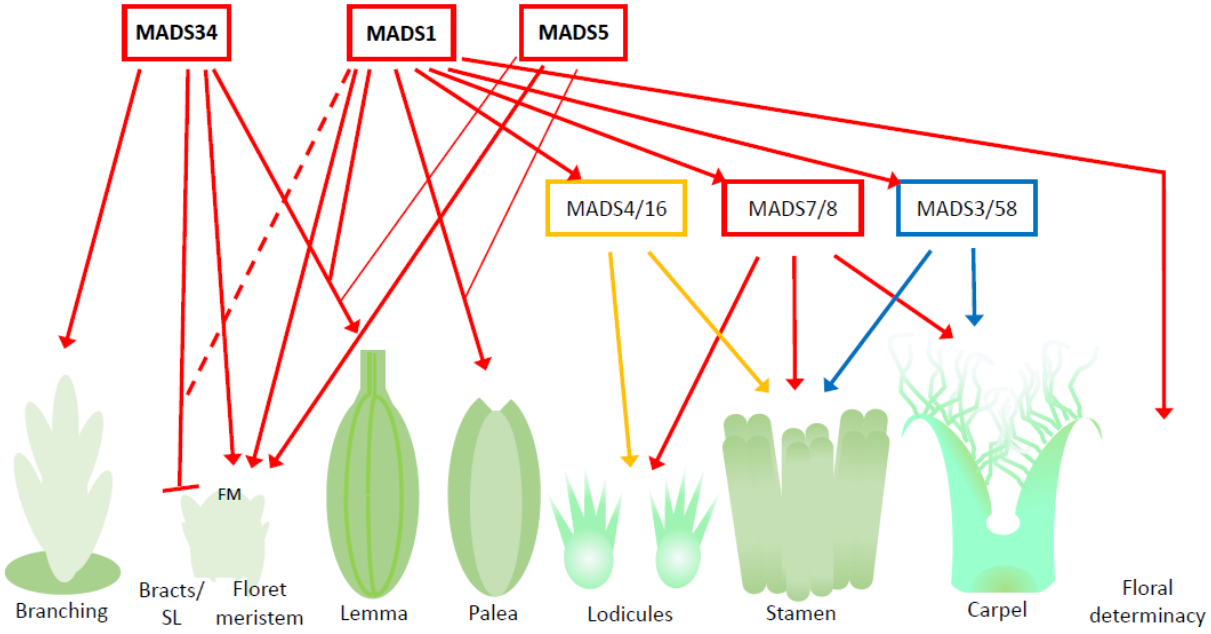

Figure 5: Schematic of the involvement of LOFSEP genes in inflorescence development and floral organ identity in a generic grass model. Left to right corresponds approximately with timing throughout inflorescence development. Red boxes and arrows from E-class/SEPALLATA genes, green from B-class, blue from C-class. While LOFSEP genes are expressed in various inflorescence meristems up to lemma and palea primordia, their effect on the later floral organs is likely indirect through stimulation of B-, C-, and SEP3-E-class genes. SL, sterile lemma (or glume); FM, floral meristem.

LOFSEP functions	MADS1	MADS5	MADS34
Branching meristem			regulate
Spikelet meristem (establish)	promote		oppose?
Bracts			supress
Sterile lemmas	supress*		supress
Lemma	floral	floral (weak)	floral
Palea	floral	floral (weak)	floral†
Floret meristem (transition)	strong	redundant	redundant
lodicules	indirect	indirect, opposite	indirect
stamen	indirect	indirect	indirect
carpel	indirect	indirect, opposite?	indirect
Floret meristem (determinacy)	strong		redundant?

Table 1: Speculative table of LOFSEP functions. This table is based on incomplete data and has a bias towards rice, where most data is currently available. Verification from mutant analysis in other grass species will be needed. *, only found in conjunction with MADS34; †, conflicting data. MADS34 may only give floral identity to the lemma or provide floral identity to the palea only in combination with at least one other LOFSEP gene.

The next steps towards deciphering LOFSEP functions in grasses and barley

Gaining a thorough understanding of the regulation of grass inflorescence architecture will be of immense value, because inflorescence architecture is an important factor in the yield of many important crops. However, even if we limit the scope to the LOFSEP genes, a lot is still unclear. While expression of LOFSEP genes has been detected in many grass species, detailed timing and localisation data are often incomplete or missing. Additionally, since LOFSEP proteins act through interaction with other MIKCc MADS-box genes, establishing co-expression is essential to make any functional predictions. Comparing detailed expression data from multiple grass species will show what is part of the generic grass inflorescence regulatory framework, and where the morphological differences between grasses could stem from.

To add detailed expression data from a relevant grass species barley is a natural choice, because of its importance as a crop, its function as a model species for the even more agronomically important wheat and the current incomplete expression data for barley. We will identify MIKCc MADS-box genes in barley and quantify their expression throughout inflorescence development with quantitative reverse transcription PCR. Given the available data from other grasses the MIKCc MADS-box genes in barley are likely expressed at the time and in the floral organs predicted by the ABCDE model. However the few MIKCc genes where the expression deviates from the ABCDE model are likely to indicate changes to the model for grasses, or barley specifically.

Functional studies through analysis of mutants are almost exclusively done for rice. Currently most available data on LOFSEP genes comes from rice, making the generic model presented above biased towards rice. To gain insight in the LOFSEP function in grasses, and the differences between grass species with contrasting inflorescence architecture we will generate LOFSEP mutants in barley. Using CRISPR/Cas9 constructs and immature embryo transformation mutants for *HvMADS1*, *HvMADS5* and *HvMADS34* will be made. Analysing the mutant phenotypes will provide answers to how much of the current understanding of LOFSEP functions in rice is applicable to grasses in general and what the LOFSEP functions in barley are specifically.

Finally, the study of LOFSEP genes in the non-branching barley inflorescence will provide a contrast with their function in the branching rice panicle. Because the evolution of the barley spike was likely reductive from a branching inflorescence, it is not unthinkable to get a barley inflorescence to branch with a change in LOFSEP gene expression. What it takes to get the barley inflorescence to branch and what changes in gene expression accompany this morphological change can provide valuable insight into the regulation of grass inflorescence architecture and may lead towards adapting the barley inflorescence architecture in new varieties through plant breeding.

References

Agrawal G, Abe K, Yamazaki M, Miyao A, Hirochika H (2005) Conservation of the E-function for floral organ identity in rice revealed by the analysis of tissue culture-induced loss-of-function mutants of the OsMADS1 gene. Plant Molecular Biology **59:** 125-135

Ambrose BA, Lerner DR, Ciceri P, Padilla CM, Yanofsky MF, Schmidt RJ (2000) Molecular and genetic analyses of the silky1 gene reveal conservation in floral organ specification between eudicots and monocots. Molecular Cell **5:** 569-579

Angenent GC, Franken J, Busscher M, Vandijken A, Vanwent JL, Dons HJM, Vantunen AJ (1995) A NOVEL CLASS OF MADS BOX GENES IS INVOLVED IN OVULE DEVELOPMENT IN PETUNIA. Plant Cell **7:** 1569-1582

Arora R, Agarwal P, Ray S, Singh AK, Singh VP, Tyagi AK, Kapoor S (2007) MADS-box gene family in rice: genome-wide identification, organization and expression profiling during reproductive development and stress. BMC Genomics **8:** 242

Becker A (2003) The major clades of MADS-box genes and their role in the development and evolution of flowering plants. Molecular Phylogenetics and Evolution **29:** 464-489

Cacharrón J, Saedler H, Theißen G (1999) Expression of MADS box genes ZMM8 and ZMM14 during inflorescence development of Zea mays discriminates between the upper and the lower floret of each spikelet. Development Genes and Evolution **209:** 411-420

Callens C, Tucker MR, Zhang DB, Wilson ZA (2018) Dissecting the role of MADS-box genes in monocot floral development and diversity. Journal of Experimental Botany **69:** 2435-2459

Christensen AR, Malcomber ST (2012) Duplication and diversification of the LEAFY HULL STERILE1 and Oryza sativa MADS5 SEPALLATA lineages in graminoid Poales. Evodevo **3**

Ciaffi M, Paolacci AR, Tanzarella OA, Porceddu E (2011) Molecular aspects of flower development in grasses. Sex Plant Reprod **24:** 247-282

Coen ES, Meyerowitz EM (1991) THE WAR OF THE WHORLS - GENETIC INTERACTIONS CONTROLLING FLOWER DEVELOPMENT. Nature **353:** 31-37

Cui R, Han J, Zhao S, Su K, Wu F, Du X, Xu Q, Chong K, Theissen G, Meng Z (2010) Functional conservation and diversification of class E floral homeotic genes in rice (Oryza sativa). Plant J **61:** 767-781

Danilevskaya ON, Meng X, Selinger DA, Deschamps S, Hermon P, Vansant G, Gupta R, Ananiev EV, Muszynski MG (2008) Involvement of the MADS-Box gene ZMM4 in floral induction and inflorescence development in maize. Plant Physiology **147:** 2054-2069

Danilevskaya ON, Meng X, Selinger DA, Deschamps S, Hermon P, Vansant G, Gupta R, Ananiev EV, Muszynski MG (2008) Involvement of the MADS-box gene ZMM4 in floral induction and inflorescence development in maize. Plant Physiol **147:** 2054-2069

Digel B, Pankin A, von Korff M (2015) Global Transcriptome Profiling of Developing Leaf and Shoot Apices Reveals Distinct Genetic and Environmental Control of Floral Transition and Inflorescence Development in Barley. Plant Cell **27:** 2318-2334

Ditta G, Pinyopich A, Robles P, Pelaz S, Yanofsky MF (2004) The SEP4 gene of Arabidopsis thaliana functions in floral organ and meristem identity. Current Biology **14:** 1935-1940

Dreni L, Zhang D (2016) Flower development: the evolutionary history and functions of the AGL6 subfamily MADS-box genes. J Exp Bot **67:** 1625-1638

Feng N, Song G, Guan J, Chen K, Jia M, Huang D, Wu J, Zhang L, Kong X, Geng S, Liu J, Li A, Mao L (2017) Transcriptome Profiling of Wheat Inflorescence Development from Spikelet Initiation to Floral Patterning Identified Stage-Specific Regulatory Genes. Plant Physiol **174:** 1779-1794

Feng N, Song GY, Guan JT, Chen K, Jia ML, Huang DH, Wu JJ, Zhang LC, Kong XY, Geng SF, Liu J, Li AL, Mao L (2017) Transcriptome Profiling of Wheat Inflorescence Development from Spikelet Initiation to Floral Patterning Identified Stage-Specific Regulatory Genes. Plant Physiology **174:** 1779-1794

Gao XC, Liang WQ, Yin CS, Ji SM, Wang HM, Su XA, Guo CC, Kong HZ, Xue HW, Zhang DB (2010) The SEPALLATA-Like Gene OsMADS34 Is Required for Rice Inflorescence and Spikelet Development. Plant Physiology **153:** 728-740

Goto K, Kyozuka J, Bowman JL (2001) Turning floral organs into leaves, leaves into floral organs. Current Opinion in Genetics & Development **11:** 449-456
Hama E, Takumi S, Ogihara Y, Murai K (2004) Pistillody is caused by alterations to the class-B MADS-box gene expression pattern in alloplasmic wheats. Planta **218:** 712-720
Harrop TW, Ud Din I, Gregis V, Osnato M, Jouannic S, Adam H, Kater MM (2016) Gene expression profiling of reproductive meristem types in early rice inflorescences by laser microdissection. Plant J **86:** 75-88
Immink RGH, Tonaco IAN, de Folter S, Shchennikova A, van Dijk ADJ, Busscher-Lange J, Borst JW, Angenent GC (2009) SEPALLATA3: the 'glue' for MADS box transcription factor complex formation. Genome Biology **10**
Khanday I, Yadav SR, Vijayraghavan U (2013) Rice LHS1/OsMADS1 Controls Floret Meristem Specification by Coordinated Regulation of Transcription Factors and Hormone Signaling Pathways. Plant Physiology **161:** 1970-1983
Kobayashi K, Maekawa M, Miyao A, Hirochika H, Kyozuka J (2010) PANICLE PHYTOMER2 (PAP2), encoding a SEPALLATA subfamily MADS-box protein, positively controls spikelet meristem identity in rice. Plant and Cell Physiology **51:** 47-57
Kwantes M, Liebsch D, Verelst W (2012) How MIKC* MADS-Box Genes Originated and Evidence for Their Conserved Function Throughout the Evolution of Vascular Plant Gametophytes. Molecular Biology and Evolution **29:** 293-302
Laudencia-Chingcuanco D, Hake S (2002) The indeterminate floral apex1 gene regulates meristem determinacy and identity in the maize inflorescence. Development **129:** 2629-2638
Li C, Dubcovsky J (2008) Wheat FT protein regulates VRN1 transcription through interactions with FDL2. Plant J **55:** 543-554
Li HF, Liang WQ, Yin CS, Zhu L, Zhang DB (2011) Genetic Interaction of OsMADS3, DROOPING LEAF, and OsMADS13 in Specifying Rice Floral Organ Identities and Meristem Determinacy. Plant Physiology **156:** 263-274
Lim J, Moon YH, An G, Jang SK (2000) Two rice MADS domain proteins interact with OsMADS1. Plant Mol Biol **44:** 513-527
Liu H, Li G, Yang X, Kuijer HNJ, Liang W, Zhang D (2019) Transcriptome profiling reveals phase-specific gene expression in the developing barley inflorescence. The Crop Journal
Malcomber ST, Kellogg EA (2005) SEPALLATA gene diversification: brave new whorls. Trends in Plant Science **10:** 427-435
Murai K (2013) Homeotic Genes and the ABCDE Model for Floral Organ Formation in Wheat. Plants-Basel **2:** 379-395
Paolacci AR, Tanzarella OA, Porceddu E, Varotto S, Ciaffi M (2007) Molecular and phylogenetic analysis of MADS-box genes of MIKC type and chromosome location of SEP-like genes in wheat (Triticum aestivum L.). Mol Genet Genomics **278:** 689-708
Paollacci AR, Tanzarella OA, Porceddu E, Varotto S, Ciaffi M (2007) Molecular and phylogenetic analysis of MADS-box genes of MIKC type and chromosome location of SEP-like genes in wheat (Triticum aestivum L.). Molecular Genetics and Genomics **278:** 689-708
Pelaz S, Ditta GS, Baumann E, Wisman E, Yanofsky MF (2000) B and C floral organ identity functions require SEPALLATA MADS-box genes. Nature **405:** 200-203
Prasad K, Parameswaran S, Vijayraghavan U (2005) OsMADS1, a rice MADS-box factor, controls differentiation of specific cell types in the lemma and palea and is an early-acting regulator of inner floral organs. Plant Journal **43:** 915-928
Reinheimer R, Kellogg EA (2009) Evolution of AGL6-like MADS box genes in grasses (Poaceae): ovule expression is ancient and palea expression is new. Plant Cell **21:** 2591-2605
Remizowa MV, Rudall PJ, Choob VV, Sokoloff DD (2013) Racemose inflorescences of monocots: structural and morphogenetic interaction at the flower/inflorescence level. Annals of Botany **112:** 1553-1566
Sang X, Li Y, Luo Z, Ren D, Fang L, Wang N, Zhao F, Ling Y, Yang Z, Liu Y, He G (2012) CHIMERIC FLORAL ORGANS1, encoding a monocot-specific MADS box protein, regulates floral organ identity in rice. Plant Physiol **160:** 788-807

Schmitz J, Franzen R, Ngyuen TH, Garcia-Maroto F, Pozzi C, Salamini F, Rohde W (2000) Cloning, mapping and expression analysis of barley MADS-box genes. Plant Molecular Biology **42:** 899-913

Shitsukawa N, Tahira C, Kassai KI, Hirabayashi C, Shimizu T, Takumi S, Mochida K, Kawaura K, Ogihara Y, Murai K (2007) Genetic and epigenetic alteration among three homoeologous genes of a class E MADS box gene in hexaploid wheat. Plant Cell **19:** 1723-1737

Smaczniak C, Immink RGH, Angenent GC, Kaufmann K (2012) Developmental and evolutionary diversity of plant MADS-domain factors: insights from recent studies. Development **139:** 3081-3098

Sorrells ME, La Rota M, Bermudez-Kandianis CE, Greene RA, Kantety R, Munkvold JD, Miftahudin, Mahmoud A, Ma X, Gustafson PJ, Qi LL, Echalier B, Gill BS, Matthews DE, Lazo GR, Chao S, Anderson OD, Edwards H, Linkiewicz AM, Dubcovsky J, Akhunov ED, Dvorak J, Zhang D, Nguyen HT, Peng J, Lapitan NL, Gonzalez-Hernandez JL, Anderson JA, Hossain K, Kalavacharla V, Kianian SF, Choi DW, Close TJ, Dilbirligi M, Gill KS, Steber C, Walker-Simmons MK, McGuire PE, Qualset CO (2003) Comparative DNA sequence analysis of wheat and rice genomes. Genome Res **13:** 1818-1827

Strable J, Wallace JG, Unger-Wallace E, Briggs S, Bradbury PJ, Buckler ES, Vollbrecht E (2017) Maize YABBY Genes drooping leaf1 and drooping leaf2 Regulate Plant Architecture. Plant Cell **29:** 1622-1641

Theissen G (2001) Development of floral organ identity: stories from the MADS house. Current Opinion in Plant Biology **4:** 75-85

Trevaskis B, Hemming MN, Dennis ES, Peacock WJ (2007) The molecular basis of vernalization-induced flowering in cereals. Trends Plant Sci **12:** 352-357

Wang KJ, Tang D, Hong LL, Xu WY, Huang J, Li M, Gu MH, Xue YB, Cheng ZK (2010) DEP and AFO Regulate Reproductive Habit in Rice. Plos Genetics **6**

Wang L, Zeng XQ, Zhuang H, Shen YL, Chen H, Wang ZW, Long JC, Ling YH, He GH, Li YF (2017) Ectopic expression of OsMADS1 caused dwarfism and spikelet alteration in rice. Plant Growth Regulation **81:** 433-442

Wu D, Liang W, Zhu W, Chen M, Ferrandiz C, Burton RA, Dreni L, Zhang D (2018) Loss of LOFSEP Transcription Factor Function Converts Spikelet to Leaf-Like Structures in Rice. Plant Physiol **176:** 1646-1664

Wu D, Liang WQ, Zhu WW, Chen MJ, Ferrandiz C, Burton RA, Dreni L, Zhang DB (2018) Loss of LOFSEP Transcription Factor Function Converts Spikelet to Leaf-Like Structures in Rice. Plant Physiology **176:** 1646-1664

xu G, Kong H (2007) Duplication and Divergence of Floral MADS-Box Genes in Grasses: Evidence for the Generation and Modification of Novel Regulators. Journal of Integrative Plant Biology **49:** 927-939

Yamaguchi T, Nagasawa N, Kawasaki S, Matsuoka M, Nagato Y, Hirano HY (2004) The YABBY gene DROOPING LEAF regulates carpel specification and midrib development in Oryza sativa. Plant Cell **16:** 500-509

Yu XX, Duan XS, Zhang R, Fu XH, Ye LL, Kong HZ, Xu GX, Shan HY (2016) Prevalent Exon-Intron Structural Changes in the APETALA1/FRUITFULL, SEPALLATA, AGAMOUS-LIKE6, and FLOWERING LOCUS C MADS-Box Gene Subfamilies Provide New Insights into Their Evolution. Frontiers in Plant Science **7**

Yuan Z, Gao S, Xue DW, Luo D, Li LT, Ding SY, Yao X, Wilson ZA, Qian Q, Zhang DB (2009) RETARDED PALEA1 controls palea development and floral zygomorphy in rice. Plant Physiol **149:** 235-244

Zahn LM, Kong H, Leebens-Mack JH, Kim S, Soltis PS, Landherr LL, Soltis DE, Depamphilis CW, Ma H (2005) The evolution of the SEPALLATA subfamily of MADS-box genes: a preangiosperm origin with multiple duplications throughout angiosperm history. Genetics **169:** 2209-2223

Zhang Z, Li H, Zhang D, Liu Y, Fu J, Shi Y, Song Y, Wang T, Li Y (2012) Characterization and expression analysis of six MADS-box genes in maize (Zea mays L.). J Plant Physiol **169:** 797-806

Zhang ZB, Li HY, Zhang DF, Liu YH, Fu J, Shi YS, Song YC, Wang TY, Li Y (2012) Characterization and expression analysis of six MADS-box genes in maize (Zea mays L.). Journal of Plant Physiology **169:** 797-806

Chapter 2: Expression profiling of MIKCc MADS-box genes reveals conserved and novel roles in barley inflorescence development

2.1 Abstract

MADS-box genes have a wide range of functions in plant reproductive development. The ABCDE model of floral organ development shows that MADS-box genes are central players for floral development in dicots, but this model remains largely unknown in many grass crops. Here we showed that expression analysis of all MIKCc MADS-box genes through barley (*Hordeum vulgare*) inflorescence development reveals co-expression groups that can be linked to developmental events. 34 MIKCc MADS-box genes were identified in the barley genome and only two orthologous genes were missing compared with other grass species, indicating there is little evolutionary divergence.

The natural variation of the 34 MIKCc MADS encoding regions was investigated using the SNP browser (https://bridge.ipk-gatersleben.de/bridge//#snpbrowser) scanning in 22530 barley varieties showed that most genomic sequences of this family are extremely conserved during evolution/domestication.

Combined expression analysis for various inflorescence developmental stages and individual floral organs by RT-qPCR showed that MADS-box genes are generally expressed at key developmental stages and floral organs in barley as predicted by the ABCDE model. However, expression patterns of some *MADS* genes, like *HvMADS58* and *HvMADS34*, were deviating from predicted patterns, placing them outside the scope of the classical ABCDE model of floral development. Co-expression in three correlation sets showed that different members of the barley MIKCc MADS-box genes are likely to be involved in the associated developmental events of inflorescence meristem (IM) initiation, floral meristem identity and floral organ determination. Thus, we proposed a potential ABCDE working model in barley where the classic model is generally upheld, but with some notable deviations: the antagonism between A-class and C-class gene expression, a central tenet of the ABC model, is abandoned in barley. This study provides new insights into MIKCc MADS-box genes in a floral ABCDE working model during barley inflorescence development.

2.2 Introduction

Flowers are often composed of four different floral organs organised in concentric whorls numbered from peripheral to central position. The outer whorls are sepals and petals in many dicots, including the model plant *Arabidopsis*, and lemma/palea and lodicules in grasses, while the inner whorls contain the male reproductive organs, the stamens, in the third whorl and the female organs, the carpels, in the fourth whorl (Figure 1C in chapter 1). Genetic studies have identified a large number of regulatory genes that control the specification of these distinct floral organs in plants (Alvarez-Buylla et al., 2010). The ABCDE model, originally proposed for *Arabidopsis* and *Antirrhinum majus*, associates the developmental determination of specific flower organs with the combinatorial activity of several classes of homeotic selector genes, most of which encode MIKCc MADS domain developmental transcription factors that cooperatively bind to DNA at conserved CArG boxes (CCA/T6GG) to regulate gene expression (Theissen and Saedler, 2001). The MIKCc genes are divided into A-, B- C- D- and E-classes where A- and E-class genes determine the first whorl organs, A-, B-, and E-class genes determine the second whorl, B-, C-, and E-class genes control the third whorl and C- and E-class genes specify the fourth whorl. D-class genes are involved in a floral quartet that determines ovule development. Individual genes within a class usually act redundantly with each other, so that single mutations often have a subtle or absent phenotype (Coen and Meyerowitz, 1991; Angenent et al., 1995; Pelaz et al., 2000). Studies demonstrate the conservation of homologs of the ABCDE genes across most flowering plants (Theissen et al., 2016), and suggest the regulatory principles of some of these homologs have been conserved during flower evolution.

MIKCc MADS transcription factors contain the conserved MADS DNA-binding domain, Intervening domain, Keratin-like domain and the C-terminal domain, while the small c stands for classic. The closest relatives are the MIKC* genes, and then the α- β- and γ-MADS box genes complete the MADS family (Kwantes et al., 2012; Smaczniak et al., 2012). Within the MIKCc family there are more groups than just the ABCDE-class genes such as the SVP-like floral repressors and the SOC1-like floral promotors (Figure 1).

The MIKCc genes in grasses

While the MIKCc classes and their roles in inflorescence development are generally conserved, the individual genes within a class often have no direct homology between grasses

and *Arabidopsis*, making them co-orthologs ((Ciaffi et al., 2011); supplemental table 1). Notably missing in the grasses is the FLC-class, which governs vernalisation and flowering time in *Arabidopsis* (Becker, 2003). Unique to grasses is the *OsMADS32* class, which is loosely related to B-class genes (Ciaffi et al., 2011).

The 11 MIKC type MADS-box genes from the last common ancestor of monocots and eudicots increased to at least 24 in the last common ancestor of rice, wheat and maize (Bremer, 2002; Ciaffi et al., 2011). During this time of duplication and diversification in the MIKC family the complex grass inflorescence and floral structures of the Poaceae family evolved. Changes in the copy number and expression pattern of MADS-box genes are closely associated with the morphological diversification of grass inflorescences (Ciaffi et al., 2011).

The ABCDE model in grasses

Generally the ABCDE model of floral organogenesis can be applied to grasses as well. The functional studies in rice produce mostly the homeotic changes predicted by the model for A-class genes (Wu et al., 2017), B-class genes (Nagasawa et al., 2003; Yadav et al., 2007; Yao et al., 2008), C- and D-class genes (Yamaguchi et al., 2006; Dreni et al., 2011) and E-class genes (Cui et al., 2010; Gao et al., 2010; Wu et al., 2018). The expression pattern and timing of MIKCc genes in other grasses indicates this likely extends to the whole grass family (Digel et al., 2015; Harrop et al., 2016; Feng et al., 2017; Callens et al., 2018; Zhu et al., 2018).

A major difference is the regulation of carpel specification in rice by the YABBY family gene *DROOPING LEAF* (*DL*) (Nagasawa et al., 2003; Yamaguchi et al., 2004). Expression of *DL* orthologs in the carpel of maize and wheat suggests its function in carpel specification is a common feature in grasses (Bommert et al., 2005). While *CRABS CLAW*, the Arabisopsis co-ortholog of *DL*, has a function in carpel development, there is no homeotic change to the carpel identity in its absence (Bowman and Smyth, 1999), indicating a change in floral organogenesis between eudicots and grasses.

Some MIKCc genes have adopted additional roles in grasses, like the A-class gene *HvMADS14* which is a vernalisation integrator in barley (Trevaskis et al., 2007), a role in the onset of the floral transition. While in rice *OsMADS34* has been shown to modulate

inflorescence branching (Gao et al., 2010; Kobayashi et al., 2010), which is not canonically an E-class role.

Transcript analysis

The inflorescence development in barley and wheat can be divided into steps by examining the development of the shoot apical meristem (SAM) and noting the emergence and shape of the inflorescence, spikelet and floret meristems followed by the sequential initiation and growth of the floral organs (Waddington et al., 1983). These Waddington stages range from the transition of the vegetative to reproductive SAM at W1, to pollination or anthesis at W10, and includes a series of developmental and cellular events (Figure 1, supplemental figure 2). However, the expression and regulation of ABCDE model components in barley inflorescence development and floret formation still remain unknown. Here, we performed transcript analysis of MIKCc genes through inflorescence developmental stages and in individual floral organs by RT-qPCR. Our findings reveal that the ABCDE model can likely be mostly applied to barley, while the deviations point to interesting adaptations that can reveal more about inflorescence development in grasses.

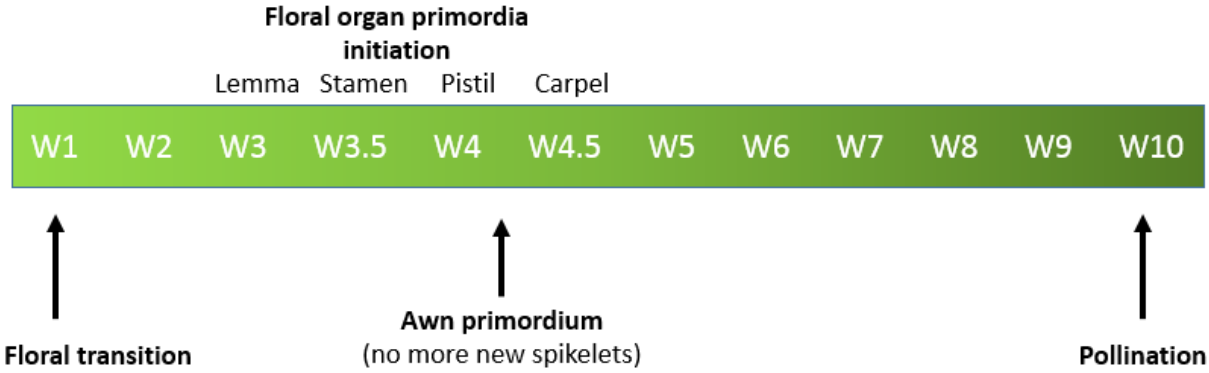

Figure 1: Waddington stages for barley and their relation to major developmental steps.

2.3 Results

Identification and phylogenetic analysis of MIKCc MADS-box genes in the barley genome

The recent barley genome assembly has 32 MIKCc MADS-box genes annotated as expressed sequences and a pseudogene strongly resembling *HvMADS14* (Mascher et al., 2017). Through comparison to homologous genes from rice, and a BLAST search for available transcript sequences of barley, two genes labelled as *HvMADS27* were found to be more related to *HvMADS23*, while *HvMADS50* and *HvMADS33* were found as transcript sequences for barley, but not present in the genome assembly. Additionally, a more accurate exon sequence was found for 9 MIKCc genes through comparison with available transcripts for *HvMADS16*, *HvMADS18*, *HvMADS55*, *HvMADS56*, and *HvMADS57*, and by analysing the genomic region with FGENESH, guided by the *OsMADS25* sequence, for *HvMADS25a/b/c/d*. This brings the total to 34 MIKCc MADS-box genes and 1 pseudogene in barley. A complete list with HORVU IDs and accession numbers for improved transcripts is given in supplemental table 1.

There is a barley homolog for 31 of the 33 complete MIKCc genes in rice, missing homologs for the A-class gene *OsMADS20* and the AGL6 like gene *OsMADS17*. There is only one copy of *OsMADS25* in rice, but four in barley, here designated *HvMADS25a*, *HvMADS25b*, *HvMADS25c* and *HvMADS25d*. Apart from these exceptions, the MIKCc genes in barley each have a clear homolog in rice. This conservation can mostly be extended to *Brachypodium* and sorghum as well (Figure 2; Supplemental table 1). The FLC-like MIKCc genes, involved in flowering time and vernalisation in *Arabidopsis* have no homologous class in grasses. Conversely the *MADS32* gene has no orthologous gene group in *Arabidopsis*.

The structure of MIKCc MADS-box genes shows some expected conservation of intron-exon pattern within the different classes of closely related genes. Most exon patterns are long-short-short-medium-short-short-long, or a variant thereof, whereas intron length, and therefore gene length, varies more widely (Figure 11). Some of the *MADS25* paralogous genes have big introns, a: 0.5kbp, b: 6kbp, c: 10kbp and d: 15kbp.

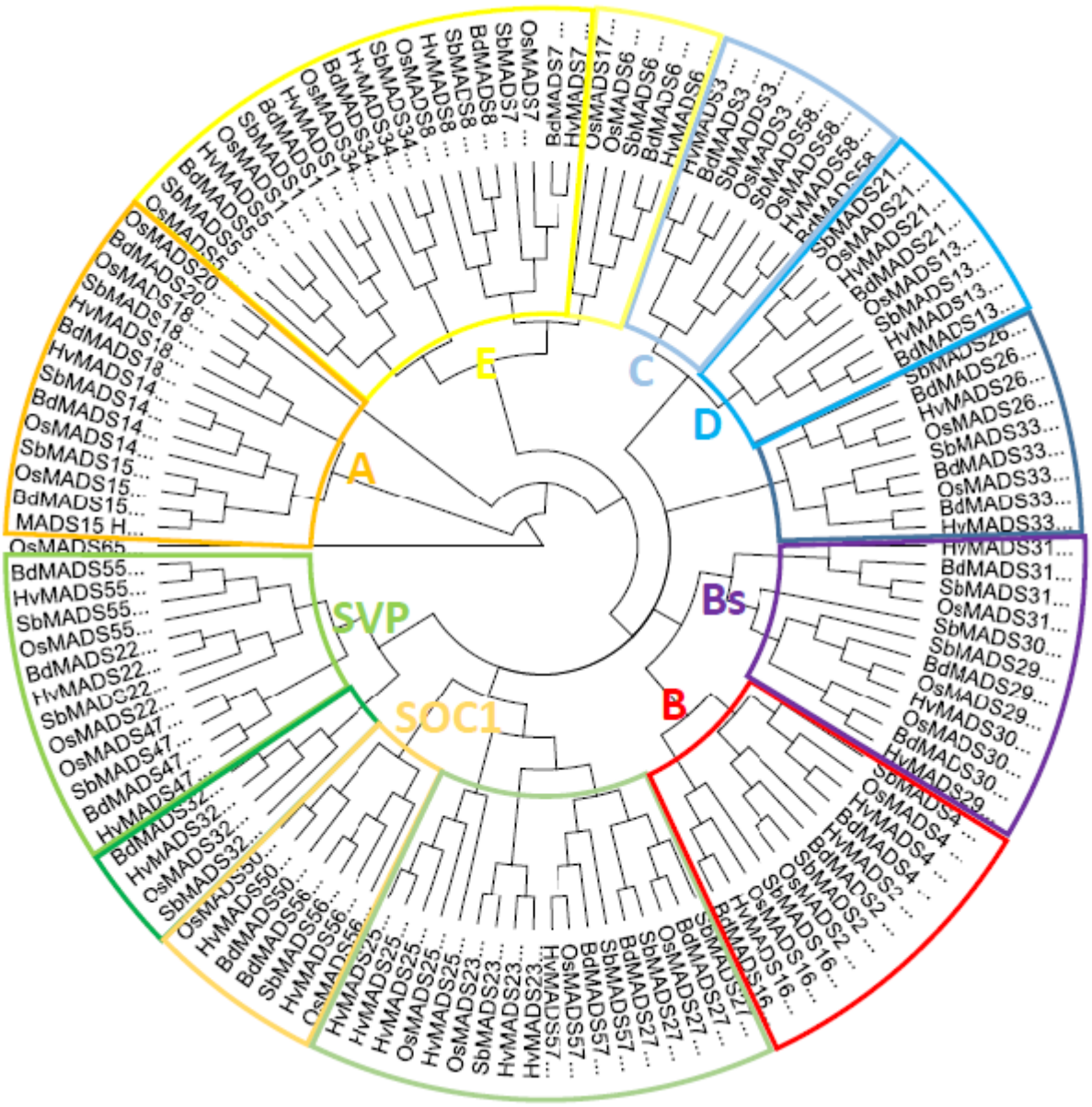

Figure 2: Phylogenetic analysis of all MIKCc type MADS-box genes in barley compared to the homologues in rice, *Brachypodium* and sorghum. The classes within the family are delimited by coloured boxes. A: A-class genes, B: B-class genes, Bs: B-sister class genes, C: C-class genes or *AGAMOUS*-like, D: D-class genes, E: E-class genes or SEPALLATA, SOC1: *SUPRESSOR OF CONSTANS1*-like genes, SVP: *SVP*/*VRT*-like genes.

Low amount of single nucleotide polymorphism shows high conservation of MIKCc genes

Not only are the MIKCc MADS-box genes conserved between grass species, between varieties of wild and domesticated barley there are only a few single nucleotide polymorphisms (SNPs). Exome sequencing of 22626 barley cultivars, landraces and wild

relatives resulted in a comprehensive SNP database, recently made accessible at IPK Gatersleben (Milner et al., 2019) https://bridge.ipk-gatersleben.de/bridge//#snpbrowser.

Only 14 out of the 34 MIKCc MADS-box genes contained any SNPs in the varieties sampled. Within these 14 genes only half exhibit amino acid changes (Table 1), though never in the first 110 amino acids, which contain the MADS domain and the Intervening domain. The lack of both natural and selected variety in these genes may just be in line with the general low sequence polymorphism of barley. In rice there are significantly more SNPs that change an amino acid, although many occur at a very low frequency (Table 1); (Mansueto et al., 2017); (http://snp-seek.irri.org/_snp.zul).

	No. of rice SNPs	Average % occurance	No. of barley SNPs
MADS14		-	
MADS15		-	2
MADS18	1	4	1
MADS20	9	10	
MADS2	1	33	
MADS4		-	1
MADS16	3	21	
MADS3	1	42	
MADS58	5	13	
MADS13	2	41	
MADS21	2	4	1
MADS1		-	
MADS5	1	8	
MADS34		-	
MADS7	2	43	
MADS8		-	
MADS6	1	17	

	No. of rice SNPs	Average % occurance	No. of barley SNPs
MADS17		-	
MADS50	3	16	
MADS56	4	25	
MADS22		-	
MADS55	1	3	
MADS47	1	22	1
MADS26	1	7	
MADS33	1	1	
MADS23	2	7	
MADS25 (C)	1	27	2
MADS27	2	5	
MADS57	1	2	
MADS29	1	49	
MADS30	9	1	
MADS31	2	27	2
MADS32	1	3	

Table 1: All SNPs resulting in an amino acid change in the MIKCc genes of rice and barley. The average percentage of the rice accessions with each SNPs is given per gene. For example, two amino acid changing SNPs were found in *OsMADS7*, on average they each occurred in 43% of the cultivars, while no amino acid changing SNPs were found in *HvMADS7*. The 3k variety set on http://snp-seek.irri.org/_snp.zul was used for rice, and the complete collection on https://bridge.ipk-gatersleben.de/bridge//#snpbrowser for barley.

Global MIKCc expression is concentrated in the inflorescence and caryopsis

The ABCDE-class MIKCc genes in barley, according to the expression data accompanying the HORVU database (Mayer et al., 2012), are predominantly expressed in the developing inflorescence at 0.5 and 1.5 cm (INF1 and INF2) and developing seed (CAR1 and CAR2) (Figure 3).

Expression in other barley tissues, such as leaf and root, is seen for the SVP-like genes *MADS22*/*47*/*55*. AGL17-like genes *MADS23a*/*b* and *MADS25a*/*b*/*c*/*d* are expressed mostly in the root and late seed development, however their total expression level is low (RPKM 8 or less), suggesting they may not be functional. *MADS27* and *MADS57* have an RPKM of 69 and 41 in roots respectively, which indicates they are likely to be functional.

Overall, the majority of MIKCc MADS-box genes are expressed in the developing inflorescence and, similar to homologs in related species, are probably involved in meristem transitions and floral organ development (Arora et al., 2007; Paollacci et al., 2007; Wei et al., 2014). However, to gain any insight into the similarities and differences in function of the MIKCc genes in barley inflorescence development, and to what extent the ABCDE model is conserved, a higher resolution expression profile from floral transition to pollination and a complete set of floral organ expression data would be required.

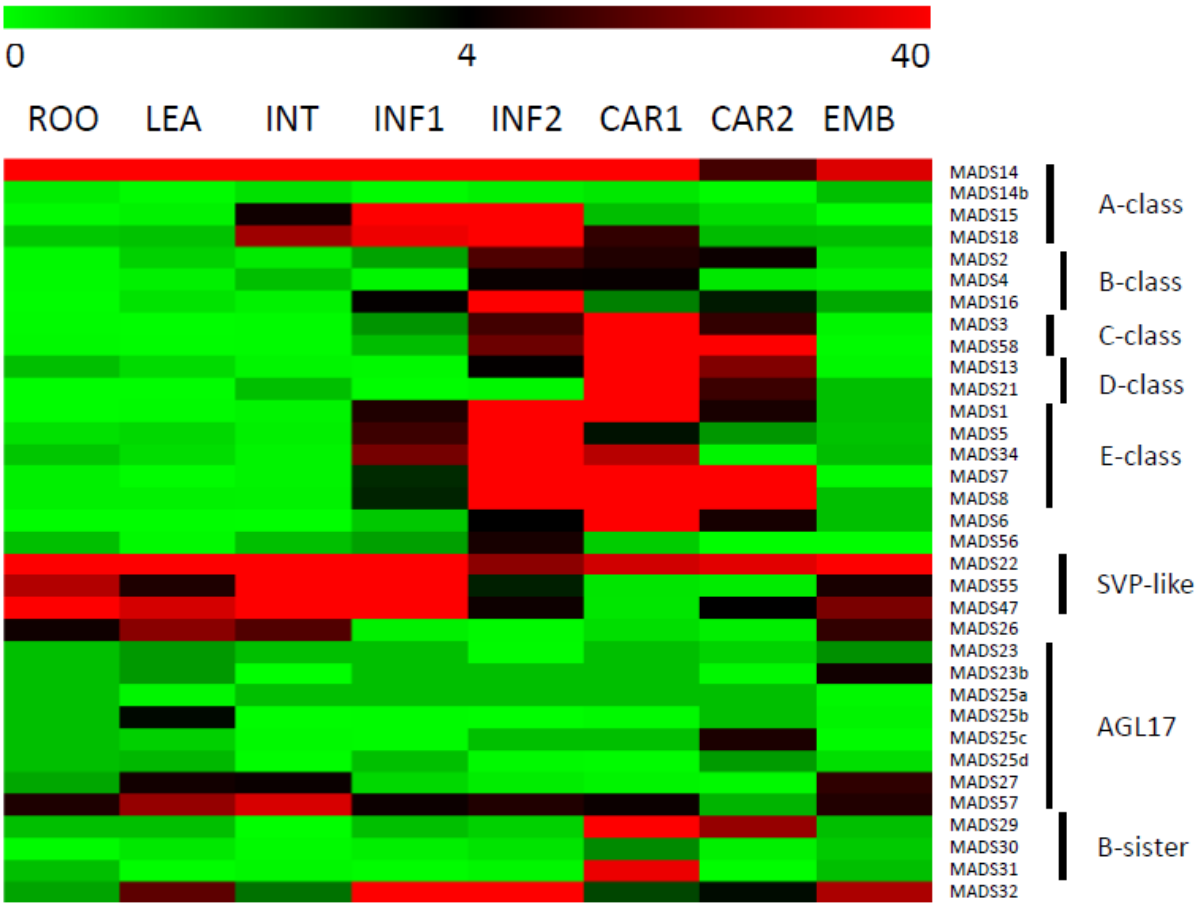

Figure 3: Global expression of MIKCc genes in different barley tissues. Absolute RPKM is plotted on a logarithmic colour scale. ROO: roots 17 DAP, LEA: leaves 17 DAP, INT: 3rd internode 42 DAP, INF1: developing inflorescence 5 mm, INF2: developing inflorescence 10-15 mm, CAR5: developing grain 5 DAP, CAR15: developing grain 15 DAP, EMB: 4 days after germination embryo. Raw data form Mayer et al, (2012).

Expression profiles of MIKCc genes in inflorescence development and floral organs

The expression profiles of MIKCc genes through barley inflorescence development (Figure 4, 5) can be related to developmental events by Waddington stage (Figure 1 and 5). Combined with expression data in the floral organs at Waddington stage W9.5 (Figure 6), a comparison to established ABCDE models in other species can be made.

A-class: The canonical A-class function in the outer floral organs would show expression starting after the lemma primordium is first formed, at W3. However expression of all three A-class genes increases earlier, at the floral transition W1, indicating a new role in earlier inflorescence development. *MADS14* expression is already established at W1, peaks at W3.5,

declines into W4.5 and peaks again at W9.5, right before pollination. The early expression of *MADS18*, along with the decline at W4.5, is less pronounced than for *MADS14*, but still recognisable (Figure 4). *MADS15* expression is closer to the expected profile of an A-class function gene, and expression is indeed confined to the lemma and palea. While *MADS14* and *MADS18* are also expressed in the lemma and palea, their expression is not confined there and *MADS14* is surprisingly more strongly expressed in the stamens than the first whorl, indicating a clear break with the classical ABCDE model (Figure 6).

B-class: The expression of B-class genes starts to increase at W3.5, where the stamen primordia are formed, and peaks right before pollination (Figure 4). B-class expression is confined to the lodicules and stamens, exactly following the ABCDE model, indicating B-class function is likely to be completely conserved in barley (Figure 6).

C-class: *MADS3* and *MADS58* both start expression around W3.5 when the stamen primordia appear, in accordance with the ABCDE model. However where *MADS3* peaks before pollination and declines quickly afterwards, *MADS58* maintains peak expression through W10, indicating subfunctionalisation of the two genes, where *MADS58* is responsible for the C-class function in the carpel (Figure 4). Both C-class genes also show some expression in the lodicules, which goes against the ABCDE model (Figure 6).

D-class: *MADS13* and *MADS21* both start significant expression only after W6.5, well after the pistil primordium is formed, which first appears at W4. Their peak expression is after pollination, and confined to the carpel, indicating that their canonical role in ovule development is likely to be conserved in barley (Figure 4).

E-class: There is a clear difference between the 'LOFSEP' genes *MADS1*, *MADS5* and *MADS34* that express earlier and sharply drop at pollination (W10) and *MADS7* and *MADS8* expression, which starts later around W3.5 and continues to rise through pollination (Figure 4). Floral organ expression shows a division along the same line, where the LOFSEP genes are mostly confined to the lemma and palea whereas *MADS7* and *MADS8* are expressed in the lodicules, stamens and carpel (Figure 6). Therefore the LOFSEP genes probably perform the E-class function in the lemma and palea, while *MADS7* and *MADS8* fulfil the E-class function in the other floral organs. In contrast to all other E-class genes, *MADS34* is strongly expressed at W2, similar to *MADS14*, hinting at a function in early inflorescence development.

SVP-like: The three SVP-like genes *MADS22*, *MADS47* and *MADS55* are highly expressed at the start of the floral transition, and quickly decline to insignificant expression at W2.5, which indicates a role at this early stage. *MADS22* has a surprising resurgence in expression to a new maximum at W9.5, exclusively in the stamens, indicating possible neofunctionalisation (Figures 5, 6).

MADS6: *MADS6*, closely related to the E-class genes, has an expression profile similar to *MADS1* (Figure 5), however in contrast to *MADS1* it is not expressed in the lemma, but is in the lodicules (Figure 6). The presence of *MADS1*, and absence of *MADS6,* in the lemma is confirmed in early inflorescence development by *in situ* hybridisation (Figure 9). *MADS1* and *MADS6* may be partially redundant, but not in the lemma and lodicules.

MADS32: *MADS32* has no equivalent in *Arabidopsis*, and thus no assigned function in the original ABCDE model. The *MADS32* expression profile starts before the initiation of the floral organs, and uniquely declines after W6.5, unlike any other MIKCc gene (Figure 5). Floral organ expression is concentrated in the lemma, palea and lodicules (Figure 6).

B-sister: *MADS29* and *MADS31* are expressed late in inflorescence development, mostly after W8.5 and are strongly expressed after pollination (Figure 5). Combined with a nearly exclusive expression in the carpel, *MADS29* and *MADS31* are likely to be involved to be in ovule and seed development (Figure 6).

SOC1-like: *MADS50* and *MADS56* expression starts early, with a peak at W2 and W2.5, much like *MADS14* and *MADS34*. Late expression is weak, and therefore the floral organ expression is not very consequential (Figures 5, 6).

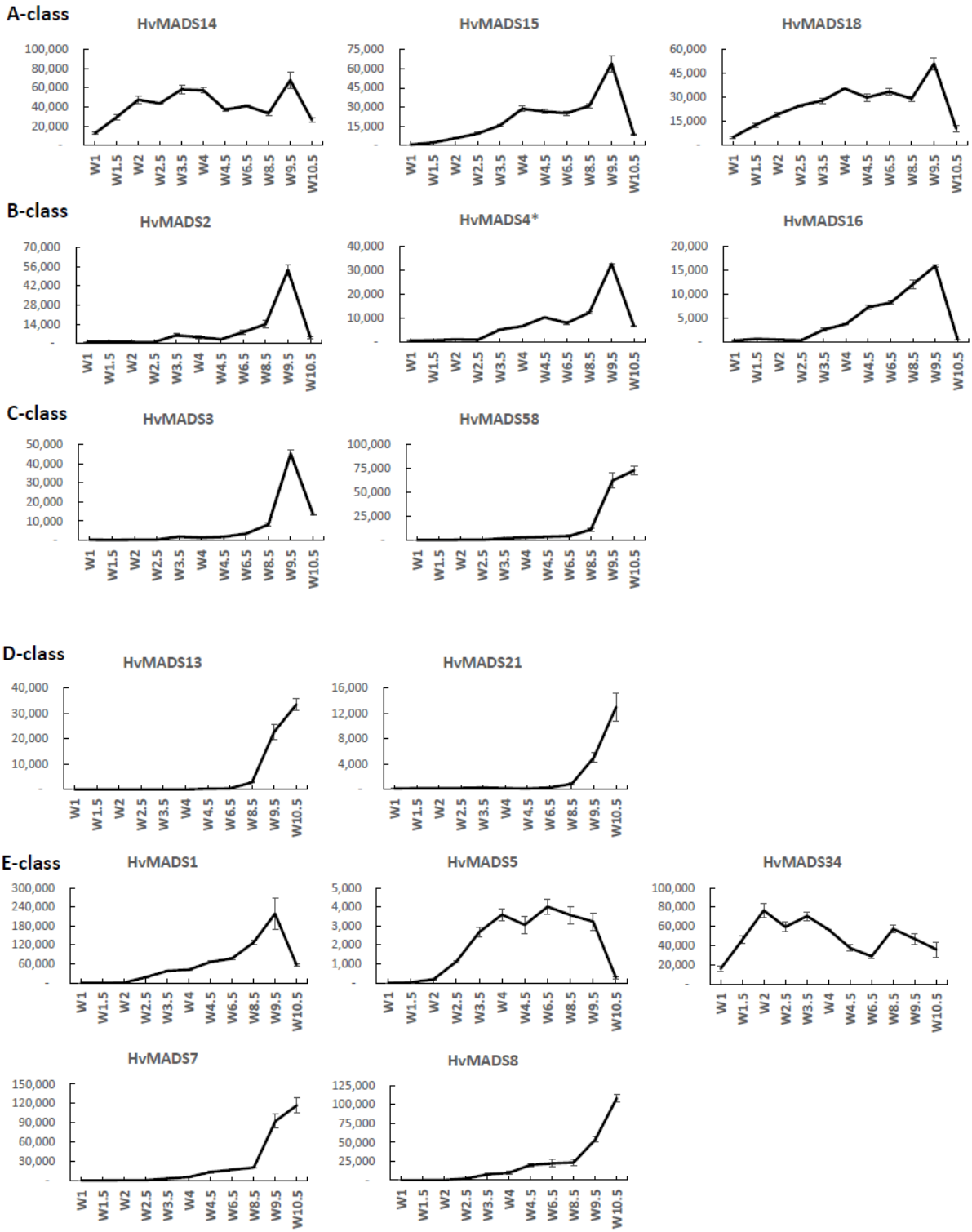

Figure 4: Expression profile of A, B, C, D and E-class MIKCc MADS-box genes in the shoot apical meristem through inflorescence development as measured by the Waddington stage in Golden Promise. Error bars are one standard deviation, based on technical replicates. **A-class**: The canonical A-class function in the outer floral organs shows expression starts after W3, where the lemma primordium is first formed. However expression of all three A-class genes increases earlier, at the floral transition W1. **B-class**: The expression of B-class genes starts to increase at W3.5, where the stamen primordia are formed, and peaks right before pollination. **C-class**: *MADS3* and *MADS58* both start expression around W3.5 when

the stamen primordia appear, however *MADS3* peaks before pollination and declines quickly afterwards, while *MADS58* maintains peak expression through to W10. **D-class**: *MADS13* and *MADS21* both start significant expression only after W6.5, well after the pistil primordium is formed, which first appears at W4. Their peak expression is after pollination. **E-class:** There is a clear difference between the LOFSEP genes *MADS1*, *MADS5*, *MADS34* that express earlier and sharply drop at pollination (W10) and *MADS7* and *MADS8* expression, which starts later around W3.5 and continues to rise through pollination.

Figure 5: Expression profile of the non-ABCDE MIKCc MADS-box genes through inflorescence development by Waddington stage in Golden Promise. Error bars are one standard deviation, based on technical replicates.

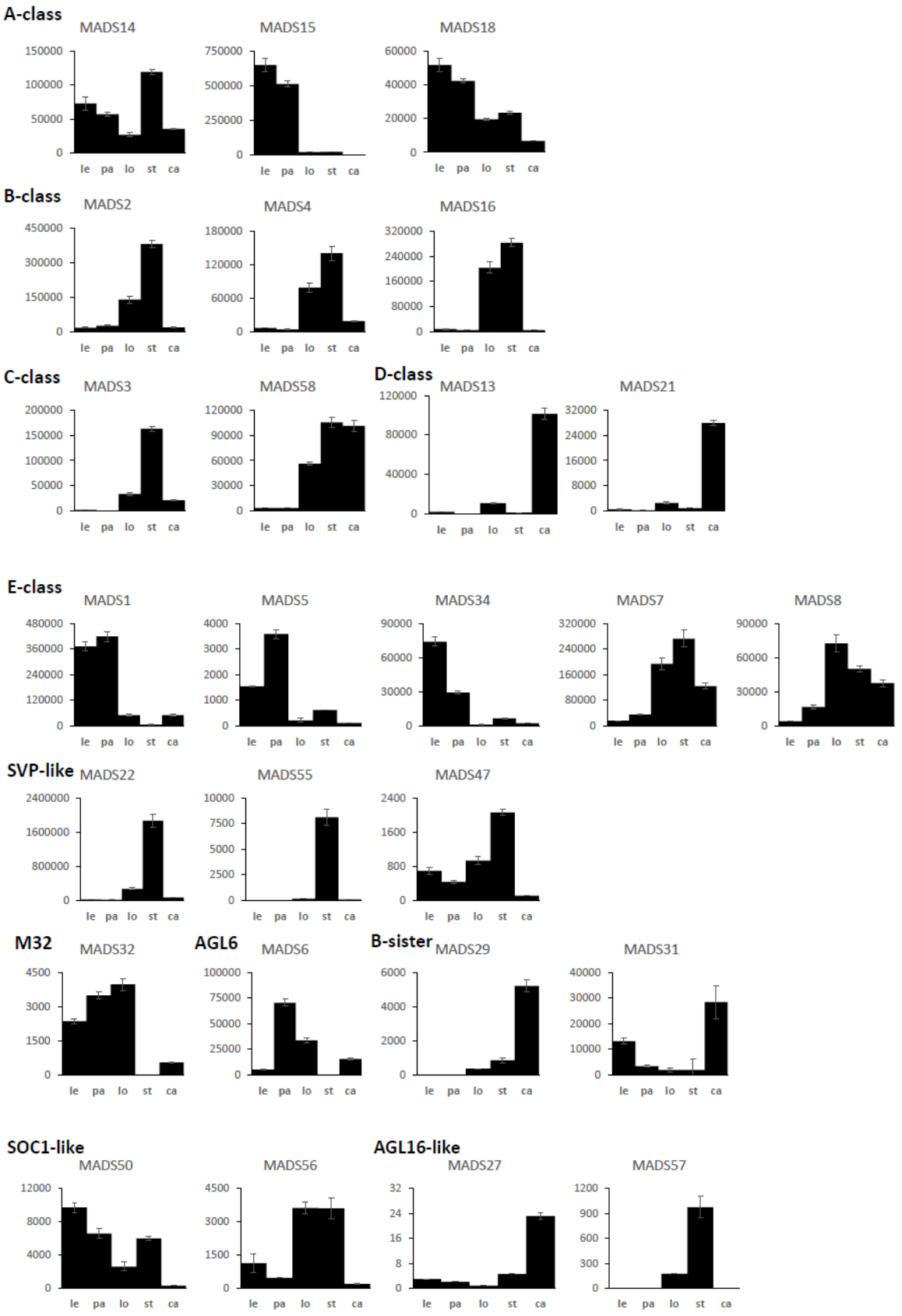

Figure 6: MIKCc MADS-box gene expression in floral organs at Waddington stage 9.5. Le: lemma, pa: palea, lo: lodicules, st: stamens, ca: carpel. Error bars are one standard deviation, based on technical replicates.

MIKCc genes with low inflorescence expression

There was no significant expression detected for several AGL16-like genes in inflorescence samples. *MADS23a* and all four *MADS25* co-orthologs are probably not expressed during the stages of inflorescence development examined here. Global expression analyses indicated that these transcripts are more prevalent in embryo, leaf and root tissue (Figure 3). Of the *AGL17*-like genes that did have measurable expression, *MADS23b*, *MADS27* and *MADS57*, the low abundance and erratic profiles preclude any meaningful speculation on their function (Figure 5). The *MADS14a* pseudogene did seem to be expressed based on primer pair tests at various temperatures, but could never be sufficiently separated from the very similar and much more abundant *MADS14* transcript to provide a clear expression profile (data not shown). The final missing profile is that of *MADS30*, a B-sister gene.

Co-expression profiles reveal a novel regulatory network among MADS-box genes in barley developing inflorescences

Correlation analysis of the expression profiles of all MIKCc MADS-box genes reveals three sets, and a less cohesive pseudoset (Figure 7; Supplemental figure 1). Correlation set 1 is expressed mostly at W1 and W1.5, during the floral transition, and quickly disappears after this stage (Figure 8). Secondly, the pseudoset is spread out over the whole time course, but has some members with high expression between W1.5 and W3.5 where none of the other sets show strong expression. This is the window for spikelet- and floret meristem initiation and development. Then follows correlation set 2, which starts at W3 and stops after W9.5, which is the timeframe where most floral organs develop. Finally correlation set 3 starts expression the latest, and generally has maximum expression at W10.5, after pollination (Figure 8).

Set 1: floral transition

The first set consists of three SVP-like genes, *MADS22*, *MADS47* and *MADS55*. The expression at W1 starts high and quickly declines to a minimum at W2.5. Remarkably, the expression of *MADS22* is up-regulated again after W2.5 and peaks at W9.5 (Figures 5, 8). As the members of this set are already a class within the MIKCc genes, it is likely they redundantly repress floral development.

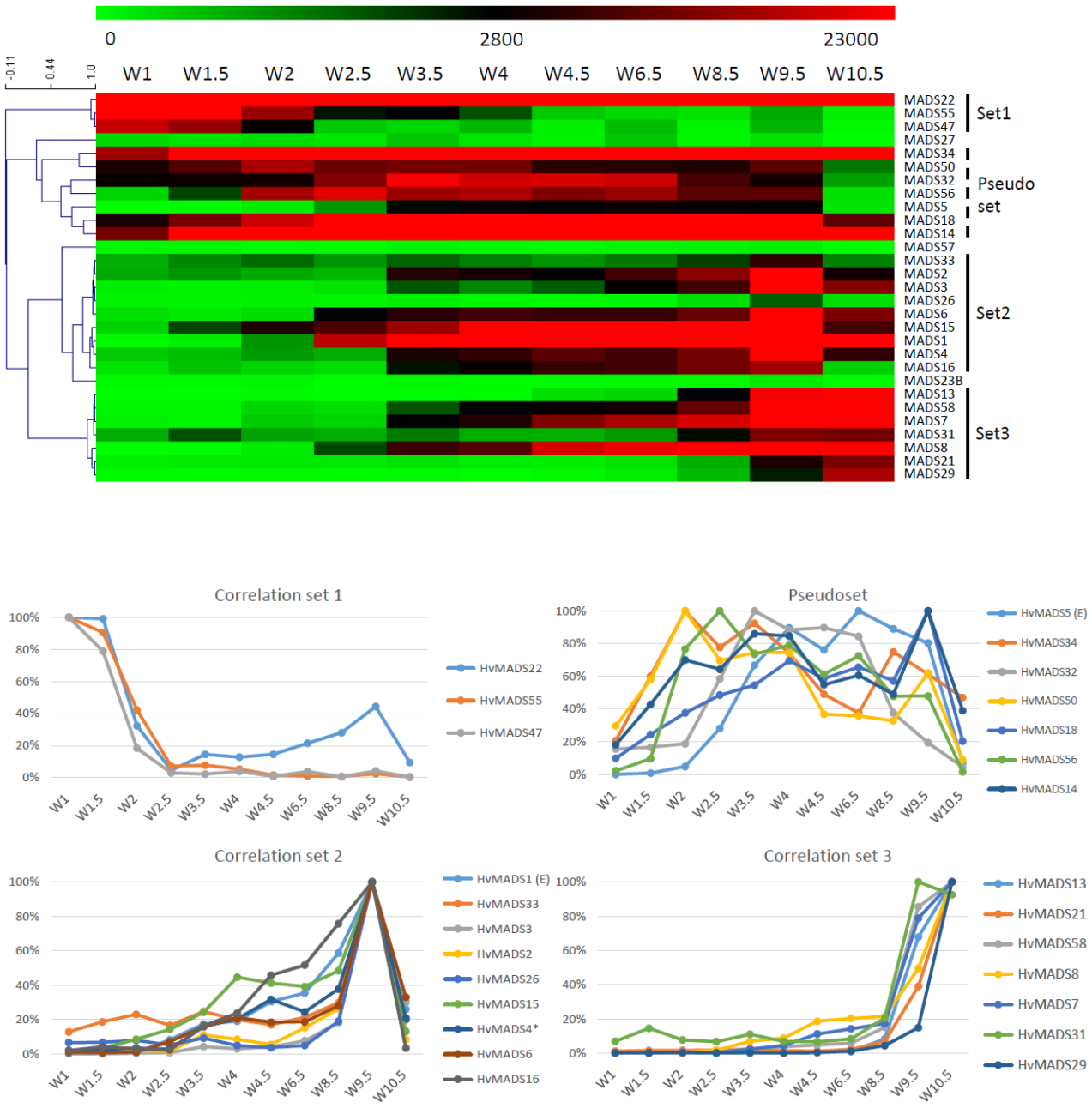

Figure 7: A) Pearson correlation of time course expression reveals 3 sets and a pseudoset. Expression is represented on a logarithmic colour scale. Correlation tree and scale bar are presented on the left side. B) Relative expression profiles through inflorescence development of the MADS-box genes within each correlation set.

Pseudoset: possibly involved in spikelet- and floret meristem

The expression of the genes in the pseudoset is not as closely correlated as the members of the other sets, but a general pattern can still be distinguished. Expression mostly rises between the floral transition (W1) and the emergence of the floral organs (W3-W4) and for some the maximum expression is also in this early timeframe. The E-class genes in the

pseudoset are LOFSEP genes *MADS5* and *MADS34*. *MADS34* really stands out from the other E-class genes with a very early high level of expression peaking at W2. *SUPRESSOR OF OVEREXPRESSION OF CONSTANS* (*SOC1*) like genes *MADS50* and *MADS56* are both expressed early in barley inflorescence development with a maximum at W2 and W2.5 respectively and have a steep decline after W4. The early expression of the members of the pseudoset indicate a function in floral development prior to the formation of the floral organs, such as a role in the spikelet- or floret meristem. The correlation of early expression of *MADS14*, *MADS34* and *MADS50* suggests the possibility of related functions (Figure 8A).

Set 2: lemma, palea, lodicule and stamen development

Correlation set 2 is not as uniform as set 1 and set 3. The expression in general is initiated around W3 to W3.5, increases to a maximum right before anthesis at W9.5 and quickly diminishes right after pollination at W10.5.

All three A-class genes are strongly expressed in the lemma and palea, although the expression of *MADS14* and *MADS18* starts significantly earlier. Three E-class genes from the LOFSEP subclade, *MADS1*, *MADS5* and *MADS34*, are strongly expressed in the lemma and palea, and hardly at all in the lodicule, stamen and carpel (Figure 6). Of these, only *MADS1* appears in correlation set 2. The strongest difference in expression between the lemma and palea is for *MADS6*, which is expressed in the palea, but hardly in the lemma. In general this indicates A- and E-class genes are expressed in the first whorl, which is consistent with the ABCDE model in other plants.

Of the A-class genes *MADS14* and *MADS18* are expressed in the lodicules. All three B-class and both C-class genes *MADS3* and *MADS58* are also expressed in the lodicules whilst the SEP3 subclade of the E-class genes, *MADS7* and *MADS8*, are also strongly expressed here. *MADS32* is expressed in the lodicules, but its expression profile in the pseudoset is not similar to that of set 2 members, most notably its early sharp decline after W6.5. Finally, *MADS6* is expessed in the lodicules. Canonically the second whorl has A-, B- and E-class gene expression so the C-class expression in barley lodicules is very unexpected, and clashes strongly with the ABCDE model.

The A-class genes *MADS14* and *MADS18* are both expressed in the stamens, for *MADS14* it is the highest expression in any floral organ. All three B-class genes and both C-class genes,

MADS3 and *MADS58* are expressed in this organ, the E-class genes *MADS7* and *MADS8* are expressed here too, while the LOFSEP genes are only marginally expressed. Surprisingly, the highest expressed MIKCc gene in the stamens is *MADS22*, an SVP-like gene from correlation set 1. Ignoring the *MADS22* expression before W2.5, the expression profile thereafter is very similar to that of correlation set 2, for *MADS16* in particular (Figure 8C). The expected B-, C-, and E-class expression for the third whorl is present in barley stamens, but the addition of A-class expression and *MADS22* is unexpected.

Set 3: Carpel and ovule development

Correlation set 3 contains the canonical members of a carpel and an ovule quartet: C-, D- and E-class genes. Additionally, the expression of set 3 genes peaks past pollination at W10.5. *MADS58*, a C-class gene that is a part of correlation set 3, shows strong expression in the carpel, while the other C-class gene *MADS3*, a member of set 2, is only marginally expressed (Figure 6). The expression of D-class genes *MADS13* and *MADS21* starts late, even compared to other set 3 members, after W6.5, and expression of these D-class genes is found almost exclusively in the carpel samples. *MADS7* and *MADS8* are expressed late in floret development and the final two genes in correlation set 3 are the B-sister genes *MADS29* and *MADS31*.

MADS2 and *MADS4* are covered by neighbouring kinase transcripts

The *HvMADS4* (HORVU1Hr1G063620) gene is covered completely by the transcript of the neighbouring gene on the opposite DNA strand, HORVU1Hr1G063610, a serine/threonine protein kinase. The two genes are positioned next to each other on chromosome H1 but the transcription of HORVU1Hr1G063610 continues far beyond its last exon. As a result any primer pair that targets *MADS4* will also amplify this protein kinase transcript. To circumvent this problem we designed a primer pair at the end of the *MADS4* transcript, and an alternative reverse primer just outside of the *MADS4* transcript. Subtracting the signal of the latter pair from the former provides a more accurate representation of the expression level of *MADS4* only, which is designated *MADS4** here.

A similar problem occurs with *MADS2* where the gene is also transcribed from the opposite direction by a neighbouring kinase, HORVU3Hr1G090990. In this case however, the kinase

expression was so low compared to the *MADS2* expression that trying to subtract it did not increase accuracy significantly.

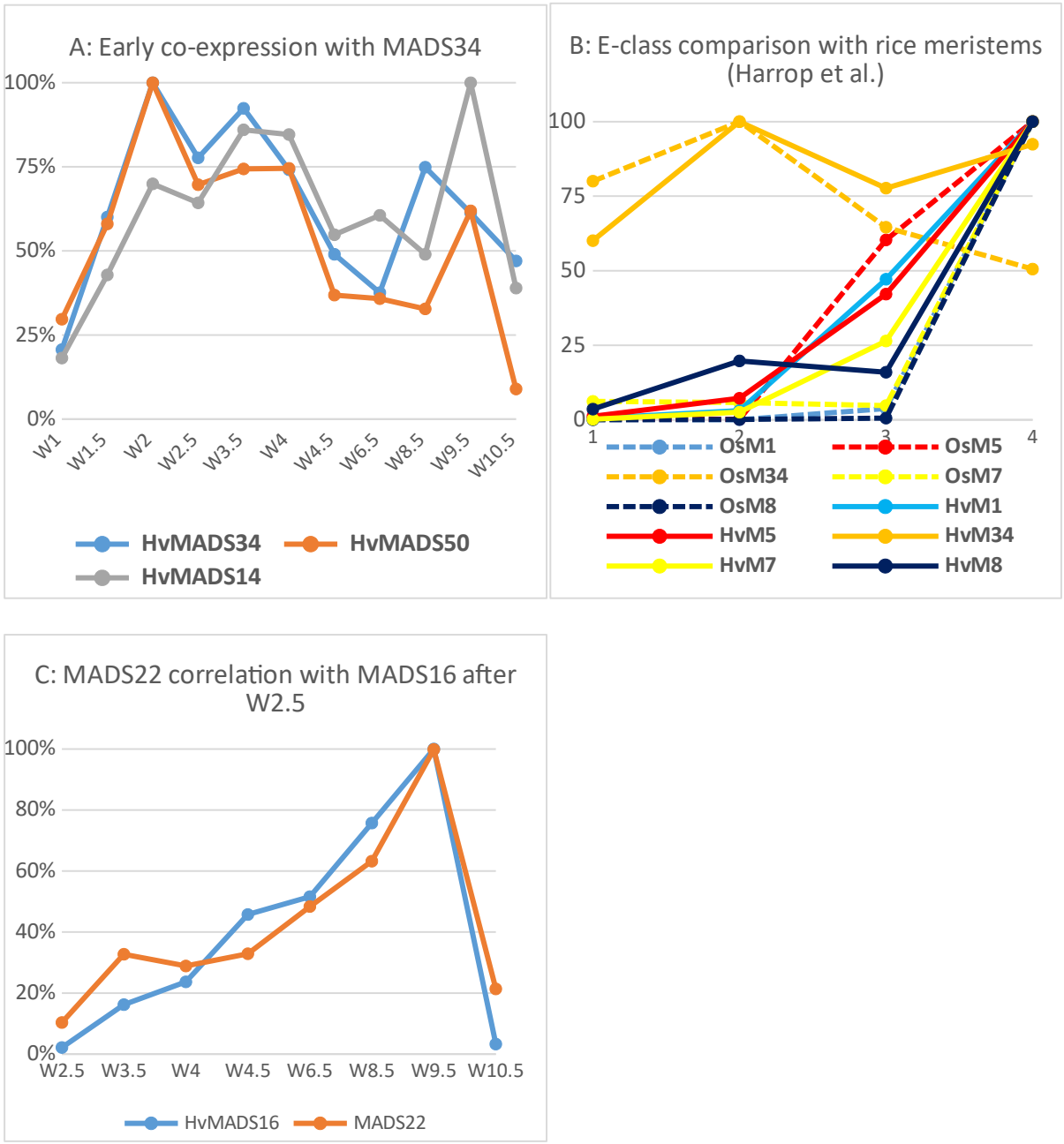

Figure 8: A) Early co-expression of *HvMADS34* with *HvMADS14* (A-class) and *HvMADS50* (*SOC1*-like). B) Comparison of early E-class gene expression in barley and rice. Analysis of the differential gene expression in the inflorescence meristem types of rice using laser microdissection followed by RNA sequencing (dashed lines) from the supplemental data of Harrop et al. (Harrop et al., 2016). While directly comparing the results of their work with expression in the early stages of the whole barley inflorescence meristem is a false equivalency, it can still provide some insights. The best matching Waddington stages W1.5 – W3.5 expression data is shown (solid lines; this thesis) C) Correlation of the relative expression of *HvMADS22* and *HvMADS16* between W2.5 and W10.5.

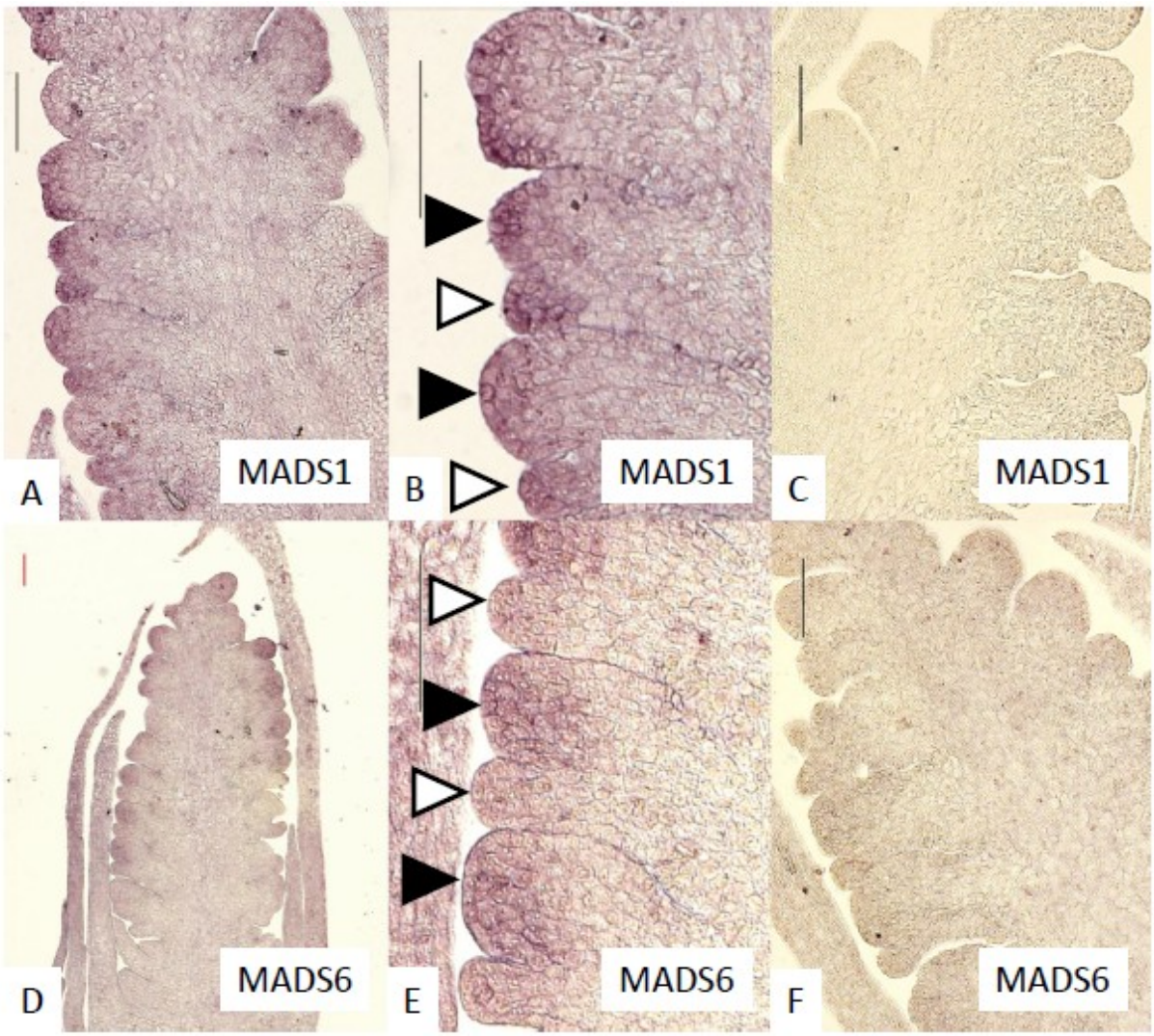

Figure 9: *In situ* hybridisation of *MADS1* and *MADS6* probes to sections of the barley inflorescence at W3. *MADS1* is expressed in the floret meristem (black arrowheads) and the lemma primordeum (white arrowheads) (A, B), but *MADS6* is more strongly expressed in the floret meristem (D, E). C and F are the sense probe controls. Scale bars: 100µm.

2.4 Discussion

Strong conservation of the MIKCc MADS-box genes in barley suggests floral organogenesis is regulated by the ABCDE model

Assesment of the SNP data shows that the MIKCc MADS-box family in barley is highly conserved, indicating random mutations are selected out consistently. The consistency in the number of genes in each class and the mostly matching homology of MIKCc genes between barley, rice, sorghum and *Brachypodium* (Figure 2) suggests that the determination of floral organs, a process dominated by the MIKCc family, is probably conserved as well. This is also reflected in the similar floral organ development among these grasses. The ABCDE model has been extrapolated to rice, maize and wheat before (Ciaffi et al., 2011), and the morphological and genetic conservation suggests it may apply to barley as well. While the MIKCc genes are highly conserved, variation in their expression profile can provide a more detailed look at the robustness of the ABCDE model in barley.

Expression profiling supports the ABCDE model in barley

Grouping MIKCc MADS-box genes using a temporal expression profile in the developing inflorescence has its drawbacks. Many shoot apical meristem samples contain spikelets and florets at multiple stages, with younger meristems near the top (Supplemental figure 2). Additionally, many of the ABCDE proteins are predicted to participate in multiple floral quartets, or even have roles before the floral organs are initiated, like some A-class and E-class genes, which also complicates expression profiles. However, these expression profiles can still be divided into 4 distinct groups mathematically (Figure 7; Supplemental figure 1). The expression profile for each gene, combined with expression data from individual floral organs, gives a clear indication of whether they conform to their expected roles within the ABCDE model, as found for homologs in rice, wheat and other plant species. Also indicated is whether their expression profile is not as expected which may hint at subfunctionalisation, neofunctionalisation or new interactions that warrant further investigation.

The inflorescence meristem expression profiles and floral organ expression of the barley MIKCc MADS-box genes show that at least some members of all canonical classes that participate in the floral quartets according to the ABCDE model are expressed at the right

time, in the right floral organs during barley inflorescence development. However, there are several strong deviations in the expression pattern of some ABCDE genes, indicating neofunctionalisation, as well as some genes conventionally outside of the ABCDE classes that may contribute to the ABCDE functions.

SVP-like MIKCc genes likely act as floral inhibitors

The high start and quick decline of *MADS22*, *MADS47* and *MADS55* expression is in accordance with previous results of RNA sequencing of barley early inflorescence meristems (Digel et al., 2015) (Supplemental figure 1) and is similar to qRT-PCR results by Trevaskis et al. (2007). In rice the same pattern can be observed through the progression of meristem types, where *OsMADS22* and *OsMADS55* expression is high in the inflorescence meristem, lower in the branch meristem and at a minimum in the spikelet meristem (Harrop et al., 2016). In the inflorescence of *Setaria viridis*, a member of the Panicoideae (e.g. maize and sorghum) again the same decline in early inflorescence development is observed (Zhu et al., 2018). In barley the expression of *MADS22* peaks again at W9.5, and this re-emergence later in floret development is only mirrored in wheat (Feng et al., 2017); (Supplemental figure 1B). *MADS22* (*BM10*) and *MADS47* (*BM1*) act as floral inhibitors and can cause partial or full floral reversion when ectopically expressed (Trevaskis et al., 2007). The expression profile of *MADS22*, *MADS47* and *MADS55* fits the function as floral inhibitors well, except for the resurgence of *MADS22* expression.

ABCDE MIKCc genes expressed before floral organ initiation may function in branch- spikelet- and floret meristems

A-class genes in barley are likely to perform A-class functions in floral organ determination (see below), however *MADS14* (*VRN1*) has an additional role in the vernalisation response and probably in establishing and maintaining inflorescence meristem identity in barley (Trevaskis et al., 2007). The early expression of *MADS18*, along with the decline at W4.5, is less pronounced than for *MADS14*, but still recognisable, indicating a potentially weaker redundant role in establishing and maintaining inflorescence meristem identity. *MADS15* is part of correlation set 2, and is therefore more likely to perform an A-class function

exclusively. A similar divide is present in wheat, where *MADS14* and *MADS18* co-homologs have reduced expression after W4, while *MADS15* co-homologs do not (Feng et al., 2017).

Mutants in rice show that *OsMADS34* is involved in inflorescence branching (Gao et al., 2010; Kobayashi et al., 2010) and unsurprisingly *OsMADS34* is highly expressed in the inflorescence branch meristem of rice (Harrop et al., 2016). When comparing E-class gene expression in the early inflorescence meristem between barley and rice, the early peak of *MADS34* expression is conserved (Figure 8b) even though the barley inflorescence doesn't branch, and no transient inflorescence branch meristem has been reported. No other E-class gene (nor *MADS6*) could provide redundancy for a potential *MADS34* function around stage W2, because their expression starts later in inflorescence development. We can only speculate that the early *MADS34* expression is merely a vestigial remnant from the ancestral inflorescence, which did have a branched morphology (Remizowa et al., 2013). The idea that the *Triticeae* spikes merely suppress inflorescence branching is given credence by the branching phenotype of a *COMPOSITUM2* mutant in barley and the tetraploid 'miracle wheat' (Poursarebani et al., 2015), which shows that most of the components for a branching inflorescence are still present in some *Triticeae*.

SOC1 is a floral promotor, and its protein can interact with A- and E-class proteins in *Arabidopsis* (Smaczniak et al., 2012). *SOC1*-like genes *MADS50* and *MADS56* are both part of the pseudoset. During early inflorescence development *MADS14*, *MADS50* and *MADS34* expression are highly correlated (Figure 9), suggesting a hypothetical branching meristem quartet in barley would include these genes.

A- and LOFSEP E-class expression dominate in the lemma and palea

The ABCDE model states the first floral whorl is defined by A- and E-class genes (Theissen and Saedler, 2001). However, whether the palea and lemma are true first whorl floral organs in grasses is still debated (reviewed by (Ciaffi et al., 2011)).

E-class: Since *MADS7* and *MADS8* are not expressed in the lemma and palea, the E-class role is likely performed by the LOFSEP genes. The quadruple knockdown of *OsMADS1/5/7/8* (leaving *OsMADS34* as the only remaining E-class gene) transforms all floral organs in the rice floret into leaf like structures, except for the lemma (Cui et al., 2010).

As *MADS34* is more strongly expressed in the lemma in barley, this may be the only floral organ where *MADS34* acts in an E-class role.

MADS32*: MADS32*, the only member of a MIKCc class unique to grasses, is not part of set 2, because it reaches its zenith at W3.5 and starts decreasing earlier than set 2 transcripts, after W6.5. So while its expression in the lemma and palea makes it likely to be a member of the lemma and palea floral quartet, its unique expression profile does not match the other members of the quartet.

AGL6: The lemma and palea are often considered collectively as the first floral whorl, but their morphology (and possibly their origin) is different. The strongest difference in expression between the lemma and palea is for *MADS6*, which is expressed in the palea, but hardly in the lemma (Figure 9). While not technically an E-class gene, *MADS6* has been reported to fulfil an E-class function (reviewed by Dreni and Zhang (2016)). In *mads6* barley inflorescences, a comparison between the palea and lemma morphology could shed light on the extent that *MADS6* is responsible for the phenotypic divide.

The lemma and palea floral quartets in barley are probably composed of A-class and LOFSEP E-class proteins, in accordance with the ABCDE model (Figure 11). In the palea *MADS6* is likely to play an E-class role in the floral quartet, possibly resulting in the morpological differences between the lemma and palea in barley.

Lodicules contain predicted A-, B, and (SEP3) E-class expression but suprising C-class expression

The second floret whorl in grasses is the lodicule, generally considered the equivalent of the eudicot petal. The second whorl is canonically determined by a floral quartet consisting of one A-class, two B-class and one E-class protein. Because of their relatively small size, compared to the other floral organs, the expression of genes in the lodicules is likely to have only a marginal effect on the expression profile of the whole inflorescence meristem.

A-class: *MADS15* is the only barley A-class gene not expressed in the lodicules. This is in contrast to *OsMADS15* which is expressed in the lodicules of rice (Kyozuka et al., 2000). The wheat *MADS15* ortholog *TaAP1-3* is expressed at an intermediate level (Paollacci et al., 2007).

B-class: All three B-class genes are expressed in the lodicules, in accordance with the ABCDE model. The two B-class proteins in the second whorl floral quartet canonically come in the form of a heterodimer of an AP3/DEF subclade member, for which *MADS16* is the only choice in barley, and a PI/GLO subclade member, which could be either *MADS2* or *MADS4* in barley. The conservation of this B-class function and mechanism in grasses is shown by the homeotic conversion of lodicules into whorl 1 like bracts in mutants of AP3/DEF subclade members *OsMADS16*/*SUPERWOMAN1* in rice (Nagasawa et al., 2003) and *SILKY* in maize (Ambrose et al., 2000). The role of *OsMADS2* and *OsMADS4* as redundant PI/GLO seems clear from the *spw1*-like phenotype (homeotic conversion of stamens to carpels) of the double knockout line (Yao et al., 2008), however the relative importance in the lodicule is not entirely resolved (discussed by Ciaffi et al. (2011)).

C-class: In barley both C-class genes *MADS3* and *MADS58* are expressed in the lodicules. The C-class orthologs in maize (*ZAG1*, *ZmM2* and *ZmM23*) and wheat (*TaAG-1* and *TaAG-2*) are not expressed in lodicules, but *TaAG3* is (Mena et al., 1996; Paollacci et al., 2007)). In Brachypodium *BdMADS18* (C-class) is expressed in the lodicules (Wei et al., 2014).

E-class: The strong expression of E-class genes MADS7 and MADS8 in the lodicules makes them the likely candidates for the E-class role in the lodicule defining floral quartet in barley. The same expression profile is shown by the rice homologs OsMADS7 and OsMADS8, which are strongly expressed in the lodicules. Furthermore, the *Osmads7/8* double mutant shows abberant lodicules (Cui et al., 2010) indicating the LOFSEP E-class genes do not redundantly cover this function. A *mads7/mads8* double mutant could confirm this role in barley, while *mads7* or *mads8* single mutants are unlikely to have a clear phenotype, because of the high similarity in expresion pattern and reported redundancy in related species (Cui et al., 2010).

MADS32: *MADS32* is expressed in the lodicules, but its expression profile in the pseudoset is not similar to that of other potential members of the lodicule quartet, most notably its early sharp decline after W6.5. So while it is expressed in the lodicule, this would point to a function independent of the strict ABCDE model, since floral quartets generally persist throughout the lifespan of a floral organ. However, in rice the *osmads32* mutants do show some homeotic conversion of the lodicules (Sang et al., 2012) and a disrupted protein interaction with *OsMADS2* and *OsMADS4* is likely to be responsible for at least part of the *OsMADS32* function (Wang et al., 2015). Therefore, *MADS32* could have a function in

lodicule determination and potentially be part of a lodicule quartet, but only in the early stages.

AGL6: *MADS6* expression in the lodicules indicates a redundant function with *MADS7* and *MADS8*. In rice the *osmads7/8* mutant did not show full homeotic conversion of the lodicules (Cui et al., 2010), which means the floral quartet is still partially functional. Since the other E-class genes *MADS1*, *MADS5* and *MADS34* are not expressed in the lodicules, *MADS6* is the most closely related gene to potentially take this role. In maize, the *MADS6* homolog *ZAG3* is also expressed in the lodicules (Thompson et al., 2009).

In summary this shows that the expected MIKCc classes are represented in the barley lodicules: A-class *MADS14* and *MADS18* (but not *MADS15*), all B-class genes and the SEP3-like *MADS7* and *MADS8* as the E-class representatives (Figure 11). Additionally, *MADS6* could provide partial redundancy for the E-class function, whilst *MADS32* has only an early function, if at all.

Stamens have expected B-, C- and (SEP3) E-class expression, but surprising A-class and *MADS22* expression

The third floral whorl that forms the stamens in dicots as well as grasses, is usually determined by a floral quartet which contains two B-class proteins (an AP3/DEF and PI/GLO heterodimer), a C-class protein and an E-class protein.

A-class: The A-class genes *MADS14* and *MADS18* are both expressed in the stamens, for *MADS14* it is the highest expression in any floral organ. The wheat homolog TaAP1-1 is expressed in all floral organs (Paollacci et al., 2007). In rice *OsMADS14* and *OsMADS18* are expressed in the stamens, but *OsMADS14* is the main actor in stamen identity (Wu et al., 2017).

B-class: All three B-class genes are expressed in the stamens. The same is true for rice, where a knockdown of either *OsMADS16* or both *OsMADS2* and *OsMADS4* results in homeotic conversion of the stamens into carpel-like organs (Yao et al., 2008). Since the *MADS2* and *MADS4* genes have a covering transcript from kinase genes that are similar to each other, and this arrangement of genes is the same in rice, there may be a conserved regulatory relation. *MADS2* and *MADS4* expression could be negatively impacted by these kinase transcripts in grasses, however their low expression in the inflorescence suggests this

effect is not strong during barley inflorescence development. Remarkably, all of the 20 SNPs found around *MADS2* occur inbetween *MADS2* and HORVU3Hr1G090990, suggesting some adaptive changes to this relationship may have occurred with selection.

C-class: Both C-class genes, *MADS3* and *MADS58* are strongly expressed in the stamens, similar to their counterparts in rice. In rice *OsMADS3* plays a more crucial role in stamen identity (Yamaguchi et al., 2006), but without available mutants the relative importance of C-class genes in barley is still uncertain.

E-class: In line with their likely role as E-class genes for the inner floral organs, *MADS7* and *MADS8* are expressed in the stamens, where the LOFSEP genes are only marginally expressed. The homologous genes in wheat, *TaSEP4* and *TaSEP3* respectively, are also predominantly expressed in the inner floral organs (Paollacci et al., 2007). In rice *OsMADS7/8* double knockdown plants the stamens were affected, but not completely abolished as in the *OsMADS1/5/7/8* quadruple knockdown lines, so *OsMADS7* and *OsMADS8* have a primary E-class function in the stamens, but not an exclusive one (Cui et al., 2010).

MADS22: Surprisingly, the most highly expressed MIKCc gene in the stamens is *MADS22*, an SVP-like gene from correlation set 1, which normally functions as a floral repressor. Ignoring the *MADS22* expression before W2.5, the expression profile thereafter is very similar to that of correlation set 2 and *MADS16* in particular (Figure 8C). The start of this increase in expression after W2.5 is visible from the early expression data of Digel et al. (2015) (Supplemental figure 1). In *Brachypodium* the *MADS22* homolog *BdMADS30* is also strongly expressed in the stamens (Wei et al., 2014). In the *MADS22* promoter, within 1kb of the start of the gene there are 12 SNPs of varying rarity. Three of these, 529572337T, 529572349T and 529572362A commonly occur together and correspond to the barley variety *Hybernum viborg*, a winter barley grown in many parts of the world. Investigating expression and phenotypic differences correlated with these SNPs may provide insight in the *MADS22* role.

In conclusion the canonical members of the third whorl floral quartet are expressed in barley stamens: *MADS16* (AP3/DEF B-class), *MADS2* or *MADS4* (PI/GLO B-class), *MADS3* or *MADS58* (C-class) and *MADS7* or *MADS8* (E-class). However the A-class genes *MADS14* and *MADS18* also show significant expression and the most highly expressed MIKCc gene is *MADS22*, an SVP-like MADS-box gene (Figure 11). While the expression profiles for

MADS14 and *MADS18* do not reveal meaningful co-expression, *MADS22* expression after W2.5 is very similar to other probable stamen quartet members (Figure 8C), suggesting the unlikely neofunctionalisation of a floral repressor into a potential member of the stamen-determining floral quartet.

C-, D, (SEP3) E-class and B-sister genes are expressed in the carpel and ovule

In the ABCDE model in *Arabidopsis*, carpel fate is induced by a quartet of two C- and two E-class genes, while the ovule quartet contains a C-, two D- and one E-class gene (Theissen et al., 2016). The floral meristem determinacy (FMD) is likely to be regulated by the remnant of the floret meristem, located within the carpel samples.

C-class: *MADS58*, a C-class gene that is part of correlation set 3, shows strong expression in the carpel, while the other C-class gene *MADS3*, a member of set 2, is only marginally expressed (Figure 4). The strong carpel expression of the C-class gene *MADS58*, in contrast to the marginal *MADS3* expression is a sign of subfunctionalisation among the C-class genes where the C-class role in carpel development is fulfilled primarily by *MADS58*. The wheat homolog of *MADS3*, *TaAG-2*, is also predominantly expressed in the stamens, compared to the carpel (Paollacci et al., 2007). An *osmads58* mutant in rice develops abnormal carpels, while the *osmads3* carpel develops almost completely normally, showing that *OsMADS58* is the primary C-class gene for carpel development (Yamaguchi et al., 2006).

D-class: The late expression of D-class genes *MADS13* and *MADS21* is consistent with a potential role in ovule development, which is the last part of the floret to initiate. Indeed expression of these D-class genes is found almost exclusively in the carpel samples (collected at W9.5), which contain the developing ovule.

E-class: *MADS7* and *MADS8*, E-class genes of the SEP3 sub-clade, are expressed late in floret development, as in wheat (Feng et al., 2017) and potentially fulfil the E-class role for the inner floral organs. The division in floral organs is striking, where the LOFSEP genes are expressed in the palea and lemma and the SEP3-like genes are dominant in the lodicules, stamens and carpel. For *MADS8* (*BM9*) this boundary at the lodicule has also been shown by *in situ* hybridisation, however it also shows *MADS1* (*BM7*) expression in the developing ovule (Schmitz et al., 2000). While at W9.5 there is a little expression of *MADS1* in the carpel samples, most of the *MADS1* expression disappears after pollination. This leads to the

conclusion that *MADS7* and *MADS8*, as members of set 3, are part of the carpel and ovule quartets, and *MADS1* may have a function during ovule development or FMD.

B-sister: The final two genes in correlation set 3 are the B-sister genes *MADS29* and *MADS31*. *AtABS*, a B-sister gene in *Arabidopsis* has been linked to endothelium development and interaction with *AtSEP3* and D-class genes suggest they may function in an additional floral quartet (Kaufmann et al., 2005). Since the SEP3-like *MADS7* and *MADS8* as well as the D-class genes are present, this same hypothetical additional quartet may be present in barley. Mutant analysis could determine whether the function of this quartet is conserved in barley, although with three B-sister genes, redundancy would necessitate a double or triple knockout line for a definitive phenotype. No expression of the B-sister gene *MADS30* was detected. Based on high similarity, *MADS30* is predicted to have an expression profile similar to the other two B-sister genes, *MADS29* and *MADS31*, though perhaps expression more exclusive to developing seeds, and therefore outside of the sample range of this experiment. *OsMADS30* is not a suitable guide for the function of its homolog in barley because the rice gene has a recent insertion and an altered expression pattern compared to related grass species (Schilling et al., 2015).

Short genes can be expressed more rapidly than long genes, and can be associated with fast dividing cells, particularly in zygotic tissue (Heyn et al, 2015). Gene structure in supplemental figure 5 shows that the B-sister genes, *MADS29*, *MADS30* and *MADS31*, are short and their expression is associated with tissues of the ovule and developing grain. Long genes take longer to express, causing a so called ‘intron delay’ that can be of regulatory significance. Additionally, longer genes with sizable introns are often more highly expressed (Heyn et al, 2015). However there does not seem to be any clear correlation between intron size and frequency of expression for MIKCc genes in barley.

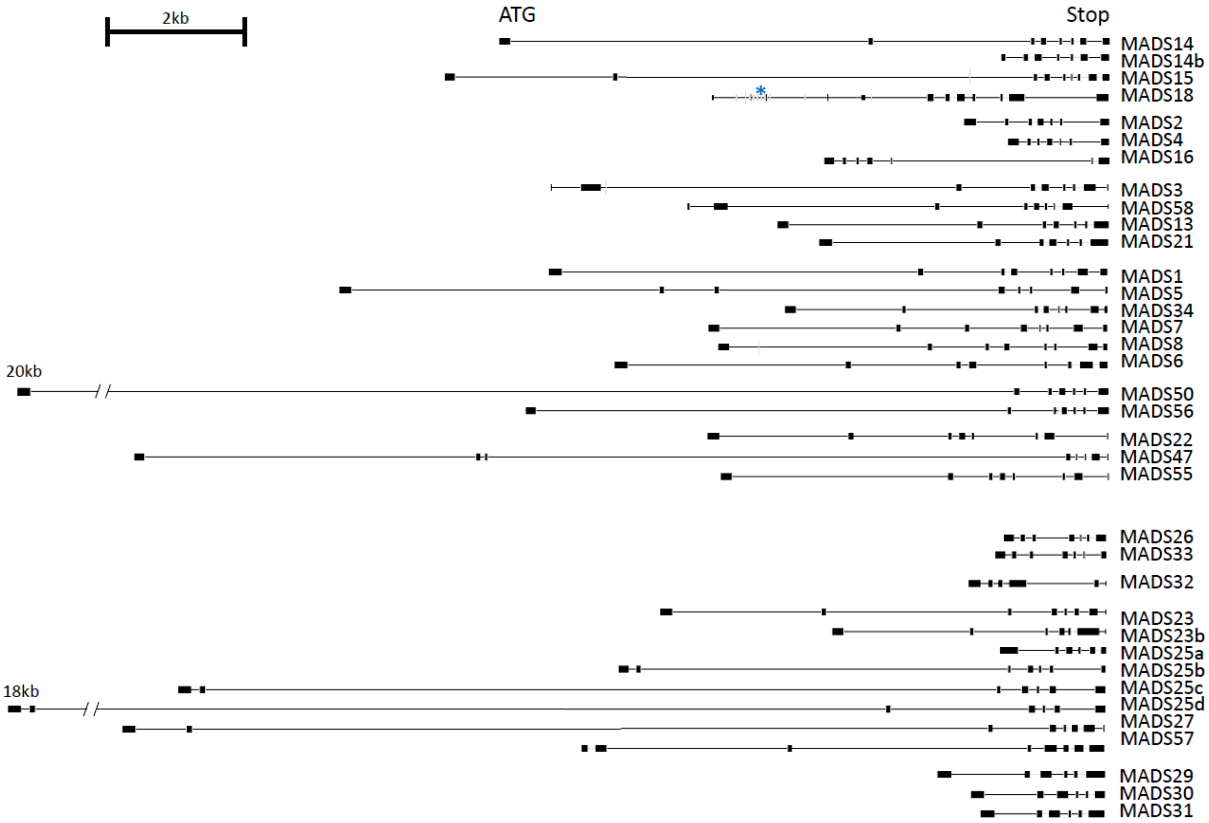

Figure 10: Structure of barley MIKCc MADS-box genes, ordered by class. The scale bar indicates the length on the genome. The star at *MADS18* labels an unresolved region in the gene structure where the genomic sequence is incomplete. For *MADS50* and *MADS25d* the total gene length on the genome is given.

In conclusion, the canonical MIKCc members of the fourth whorl quartet are present in the barley carpel: C-class gene *MADS58* and E-class genes *MADS7* and *MADS8*. The ovule quartet is also represented in the carpel samples: *MADS58* as the C-class gene, both D-class genes (*MADS13* and *MADS21*) and two E-class genes: *MADS7* and *MADS8* (Figure 11). The additional expression of B-sister genes in this correlation set may imply a redundant function in the carpel or the ovule determining quartet, however it is more likely to be related to a function in the endothelium and other ovule and early seed roles. The B-sister proteins in eudicots have been shown to interact with C-, D- and E-class proteins, and the mutant has defects in the endothelium (de Folter et al., 2006).

Correlation pseudoset: branch-, spikelet-, floret meristem

The loosely correlated genes in the pseudoset display early expression in the window between the floral transition and the start of floral organ formation, when the spikelet and

floret meristems are formed. The sudden downturn in expression between W4 and W4.5 that many members of the pseudoset have in common (Figure 7B), coincides with the end of the formation of new spikelet meristems at the awn primordium stage (Alqudah and Schnurbusch, 2014). This indicates that members of this pseudoset could be involved in the determination of some of the meristems of the inflorescence, like the inflorescence-, spikelet- and floret meristems.

Correlation set 2: Lemma, palea, lodicule and stamen determination

Correlation set 2 is not as uniform as set 1 and set 3, and it seems the temporal expression profile alone is not sufficient to distinguish the members of the floral quartets for the lemma/ palea, lodicule and stamen. The expression in general is initiated around W3, where the lemma primordium first appears, and W3.5 when the stamen primordia are initiated. If the progression of whorls is maintained, the palea and lodicule primordia are also formed in this interval, although they are not visible from the outside of the developing floret meristem (Supplemental figure 2). The quick decline in expression right after pollination at W10.5 is consistent with the rapid withering of the stamens and lodicules after they have fulfilled their purpose, and the growth arrest of the palea and lemma. Combined, this means the initiation, growth and decline of the first three floral whorls are timed very similarly, making them difficult to distinguish by their expression profile alone.

Additionally, the ABCDE model predicts that many of these MIKCc genes will have a role in more than one floral quartet. For example, B-class genes are canonically part of both second and third whorl quartets, mixing the expression profiles even more.

The inability to untangle these expression profiles means they all group together in correlation set 2 and the floral organ specific expression data are needed to identify these potential floral quartet members. However, the individual floral organ samples collected near the end of floral development at W9.5 are not nescesarily representative for floral organ initiation and early development. Therefore they will have to be compared back to their temporal expression profiles.

Correlation set 3: Carpel and ovule

Correlation set 3 contains the canonical members of a carpel and an ovule quartet: C-, D- and E-class genes. The late start of expression in this set, generally during or after the initiation of

the carpel primordium at W4, indicates a role in the fourth whorl. Additionally, persistence of expression past pollination at W10.5 also points to the carpel and ovule, which don't wither right after pollination, unlike the stamens.

Whorls 2 and 3 could be delimited not by *MADS58*, but by *MADS32*

The suprising expression of C-class genes *MADS3* and *MADS58* in lodicules is hard to explain. While the lodicules at W9.5 have to be peeled away from the carpel, and it is not unthinkable some carpel tissue was mixed in, the expression of *MADS58* in the lodicules is over half that of the carpel, and cannot be explained by admixture alone. One of the central regulatory mechanisms in the ABCDE model is the antagonistic role of A- and C-class genes. In rice the C-class genes have a role in supressing additional lodicule formation (Yamaguchi et al., 2006) and since maize does not express C-class genes in the lodicules this is potentially unique to barley, *Brachypodium* and wheat. There is nothing radically different in the barley lodicule compared to other grasses. Confirmation by *in situ* hybridisation and follow-up with mutant analysis could shed more light on the implications of this puzzling find.

The separation of expression domains of the A-class and C-class genes, by mutual negative regulation, is one of the core tenets of the ABC model as originally devised in *Arabidopsis*. Here we show that in barley, A-class genes are expressed in the inner floral organs, and C-class transcripts show up in the second whorl floral organs, the lodicules. There is no canonical floral quartet that contains both A- and C-class genes, nor is it clear what floral organ this would give rise to. Clearly the very distinct outer and inner organs in the barley floret are not primarily delimited by an A-C divide. This begs the question what it is that makes the lodicules and stamens develop so differently if A-, B-, C- and E-class genes are expressed in both. If we stay within the confines of MIKCc MADS-box genes in floral quartets, the only likely candidates are *MADS32* and *MADS6*, which are expressed in the lodicules, but not the stamens, and perhaps *MADS22*, which is almost exclusively expressed in the stamen. Interaction between *OsMADS32* and rice B-class genes has been demonstrated, and mutants of *OsMADS32* do show homeotic conversion of the lodicules, but not in the stamens (Wang et al., 2015). This, combined with the early decline in expression of *MADS32* around W6.5, indicates that while *MADS32* is probably part of the answer, there must be another player involved in the lodicule-stamen divide.

Some basal angiosperms have a more gradual transition between their floral organs, which doesn't fit with the ABCDE model which results in discrete floral whorls. This is accompanied by a more gradual change in gene expression in these taxa and is captured in the 'fading borders' model (Buzgo et al., 2004; Soltis et al., 2007), which states that the gradually rising expression of for example C-class genes, and the slowly fading expression of A-class genes results in intermediate floral organs with some characteristics from the adjacent organs. This may be the ancestral angiosperm ABC model, where only later more stringent restrictions on the expression evolved to separate the 2nd and 3rd whorls, resulting in the A-C antagonism in the ABCDE model for eudicots, and perhaps a different solution evolved in grasses, involving *MADS32*.

Adapting the ABCDE model for barley

Overall the ABCDE model for grasses still follows the same basic structure as the model from *Arabidopsis*, the addition of DELLA notwithstanding (Ciaffi et al, 2011). The results presented here show that this generally holds true in barley as well, although there are some deviations. However, when looking at the MIKCc genes outside the ABCDE-classes, the most strongly expressed genes are *MADS22* in the stamens, usually classified as a floral repressor, and *MADS32*, which may be crucial for the discrete border between the outer and inner floral organs (Figure 11).

Because MIKCc proteins function in floral quartets, the next step to gain more insight into the potentially changed roles of these genes should be protein interaction studies. This could test the potential role of *MADS22* in the stamen quartet and *MADS32* or *MADS6* in the lodicule quartet. However, beyond that there are other functions in grass inflorescence development that are regulated by MIKCc genes that may operate in the same cooperative way. So there may be further MIKCc quartets, such as one that regulates the identity of the spikelet or floret meristem. Potential members of such a quartet would be expressed before the floral organ primordia form and are probably composed of members of the pseudoset (Figure 11B).

So far, when discussing the ABCDE model, the floral organs have often been considered indivisible units that either gain the correct identity or are homeotically converted. In the barley stamens, ten different MIKCc genes from five classes are strongly expressed (Figure 11A), which are unlikely to form just one floral quartet. There may be variants of the stamen

quartet that help define specific tissues within the stamens or even complete quartets. Alternatively some of these MIKCc genes may have a function in stamens independent of a floral quartet structure. A somewhat similar tissue specific expression of MIKCc genes has been shown in the ovule of rice (Kubo et al., 2013).

To test the predicted functions of barley MIKCc genes, mutants will be instrumental. However the widespread redundancy among the MADS-box genes is likely to necessitate double and triple mutants to observe a strong phenotype.

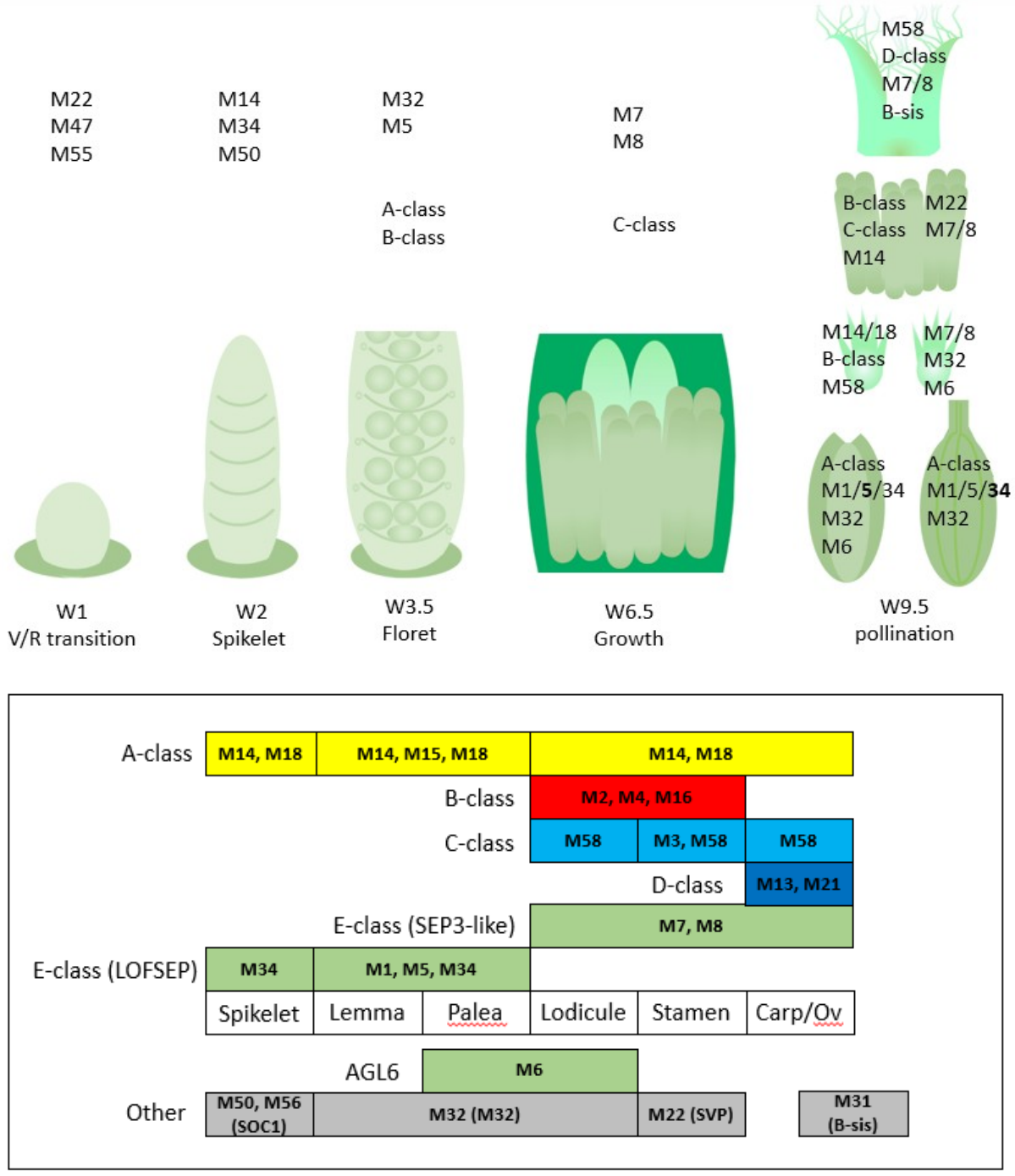

Figure 11: In this figure 'MADS' is abbreviated as 'M'. A) Prominent expression of the MIKCc MADS-box genes through developmental stages (bottom row) and the floral organs of barley (column on the right). B) Schematic of an adapted ABCDE model for barley floral development. Canonical ABCDE genes are depicted above the floral organs where they are expressed, while additional expressed MIKCc genes are shown below. Expression before the start of floral organ primordia initiation is given in the leftmost column, tentatively labelled 'spikelet'.

2.5 Materials and methods

Identification of MIKCc genes

Barley MIKCc MADS-box genes were identified by name and BlastP searches, using rice homologues, in the HORVU dataset (https://webblast.ipk-gatersleben.de/barley_ibsc/downloads/) using the Geneious software version 8.1.3 (Biomatters). Additional genes, and more accurate transcript sequences, were found using an online BlastP search at NCBI (https://blast.ncbi.nlm.nih.gov/Blast.cgi). Where no known transcript sequences were available the FGENESH+ protein-based gene prediction tool (Solovyev V.V. 2007) was used to identify the most likely transcripts. Genes were named after their rice homologs, rather than the previous names used in barley, to standerdise naming and make functional comparisons to other grasses easier (Supplemental table 1).

Phylogenetic analysis

MIKCc MADS-box genes from rice, sorghum and *Brachypodium* were collected from published data (Arora et al., 2007; Wei et al., 2014). Protein sequences were used in a neighbour joining algorithm to construct the tree in Geneious 8.1.3 (Biomatters Ltd) bootstrapping with 1000 replicates.

SNP analysis

A list of barley SNPs was composed using the comprehensive SNP database, recently made accessible at IPK Gatersleben (Milner et al., 2019) (https://bridge.ipk-gatersleben.de/bridge//#snpbrowser, accessed April 2019). Gene locations were found by HORVU number where available, otherwise by position on the chromosome. Exon and amino acid changes were assessed by comparison to an alignment of cDNA sequences and chromosome fragments in Geneious 8.1.3 (Biomatters Ltd). Rice SNPs were collected using the online interface of the SNP database (Mansueto et al., 2017); (http://snp-seek.irri.org/_snp.zul, accessed June 2019).

Meristem sampling

Golden Promise was grown in a growth room with 16h light at 15°C day and 10°C night temperatures, at 70% humidity, in 8cm square pots containing coco-peat standing in closed trays and watered from below every two days. A midday light maximum of 500 µmole photons m^{-2} s^{-1} was used.

Meristem samples were taken from the main stem and examined under a dissecting microscope. Meristems exactly matching the desired Waddington stage were immediately frozen in liquid nitrogen, and stored at -80°C

For the early stages, where the meristem was less than 1mm, as much as 30 meristems were taken per sample. This number gradually decreased to 1 at W9.5, where 5 separate samples were taken, and combined at a later stage, such that each final sample comes from at least 5 individual plants. To capture the changes in expression through pollination one additional stage was introduced, dubbed W10.5, which was taken three days after pollination (Figure 1).

Additionally, floral organ samples were taken at Waddington stage 9.5 from each floral whorl.

RNA extraction

Total RNA extraction was performed with the Qiagen Plant RNA Kit, Ambion Turbo RNA-free Kit, and cDNA synthesis with Superscript III reverse transcriptase (Invitrogen) according to the manufacturer's instructions.

Real-time q-PCR

Primers were designed across the stop codon of each gene; forward in the gene and reverse in the 3'UTR (supplemental table 3). This is not only to avoid problems with sequence similarity between closely related genes, but also because the RNA in this position is less likely to be degraded.

RT-qPCR was performed as described by Burton et al. (2008). The quantity of the cDNA was assessed with four standard genes (*HvGAP*, *HvCyclophilin*, *HvTubulin* and *HvHSP70*) and normalised over the time course and floral organ samples individually using the best matching three. The standard deviation was calculated from three technical replicates.

Expression correlation analysis was done using the Pearson correlation function in MeV4.9 (http://mev.tm4.org).

RNA in situ hybridisation

Meristems were obtained as described, but instead of liquid nitrogen were collected into fixative solution FAA and vacuum infiltrated. Samples were dehydrated in an ethanol series which was subsequently swapped for D-lemonene (HistoChoice, Sigma), and finally paraffin wax (Paramat pastillated, Gurr) at 60°C. Embedded samples were cut into 6-8µm sections on a Leica RM2265 microtome and placed on lysine coated slides.

Dioxigenin labelled probes were made, in sense and antisense configuration, using the DIG labelling kit (Roche Diagnostics), following the manufacturer's instructions. Primers used to generate the probes are listed in supplemental table 3.

Slides were dewaxed in D-lemonene and rehydrated in an ethanol series (2x 100%, 95% ethanol and 85% and 75% ethanol with 0.85%NaCl). The following steps were performed with an InsituPro robot (Invatis): Finalise rehydration, proteinase K digestion, re-dehydration. Re-dehydration was finalised with a reverse of the rehydration steps above, and the slides dried at 37°C. The following steps were also performed with the InsituPro robot: Hybridisation, stringent washes, RNAse digestion, immunolabelling (AntiDIG-APconjugate, Roche) and washing. Substrate (NBT/BCIP, Roche) was added according to the manufacturer's instructions and incubated overnight in the dark. Slides were fixed with ImmunoHistoMount (Sigma-Aldrich), and observed with a Nikon Ni-E optical microscope. Pictures were processed for colour, brightness and contrast in GIMP2.10.2 (www.gimp.org).

Additional expression data

Transcript data for barley early inflorescence development was collected from supplemental dataset 3 (Digel et al., 2015), selecting only the introgression line (S42-IL017) inflorescence samples grown in long day conditions.

Expression data for rice early inflorescence meristem types was collected from supplemental data S1 (Harrop et al., 2016), selecting the MADS-box genes by name search.

Expression data for wheat inflorescence development was collected from supplemental table S4 “List of wheat homeologs similar to rice MADS-box genes” (Feng et al., 2017).

References

Alqudah AM, Schnurbusch T (2014) Awn primordium to tipping is the most decisive developmental phase for spikelet survival in barley. Functional Plant Biology **41:** 424

Alvarez-Buylla ER, Benítez M, Corvera-Poiré A, Chaos Cador A, de Folter S, Gamboa de Buen A, Garay-Arroyo A, García-Ponce B, Jaimes-Miranda F, Pérez-Ruiz RV, Piñeyro-Nelson A, Sánchez-Corrales YE (2010) Flower development. The arabidopsis book **8:** e0127-e0127

Ambrose BA, Lerner DR, Ciceri P, Padilla CM, Yanofsky MF, Schmidt RJ (2000) Molecular and genetic analyses of the silky1 gene reveal conservation in floral organ specification between eudicots and monocots. Molecular Cell **5:** 569-579

Angenent GC, Franken J, Busscher M, Vandijken A, Vanwent JL, Dons HJM, Vantunen AJ (1995) A NOVEL CLASS OF MADS BOX GENES IS INVOLVED IN OVULE DEVELOPMENT IN PETUNIA. Plant Cell **7:** 1569-1582

Arora R, Agarwal P, Ray S, Singh AK, Singh VP, Tyagi AK, Kapoor S (2007) MADS-box gene family in rice: genome-wide identification, organization and expression profiling during reproductive development and stress. BMC Genomics **8:** 242

Becker A (2003) The major clades of MADS-box genes and their role in the development and evolution of flowering plants. Molecular Phylogenetics and Evolution **29:** 464-489

Bommert P, Satoh-Nagasawa N, Jackson D, Hirano H-Y (2005) Genetics and Evolution of Inflorescence and Flower Development in Grasses. Plant and Cell Physiology **46:** 69-78

Bowman JL, Smyth DR (1999) CRABS CLAW, a gene that regulates carpel and nectary development in Arabidopsis, encodes a novel protein with zinc finger and helix-loop-helix domains. Development **126:** 2387-2396

Bremer K (2002) Gondwanan evolution of the grass alliance of families (Poales). Evolution **56:** 1374-1387

Burton RA, Jobling SA, Harvey AJ, Shirley NJ, Mather DE, Bacic A, Fincher GB (2008) The genetics and transcriptional profiles of the cellulose synthase-like HvCslF gene family in barley. Plant Physiol **146:** 1821-1833

Buzgo M, Soltis DE, Soltis PS, Ma H (2004) Towards a comprehensive integration of morphological and genetic studies of floral development. Trends in Plant Science **9:** 164-173

Callens C, Tucker MR, Zhang D, Wilson ZA (2018) Dissecting the role of MADS-box genes in monocot floral development and diversity. J Exp Bot **69:** 2435-2459

Ciaffi M, Paolacci AR, Tanzarella OA, Porceddu E (2011) Molecular aspects of flower development in grasses. Sex Plant Reprod **24:** 247-282

Coen ES, Meyerowitz EM (1991) THE WAR OF THE WHORLS - GENETIC INTERACTIONS CONTROLLING FLOWER DEVELOPMENT. Nature **353:** 31-37

Cui R, Han J, Zhao S, Su K, Wu F, Du X, Xu Q, Chong K, Theissen G, Meng Z (2010) Functional conservation and diversification of class E floral homeotic genes in rice (Oryza sativa). Plant J **61:** 767-781

de Folter S, Shchennikova AV, Franken J, Busscher M, Baskar R, Grossniklaus U, Angenent GC, Immink RGH (2006) A B-sister MADS-box gene involved in ovule and seed development in petunia and Arabidopsis. Plant Journal **47:** 934-946

Digel B, Pankin A, von Korff M (2015) Global Transcriptome Profiling of Developing Leaf and Shoot Apices Reveals Distinct Genetic and Environmental Control of Floral Transition and Inflorescence Development in Barley. Plant Cell **27:** 2318-2334

Dreni L, Pilatone A, Yun D, Erreni S, Pajoro A, Caporali E, Zhang D, Kater MM (2011) Functional analysis of all AGAMOUS subfamily members in rice reveals their roles in reproductive organ identity determination and meristem determinacy. Plant Cell **23:** 2850-2863

Dreni L, Zhang D (2016) Flower development: the evolutionary history and functions of the AGL6 subfamily MADS-box genes. Journal of Experimental Botany **67:** 1625-1638

Feng N, Song G, Guan J, Chen K, Jia M, Huang D, Wu J, Zhang L, Kong X, Geng S, Liu J, Li A, Mao L (2017) Transcriptome Profiling of Wheat Inflorescence Development from Spikelet Initiation to Floral Patterning Identified Stage-Specific Regulatory Genes. Plant Physiol **174:** 1779-1794

Gao X, Liang W, Yin C, Ji S, Wang H, Su X, Guo C, Kong H, Xue H, Zhang D (2010) The SEPALLATA-like gene OsMADS34 is required for rice inflorescence and spikelet development. Plant Physiol **153:** 728-740

Harrop TW, Ud Din I, Gregis V, Osnato M, Jouannic S, Adam H, Kater MM (2016) Gene expression profiling of reproductive meristem types in early rice inflorescences by laser microdissection. Plant J **86:** 75-88

Kaufmann K, Anfang N, Saedler H, Theissen G (2005) Mutant analysis, protein-protein interactions and subcellular localization of the Arabidopsis B-sister (ABS) protein. Molecular Genetics and Genomics **274:** 103-118

Kobayashi K, Maekawa M, Miyao A, Hirochika H, Kyozuka J (2010) PANICLE PHYTOMER2 (PAP2), encoding a SEPALLATA subfamily MADS-box protein, positively controls spikelet meristem identity in rice. Plant Cell Physiol **51:** 47-57

Kubo T, Fujita M, Takahashi H, Nakazono M, Tsutsumi N, Kurata N (2013) Transcriptome Analysis of Developing Ovules in Rice Isolated by Laser Microdissection. Plant and Cell Physiology **54:** 750-765

Kwantes M, Liebsch D, Verelst W (2012) How MIKC* MADS-Box Genes Originated and Evidence for Their Conserved Function Throughout the Evolution of Vascular Plant Gametophytes. Molecular Biology and Evolution **29:** 293-302

Kyozuka J, Kobayashi T, Morita M, Shimamoto K (2000) Spatially and temporally regulated expression of rice MADS box genes with similarity to Arabidopsis class A, B and C genes. Plant and Cell Physiology **41:** 710-718

Mansueto L, Fuentes RR, Borja FN, Detras J, Abriol-Santos JM, Chebotarov D, Sanciangco M, Palis K, Copetti D, Poliakov A, Dubchak I, Solovyev V, Wing RA, Hamilton RS, Mauleon R, McNally KL, Alexandrov N (2017) Rice SNP-seek database update: new SNPs, indels, and queries. Nucleic Acids Research **45:** D1075-D1081

Mascher M, Gundlach H, Himmelbach A, Beier S, Twardziok SO, Wicker T, Radchuk V, Dockter C, Hedley PE, Russell J, Bayer M, Ramsay L, Liu H, Haberer G, Zhang XQ, Zhang QS, Barrero RA, Li L, Taudien S, Groth M, Felder M, Hastie A, Simkova H, Stankova H, Vrana J, Chan S, Munoz-Amatrian M, Ounit R, Wanamaker S, Bolser D, Colmsee C, Schmutzer T, Aliyeva-Schnorr L, Grasso S, Tanskanen J, Chailyan A, Sampath D, Heavens D, Clissold L, Cao SJ, Chapman B, Dai F, Han Y, Li H, Li X, Lin CY, McCooke JK, Tan C, Wang PH, Wang SB, Yin SY, Zhou GF, Poland JA, Bellgard MI, Borisjuk L, Houben A, Dolezel J, Ayling S, Lonardi S, Kersey P, Lagridge P, Muehlbauer GJ, Clark MD, Caccamo M, Schulman AH, Mayer KFX, Platzer M, Close TJ, Scholz U, Hansson M, Zhang GP, Braumann I, Spannagl M, Li CD, Waugh R, Stein N (2017) A chromosome conformation capture ordered sequence of the barley genome. Nature **544:** 426-+

Mayer KFX, Waugh R, Langridge P, Close TJ, Wise RP, Graner A, Matsumoto T, Sato K, Schulman A, Muehlbauer GJ, Stein N, Ariyadasa R, Schulte D, Poursarebani N, Zhou RN, Steuernagel B, Mascher M, Scholz U, Shi BJ, Langridge P, Madishetty K, Svensson JT, Bhat P, Moscou M, Resnik J, Close TJ, Muehlbauer GJ, Hedley P, Liu H, Morris J, Waugh R, Frenkel Z, Korol A, Berges H, Graner A, Stein N, Steuernagel B, Taudien S, Groth M, Felder M, Lonardi S, Duma D, Alpert M, Cordero F, Beccuti M, Ciardo G, Ma Y, Wanamaker S, Stein N, Close TJ, Platzer M, Brown JWS, Schulman A, Platzer M, Fincher GB, Muehlbauer GJ, Sato K, Taudien S, Sampath D, Swarbreck D, Scalabrin S, Zuccolo A, Vendramin V, Morgante M, Schulman A, Int Barley Genome Sequencing C (2012) A physical, genetic and functional sequence assembly of the barley genome. Nature **491:** 711-+

Mena M, Ambrose BA, Meeley RB, Briggs SP, Yanofsky MF, Schmidt RJ (1996) Diversification of C-function activity in maize flower development. Science **274:** 1537-1540

Milner SG, Jost M, Taketa S, Mazón ER, Himmelbach A, Oppermann M, Weise S, Knüpffer H, Basterrechea M, König P, Schüler D, Sharma R, Pasam RK, Rutten T, Guo G, Xu D, Zhang J, Herren G, Müller T, Krattinger SG, Keller B, Jiang Y, González MY, Zhao Y, Habekuß A, Färber S, Ordon F, Lange M, Börner A, Graner A, Reif JC, Scholz U, Mascher M, Stein N (2019) Genebank genomics highlights the diversity of a global barley collection. Nature Genetics **51:** 319-326

Nagasawa N, Miyoshi M, Sano Y, Satoh H, Hirano H, Sakai H, Nagato Y (2003) SUPERWOMAN1 and DROOPING LEAF genes control floral organ identity in rice. Development **130:** 705-718

Paollacci AR, Tanzarella OA, Porceddu E, Varotto S, Ciaffi M (2007) Molecular and phylogenetic analysis of MADS-box genes of MIKC type and chromosome location of SEP-like genes in wheat (Triticum aestivum L.). Molecular Genetics and Genomics **278:** 689-708

Pelaz S, Ditta GS, Baumann E, Wisman E, Yanofsky MF (2000) B and C floral organ identity functions require SEPALLATA MADS-box genes. Nature **405:** 200-203

Poursarebani N, Seidensticker T, Koppolu R, Trautewig C, Gawronski P, Bini F, Govind G, Rutten T, Sakuma S, Tagiri A, Wolde GM, Youssef HM, Battal A, Ciannamea S, Fusca T, Nussbaumer T, Pozzi C, Boerner A, Lundqvist U, Komatsuda T, Salvi S, Tuberosa R, Uauy C, Sreenivasulu N, Rossini L, Schnurbusch T (2015) The Genetic Basis of Composite Spike Form in Barley and 'Miracle-Wheat'. Genetics **201:** 155-+

Remizowa MV, Rudall PJ, Choob VV, Sokoloff DD (2013) Racemose inflorescences of monocots: structural and morphogenetic interaction at the flower/inflorescence level. Annals of Botany **112:** 1553-1566

Sang XC, Li YF, Luo ZK, Ren DY, Fang LK, Wang N, Zhao FM, Ling YH, Yang ZL, Liu YS, He GH (2012) CHIMERIC FLORAL ORGANS1, Encoding a Monocot-Specific MADS Box Protein, Regulates Floral Organ Identity in Rice. Plant Physiology **160:** 788-807

Schilling S, Gramzow L, Lobbes D, Kirbis A, Weilandt L, Hoffmeier A, Junker A, Weigelt-Fischer K, Klukas C, Wu F, Meng Z, Altmann T, Theissen G (2015) Non-canonical structure, function and phylogeny of the B-sister MADS-box gene OsMADS30 of rice (Oryza sativa). Plant Journal **84:** 1059-1072

Schmitz J, Franzen R, Ngyuen TH, Garcia-Maroto F, Pozzi C, Salamini F, Rohde W (2000) Cloning, mapping and expression analysis of barley MADS-box genes. Plant Molecular Biology **42:** 899-913

Smaczniak C, Immink RGH, Angenent GC, Kaufmann K (2012) Developmental and evolutionary diversity of plant MADS-domain factors: insights from recent studies. Development **139:** 3081-3098

Smaczniak C, Immink RGH, Muino JM, Blanvillain R, Busscher M, Busscher-Lange J, Dinh QD, Liu SJ, Westphal AH, Boeren S, Parcy F, Xu L, Carles CC, Angenent GC, Kaufmann K (2012) Characterization of MADS-domain transcription factor complexes in Arabidopsis flower development. Proceedings of the National Academy of Sciences of the United States of America **109:** 1560-1565

Soltis DE, Chanderbali AS, Kim S, Buzgo M, Soltis PS (2007) The ABC model and its applicability to basal angiosperms. Annals of Botany **100:** 155-163

Theissen G, Melzer R, Rumpler F (2016) MADS-domain transcription factors and the floral quartet model of flower development: linking plant development and evolution. Development **143:** 3259-3271

Theissen G, Saedler H (2001) Plant biology - Floral quartets. Nature **409:** 469-471

Thompson BE, Bartling L, Whipple C, Hall DH, Sakai H, Schmidt R, Hake S (2009) bearded-ear Encodes a MADS Box Transcription Factor Critical for Maize Floral Development. Plant Cell **21:** 2578-2590

Trevaskis B, Hemming MN, Dennis ES, Peacock WJ (2007) The molecular basis of vernalization-induced flowering in cereals. Trends Plant Sci **12:** 352-357

Trevaskis B, Tadege M, Hemming MN, Peacock WJ, Dennis ES, Sheldon C (2007) Short Vegetative Phase-Like MADS-Box Genes Inhibit Floral Meristem Identity in Barley. Plant Physiology **143:** 225-235

Waddington SR, Cartwright PM, Wall PC (1983) A Quantitative Scale of Spike Initial and Pistil Development in Barley and Wheat. Annals of Botany **51:** 119-130

Wang HH, Zhang L, Cai Q, Hu Y, Jin ZM, Zhao XX, Fan W, Huang QM, Luo ZJ, Chen MJ, Zhang DB, Yuan Z (2015) OsMADS32 interacts with PI-like proteins and regulates rice flower development. Journal of Integrative Plant Biology **57:** 504-513

Wei B, Zhang RZ, Guo JJ, Liu DM, Li AL, Fan RC, Mao L, Zhang XQ (2014) Genome-wide analysis of the MADS-box gene family in Brachypodium distachyon. PLoS One **9:** e84781

Wu D, Liang W, Zhu W, Chen M, Ferrandiz C, Burton RA, Dreni L, Zhang D (2018) Loss of LOFSEP Transcription Factor Function Converts Spikelet to Leaf-Like Structures in Rice. Plant Physiol **176:** 1646-1664

Wu F, Shi X, Lin X, Liu Y, Chong K, Theissen G, Meng Z (2017) The ABCs of flower development: mutational analysis of AP1/FUL-like genes in rice provides evidence for a homeotic (A)-function in grasses. Plant J **89:** 310-324

Yadav SR, Prasad K, Vijayraghavan U (2007) Divergent regulatory OsMADS2 functions control size, shape and differentiation of the highly derived rice floret second-whorl organ. Genetics **176:** 283-294

Yamaguchi T, Lee DY, Miyao A, Hirochika H, An G, Hirano HY (2006) Functional diversification of the two C-class MADS box genes OSMADS3 and OSMADS58 in Oryza sativa. Plant Cell **18:** 15-28

Yamaguchi T, Nagasawa N, Kawasaki S, Matsuoka M, Nagato Y, Hirano HY (2004) The YABBY gene DROOPING LEAF regulates carpel specification and midrib development in Oryza sativa. Plant Cell **16:** 500-509

Yao SG, Ohmori S, Kimizu M, Yoshida H (2008) Unequal genetic redundancy of rice PISTILLATA orthologs, OsMADS2 and OsMADS4, in lodicule and stamen development. Plant Cell Physiol **49:** 853-857

Zhu C, Yang J, Box MS, Kellogg EA, Eveland AL (2018) A Dynamic Co-expression Map of Early Inflorescence Development in Setaria viridis Provides a Resource for Gene Discovery and Comparative Genomics. Front Plant Sci **9:** 1309

Supplementary data

	Arabidopsis	Oryza name	Oryza ID	Barley ID	alt sequence	Legacy barley names
A-class	AP1, CAL, FUL	MADS14	Os03g0752800	HORVU5Hr1G095630.3		BM5, VRN1
				HORVU1Hr1G047550.1		'HvAP1b'
		MADS15	OS07G0108900	HORVU2Hr1G063800.7	AK249833.1	BM8
		MADS18	OS07G0605200	*inc HORVU0Hr1G003020.3	AK361227.1	BM3
		MADS20	OS12G0501700	no equivalent		
B-class	PI	MADS2	OS01G0883100	HORVU3Hr1G091000.8		
		MADS4	OS05G0423400	HORVU1Hr1G063620.2		
	AP3	MADS16	OS06G0712700	*inc HORVU7Hr1G091210.4	AK373398.1	
C-class	AG, SHP1/2, STK	MADS3	OS01G0201700	HORVU3Hr1G026650.1		HvAG1
		MADS58	OS05G0203800	HORVU1Hr1G029220.1		HvAG2
D-class		MADS13	OS12G0207000	HORVU1Hr1G023620.1		
		MADS21	OS01G0886200	HORVU1Hr1G064150.2		
E-class	SEP1/2/4	MADS1	OS03G0215400	HORVU4Hr1G067680.2		HvMADS7
		MADS5	OS06G0162800	HORVU7Hr1G025700.6		
		MADS34	OS03G0753100	HORVU5Hr1G095710.1		
	SEP3	MADS7	OS08G0531700	HORVU7Hr1G054220.1		
		MADS8	OS09G0507200	HORVU5Hr1G076400.1		M9
AGL6	AGL6/13	MADS6	OS02G0682200	HORVU6Hr1G066140.9		AGL6
		MADS17	OS04G0580700	no equivalent		
	FLC, FCL1/2, AGL27/31	no equivalent in rice/barley/Bd				
	AGL14/19/42,SOC1(AGL20	MADS50	OS03G0122600	no horvu number	AK368348.1	SOC1-1
		MADS56	OS10G0536100	*inc HORVU1Hr1G051660.8	JN673265	SOC1-L
	AGL24, SVP(AGL22)	MADS22	OS02G0761000	HORVU6Hr1G077300.1		BM10
		MADS55	OS06G0217300	*inc HORVU7Hr1G036130.1	AK356695.1	VRT2
		MADS47	OS03G0186600	HORVU4Hr1G077850.3		BM1
	AGL12	MADS26	OS08G0112700	HORVU7Hr1G076310.14	AK370468.1	
		MADS33	OS12G0206800	no horvu number	AK250031.1	
	AGL16/17/44/21	MADS23	OS08G0431900	HORVU1Hr1G008290.1		
				HORVU1HR1G008300.3		M23b
		MADS25	OS04G0304400	M25a HORVU5Hr1G000480.1		
				M25b HORVU5Hr1G000370.3		
				M25c HORVU7Hr1G023940.2		
				M25d HORVU7Hr1G024000.1		
		MADS27	OS02G0579600	HORVU2Hr1G080490.1		
		MADS57	OS02G0731200	*inc HORVU6Hr1G073040.13		AK363243.1
B-sister	ABS	MADS29	OS02G0170300	HORVU6Hr1G032220.8		
		MADS30	OS06G0667200	HORVU7Hr1G108280.4	AK375718	
		MADS31	OS04G0614100	HORVU2Hr1G098930.2		
	no At equivalent	MADS32	OS01G0726400	HORVU3Hr1G068900.3		

Supplemental table 1: The MIKCc MADSbox gene family in barley compared to rice. The *Arabidopsis* co-orthologs are given per gene class where available, as the relation within classes is generally not homologous.

Set1	MADS22	MADS55	MADS47
MADS22	1		
MADS55	0.923	1	
MADS47	0.946	0.979	1

Colors:
>0.95
>0.90
>0.75
>0.50
<0.50

Pseudoset	MADS34	MADS50	MADS32	MADS56	MADS5	MADS18	MADS14
MADS34	1						
MADS50	0.789	1					
MADS32			1				
MADS56	0.611	0.640	0.683	1			
MADS5			0.688	0.504	1		
MADS18				0.576	0.837	1	
MADS14	0.620	0.654		0.672	0.555	0.839	1

Set2	MADS33	MADS2	MADS26	MADS3	MADS6	MADS4*	MADS16	MADS15	MADS1
MADS33	1								
MADS2	0.982	1							
MADS26	0.984	0.972	1						
MADS3	0.956	0.958	0.986	1					
MADS6	0.937	0.957	0.950	0.976	1				
MADS4*	0.925	0.965	0.912	0.929	0.971	1			
MADS16	0.749	0.822	0.697	0.712	0.787	0.910	1		
MADS15	0.842	0.887	0.789	0.801	0.894	0.953	0.928	1	
MADS1	0.860	0.925	0.848	0.880	0.932	0.971	0.945	0.940	1

Set3	MADS13	MADS58	MADS7	MADS31	MADS21	MADS8	MADS29
MADS13	1						
MADS58	0.991	1					
MADS7	0.989	0.995	1				
MADS31	0.964	0.986	0.969	1			
MADS21	0.968	0.928	0.937	0.869	1		
MADS8	0.955	0.937	0.962	0.872	0.966	1	
MADS29	0.887	0.822	0.842	0.737	0.974	0.928	1

Supplemental table 2: Individual correlation score table for set1, set2, set3 and the pseudoset. Green backgrounds indicate correlation over 0.95.

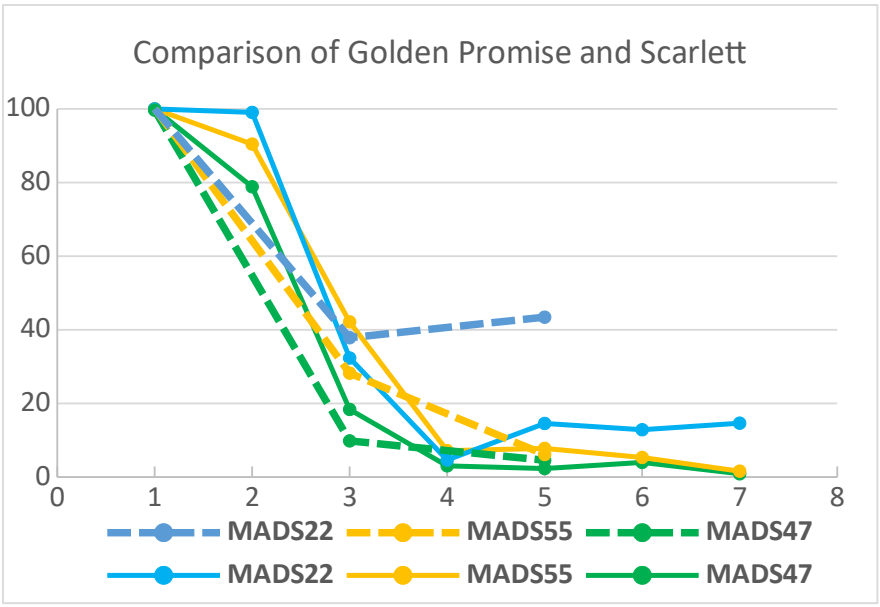

Supplemental figure 1A: Comparison of SVP-like MADS-box gene expression profiles during early inflorescence development in Scarlett (Ppd-H1) (Digel et al. 2015; dashed lines) and Golden Promise (this thesis; solid lines). Expression is given as a percentage of the maximum recorded expression, which is at Waddington stage 1 (W1) for all three genes from both varieties. The same pattern of a rapid decline in expression before W2, followed by a continued slower decline for M55 and M47, while M22 rebounds, is preserved.

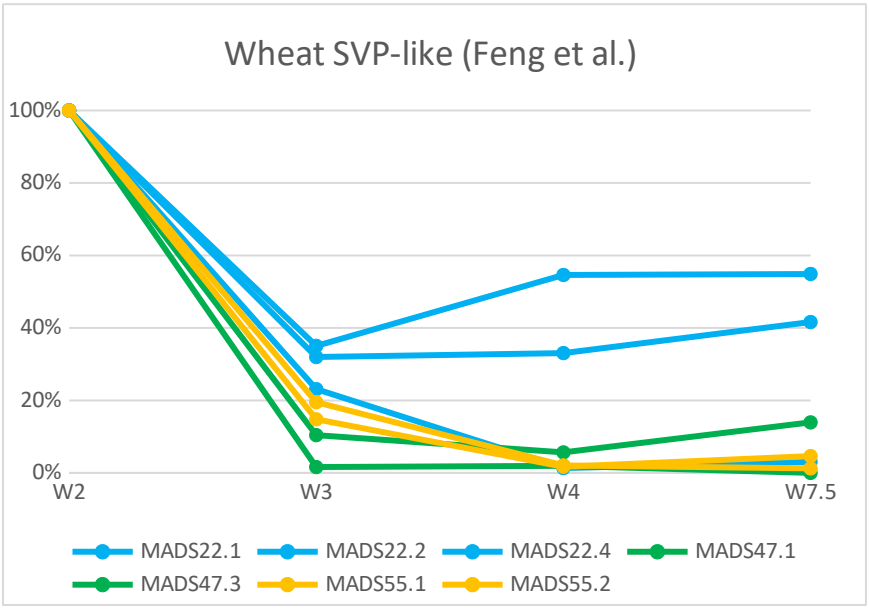

Supplemental figure 1B: Relative expression of the SVP-like genes in wheat, by Waddington stage. All expression declines after the floral transition, and the MADS47 and MADS55 ortholog expression remains low. Two out of three MADS22 orthologs show a resurgence later in inflorescence development reminiscent of the expression in barley.

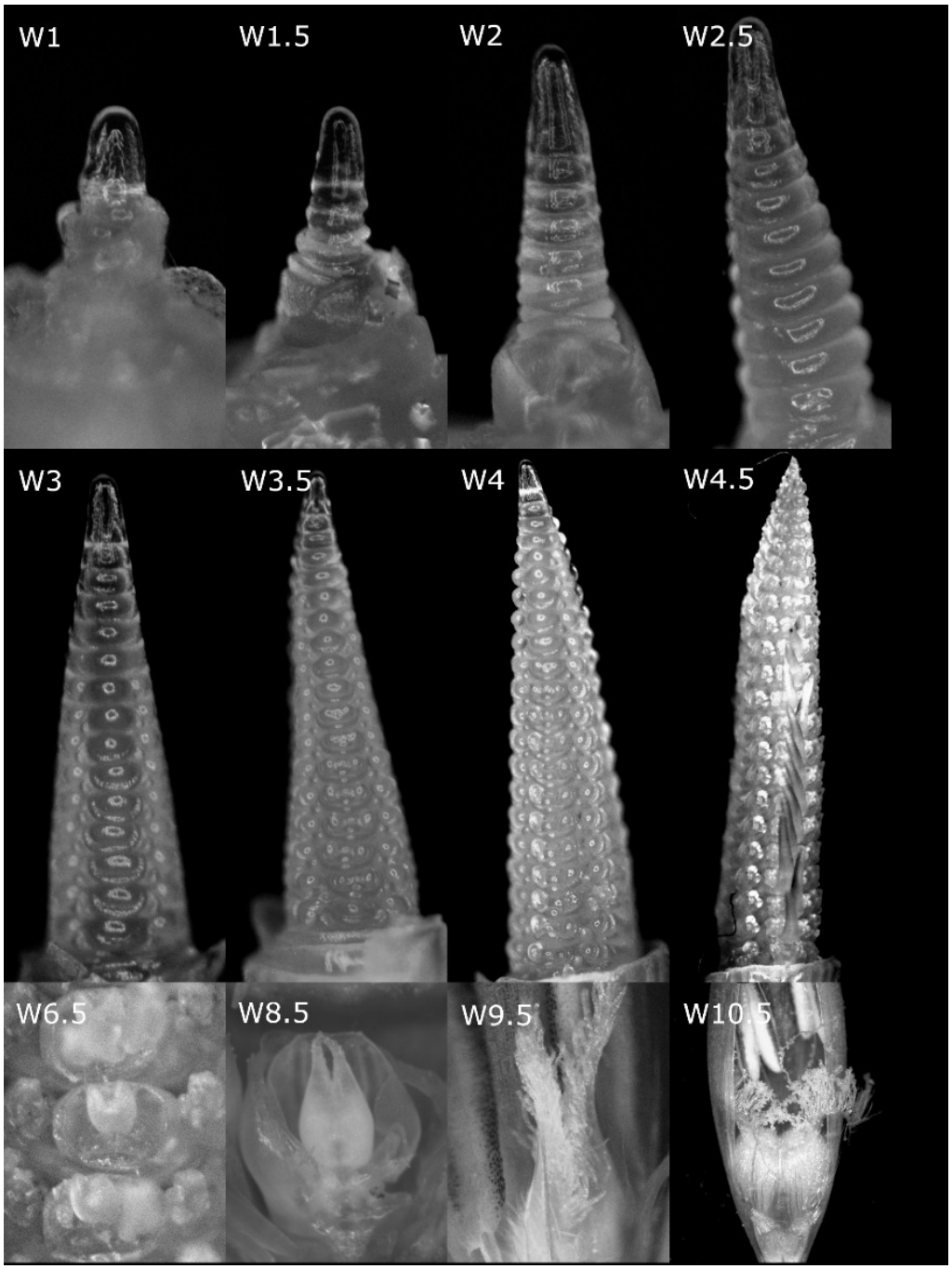

Supplemental figure 2: Waddington stages as sampled. W1: vegetative meristem starting elongation, W1.5: early reproductive meristem, W2: double ridge, W2.5: triple mound (initiation of central and lateral spikelets), W3: lemma primordium, W3.5: stamen primordia, W4: pistil primordium, W4.5: carpel primordium; awn primordium; inflorescence apex diminishes (no more new spikelets are formed), W6.5: styles are prominent on the pistil (here made visible by removing the lemma and stamens), W8.5: stigmatic branches elongating and hair forms on the ovary wall, W9.5: styles and stigmatic braches are spreading, W10.5: pollen has fertilised the ovule; styles, stigmatic branches and stamens wither; palea and lemma cease growth.

Gene	Forward primer	Reverse primer	
MADS14	CAGCGGCGGCAGGCGAGAG	CCAGGCTGGCCGCTGCAAC	
MADS14b	AGCTCACTGAAAGATATCAGAT	ATCCTCTGCCCTCACGCCTAT	*
MADS15	ATATGCCTACCGCCATGGAT	ATACAGCGAACCAGCATTCC	
MADS18	ACCAGCACAAGCAAACAACA	TGCAGGAAAAGCTCAAGACA	
MADS2	CCAGCATGATATCGCCTTG	TCGAGCCAGTGGTGGATAA	
MADS4	ATGCCAAGATGTTCCTGGTC	TTTGGCACCTTAGCCATCAT	
MADS16	CGGCAAGTACCACGAGTTCT	CGTCCAGATCTTCACCCATC	
MADS3	GCAGCAGCAGCATTACTCC	ACACATGCACGCGACAGTA	
MADS58	ATCATGCAGCAGCCTCAGT	GGTGTGGCCAAGCCTTAAT	
MADS13	TCAGCTGAACCTAGGCTGC	TTTGACAGGAATAGTTGAGTACTGGT	
MADS21	CTCTTCACCTCGGCTACGA	TCTTCACAACACGCACACG	
MADS1	TCGTCTGCAGGTTGGATATG	CAGCGTACAACGCAGCTTAG	
MADS5	CCTGGATCACATGAACAATGA	CGAAATGCGCACATGTCTAT	
MADS34	ATTTCGTGGCATGGATGTG	AACACAAAAGCAGCCGAGTT	
MADS7	ACCCTCCTGAGTCCCTGAA	ACGAAAGTTGCACGCAAAA	
MADS8	CTCAGGAGCAGATAAACAACG	GTACGCGAACGCGGTACTA	
MADS6	CCAATAATATTCCACGGAGCA	ACGCAGGGTACTTCTCGTGT	
MADS50	ACGCGGTTGAAGTGGAGAC	CTGCTGCTTGCAACTCCAT	
MADS56	GGCTGTCAGGTCAATCCAA	CATCGTCGCAGCAGCTAAT	
MADS22	TGCCATGGAAGTAACAGTAGTTG	TCGCTTCAGCTGCAAGTTT	
MADS55	CTCGCAGGACAATGACGAC	TGCGCATTGCAGACATAAA	
MADS47	CACCAACACGTCGTATCCA	CATCCAGTGCGCTCAAACT	
MADS26	TGGACTGATCGACGTAGGC	AGGCCTTAAGGGCACTCCT	
MADS33	AATTGAGCAGAGCGGGTTT	GCAATCTGCGAACTGTTCAA	
MADS23	TGAGCAACCACAATCACCA	CATCCCGGATTCAACACAG	
MADS23b	GCCGGGCGATTACTAGTTC	CCGATCATCTCCCAAACCT	
MADS25a	CATGTTATCCTCCAAGCCAGA	TCCAACTCACAGCTGACTCTGT	*
MADS25b	AGCAGCTCGAAAGTTGCTG	CATCCTCATGCTCCTGCTG	*
MADS25c	GCCAGTGGAAGCAACTCAA	TACTGCATGCTGTGGACGA	*
MADS25d	CACTGGAAGCAGCTCCAAA	GCTTGCAGTGGACGAGGTA	*
MADS27	GAGCATACTGCACCGCCTA	CGTCACATGCGAACCACTT	
MADS57	CTCCAGCACTGGGACTTCA	AGCGCACAACATGCTACATT	
MADS29	GAAGAGATTAACCACGAT	TCCAAGATATGCTCCTT	
MADS31	ATGAACCCGAAGCTGTTCC	AAGCTCCGATCATCCATCC	
MADS32	GCCTGGACCTCAAACTTGG	AGTCCAGCCCAGCCTAAAC	
HORVU1Hr1G063610	TTCTCGTGTTTGTTCTGGTCA	ATGCCAAGATGTTCCTGGTC	
GAP	GTGAGGCTGGTGCTGATTACG	TGGTGCAGCTAGCATTTGAGAC	Burton et al, 2008
Cyclophilin	CCTGTCGTGTCGTCGGTCTAAA	ACGCAGATCCAGCAGCCTAAAG	Burton et al, 2008
Tubulin	AGTGTCCTGTCCACCCACTC	AGCATGAAGTGGATCCTTGG	Burton et al, 2008
SP70	CGACCAGGGCAACCGCACCAC	ACGGTGTTGATGGGGTTCATG	Burton et al, 2008

*) did not result in usable expression data

Supplemental table 3: Primers used in quantification by RT-qPCR, and normalisation.

Gene	probe		primer
HvMADS 1	Sense	F	TAATACGACTCACTATAGGGAGATACCGCACCTGCAACTC
		R	GGTGTCTTGCAGCTTCTTCC
	Antisense	F	AGATACCGCACCTGCAACTC
		R	TAATACGACTCACTATAGGGGGTGTCTTGCAGCTTCTTCC
HvMADS 6	Sense	F	TAATACGACTCACTATAGGGGGCACAACAAAAACATTGGA
		R	GTGCTTGAGTTGCCTGTTGA
	Antisense	F	GGCACAACAAAAACATTGGA
		R	TAATACGACTCACTATAGGGGTGCTTGAGTTGCCTGTTGA

Supplemental table 4: Primers for the generation of *in situ* hybridisation RNA probes.

Chapter 3: Generation of a barley *hvmads1* mutant using a genome-editing approach

3.1 Abstract

LOFSEP genes in rice are involved in inflorescence morphology, in addition to their E-class function in floral organogenesis. In the *osmads1* mutant the lemma, palea and lodicules are transformed into leaf like structures, the number of inner floral organs is changed and floral determinacy is reduced. *OsMADS34* suppresses the outgrowth and differentiation of the sterile lemma, bracts and has a role in panicle branching.

Mutants for *HvMADS1*, *HvMADS5* and *HvMADS34* were generated in barley by *Agrobacterium*-mediated transformation of immature embryos with CRISPR/Cas9 constructs. No mutant phenotype was observed for *hvmads5* and *hvmads34*, and for *hvmads1* the phenotype is limited to shorter awns and increased tillering. The contrast between the severity of LOFSEP mutants in the rice and barley spikelet suggests there is additional redundancy between the LOFSEP genes in barley.

The shorter awns on *hvmads1* are likely independently regulated from the brassinosteroid pathway and *SHORT AWN2* (*LKS2*). The additional tillers do not result in higher yield, because fertility and grain weight are reduced. Reduced grain weight could be the result of the smaller photosynthetic contribution from the shorter awns and competition for plant resources by additional tillers during the grain filling phase.

3.2 Introduction

The flowers of plants are not only essential for reproductive success, but also crucial for crop yield. Therefore understanding the development of inflorescences is not only of fundamental scientific importance but also instrumental in feeding a growing world population over the coming decades. Barley (*Hordeum vulgare*) is an important food and feed crop in many regions of the world, and has a more accessible genome compared to the agronomically important hexaploid wheat (*Triticum aestivum)*. It is therefore an ideal model to explore factors influencing inflorescence morphology.

The barley inflorescence, called a spike, does not form branches like the rice (*Oryza sativa*) panicle. Instead the spikelet primordia form in a distichous manner at each rachis node, directly on the main floral axis in groups of three at the triple mount stage, W2.5 (Waddington et al., 1983). In two-row barley varieties only the central spikelet produces a single fertile floret, while in six-row barley all three spikelets fully develop (Koppolu et al., 2013). Each spikelet produces a floret flanked by two glumes. Within the floret the floral organs are initiated sequentially from the outer lemma, palea and two lodicules, to the inner whorls containing three stamens and one carpel. At Waddington stage 4.5 the awn primordium forms at the apex of the developing lemma (Waddington et al., 1983).

The ABCDE model

Some of the key drivers of flower morphology are the MADS-box genes that determine the identity of the floral organs, as described in the ABCDE model. In the ABCDE model the expression of A-class genes in floral organ primordia will lead to development into sepals, A-class and B-class to petals, B-class and C-class to stamens, and C-class alone to carpels (Coen and Meyerowitz, 1991). This model was later refined to include D-class genes which are involved in ovule identity specification (Angenent et al., 1995). The ABCDE model was rounded out by the addition of E-class genes, which are essential in all floral whorls for proper floral organ specification (Pelaz et al., 2000). Genes within each class often act (partially) redundantly.

When considering the lemma and palea as the equivalent of sepals and the lodicules as the equivalent of petals in grass florets, the ABCDE model can be applied mostly unchanged to monocots (Ciaffi et al., 2011; Murai, 2013). Adaptations to the ABCDE model for grasses are discussed in more details in chapter 1, and adaptations specific to barley are suggested in chapter 2.

Expression and role of SEPALLATA in inflorescence development

SEPALLATA (SEP) are E-Class MADS-box genes, likely to be involved in organogenesis in the barley floret much like other monocots. The SEPs can be divided into two subclades: the SEP3 clade and the LOFSEP clade (Malcomber and Kellogg, 2005; Zahn et al., 2005). In rice the LOFSEP clade is formed by *OsMADS1*, *OsMADS5* and *OsMADS34*, while the SEP3

clade is represented by *OsMADS7* and *OsMADS8*. The AGL6-clade, a sisterclade to SEP, has two members in rice, *OsMADS6* and *OsMADS17*, but only *HvMADS6* in barley (Callens et al., 2018). This MIKCc MADS-box gene, the closest relative to the SEP genes, contributes to E-class function in rice and other monocot species (Dreni and Zhang, 2016). The SEP3 clade members in both rice and barley are expressed late in floret development and likely perform the E-class function in the inner floral organs (Cui et al., 2010). The genes in the LOFSEP clade are expressed predominantly in the outer floral organs and likely fulfil the E-class role in the lemma, palea and perhaps in the lodicules (Callens et al., 2018).

OsMADS1 has an important role in floret meristem identity

The RNAi knockdown lines of *OsMADS1* have a leafy glume-like lemma and a leafy palea missing the marginal tissue, as well as glume like lodicules and stamens and multiple carpels (Prasad et al., 2005; Khanday et al., 2013). In a knockout mutant of *osmads1* the lemma, palea and lodicules are transformed into leaf like structures, and the number of inner floral organs is changed (Gao et al., 2010). A similar phenotype is also observed in an epigenetically silenced *osmads1* mutant, although the inner floral organs also seem homeotically affected (Wang et al., 2010). Closer observation of the *osmads1* mutant also revealed occasional twin florets, complete absence of the inner floral organs, or completely missing lodicules, stamens and carpel (Wu et al., 2018). *OsMADS1* is expressed in the spikelet primordium at stage sp4 (comparable to W3 in barley), in the lemma and palea, and weakly in the carpel primordia (Gao et al., 2010). Expression in the carpel primordium is not uniform, but seems to be concentrated in a polar fashion. Combined these results show that OsMADS1 is needed for proper floral organ development in all whorls, but is not expressed in lodicules and stamens, and only weakly in carpels, so some of its function is performed indirectly (Chapter 1).

In the double mutant *osmads1 osmads15* the florets revert to plantlets, abandoning their reproductive trajectory for a vegetative fate, indicating that OsMADS1 is important for FM identity (Wang et al., 2010).

OsMADS5 has no unique functions

OsMADS5 is the least studied of the LOFSEP genes. The duplication event leading to the split of the *OsMADS1* and *OsMADS5* lineages has been mapped to the base of the grass family. Subsequently *OsMADS5* lost the end of its C-terminal domain by the introduction of a premature stop codon (Christensen and Malcomber, 2012).

The *osmads5* mutant has no discernible phenotype, except perhaps an attachment of the lodicules to the lemma (Agrawal et al., 2005; Wu et al., 2018). The lack of a phenotype is likely due to redundancy in its function with *OsMADS1* and *OsMADS34*, and indeed double and triple mutants show enhanced phenotypes (Wu et al., 2018).

OsMADS34 has a role in regulating panicle branching and supressing sterile lemmas and glumes

The mutant os*mads34* sterile lemmas grow much larger than in the wild type, and have a lemma/palea and leaf like character. While the sterile lemmas normally have only one vascular bundle, the mutants have five to eleven. Also the cell types present in the mutant sterile lemmas are similar to those normally found in the lemma, palea or leaves. Together this indicates that OsMADS34 is essential in the specification of sterile lemmas (Gao et al., 2010; Kobayashi et al., 2010; Wu et al., 2018), or in other words, OsMADS34 suppresses the outgrowth and differentiation of the sterile lemmas. Outgrowth of some of the rudimentary glumes was observed in some *osmads34* mutants as well, which indicates that the suppression of these lateral outgrowths may be regulated in a similar way by *OsMADS34*, however these similarities are limited, because this phenotype is not always present and not found in all mutants of *OsMADS34* (Kobayashi et al., 2010).

Osmads34 mutants also have an inflorescence architecture phenotype, where there are more primary branches and fewer secondary branches and spikelets in the panicle (Gao et al., 2010), while Kobayashi et al. (2010) observe a similar increase in primary branches, but rather an increase in secondary branch formation as well as the appearance of tertiary branches and ultimately more spikelets.

Quantitative RT-PCR shows expression of *OsMADS34* in roots, culms, leaves and the inflorescence (Gao et al., 2010), although the mutant only has a phenotype in the inflorescence, where the expression is strongest. Within the developing inflorescence

OsMADS34 is expressed in the early inflorescence meristem, then highly expressed in the primary and secondary branch meristems and in the early primordia within the spikelet, the glume and sterile lemma primordia, and finally some expression is seen in the early floral organ primordia (Gao et al., 2010; Kobayashi et al., 2010; Harrop et al., 2016). A more in-depth exploration of the rice LOFSEP mutant phenotypes, including the double and triple mutants, is given in the introductory chapter of this thesis.

LOFSEP mutants may give insight into barley inflorescence and spikelet development

To understand the molecular control of barley spike and spikelet morphogenesis, a good start would be studying homologs of known genes from the model plant rice, that are involved in inflorescence development. All five rice SEPs have a homolog in barley and expression patterns are very similar (Schmitz et al., 2000; Digel et al., 2015); (Chapter 2). No functional research on barley SEPs has been reported so far, which was also noted in a recent review on ABCDE genes in grasses (Callens et al., 2018). There are no readily available mutants for SEPALLATA in barley, and the genes are highly conserved, especially across the MADS domain at the start, where no SNPs have been reported (Chapter 2). Therefore a straightforward way to study SEPALLATA function in barley is to create CRISPR/Cas9 knockout mutants. This could be done firstly for the LOFSEP genes individually, as they show the more interesting phenotypes related to inflorescence and spikelet morphology in rice. However, the possible redundancy in function among the LOFSEP genes means double and triple knockout mutants may later be required to see the more severe phenotypes.

Because there are no other types of SEPALLATA mutants available for validation in barley, the veracity of the resulting phenotype can be strengthened by creating the same mutations in more than one barley variety. Golden Promise (GP) is a two row spring barley variety that originates from Scotland, has a relatively long generation time of three months, but is the easiest known variety for barley transformation (Harwood, 2014; Hisano et al., 2017). WI4330 (WI) is also a two row spring barley, but is more acclimated to growth temperatures in Australia and is a former elite breeding line used at the University of Adelaide. WI4330 is much harder to transform, with transformation frequencies up to 7.3% (Lim et al., 2018), but has a shorter generation time. Hence these two cultivars are ideal choices for transformation and subsequent phenotyping.

CRISPR/Cas9 targeted mutagenesis

Clustered regularly interspaced short palindromic repeats (CRISPR)/Cas9 is a molecular toolkit that can be used for *in vivo* targeted gene editing, adapted from prokaryote defences against viral DNA (Barrangou, 2015). The CRISPR associated protein 9 (Cas9) can create double strand breaks in DNA where a matching sequence for its incorporated guide-RNA is found, as well as the protospacer adjacent motif (PAM) of NGG. These double strand breaks are then repeatedly repaired by error prone repair mechanisms of the cell, and cut again by Cas9, until a mutation is introduced and the guide RNA no longer matches the DNA sequence. If this mutation is introduced into germ line cells, it has become a heritable allele, and if both alleles are affected with a mutation inducing a frame shift near the start of an open reading frame, a knockout line for the target gene has been created.

Creating knockout mutants in barley will provide valuable information on the practical applicability of CRISPR/Cas9 in barley. Knockout mutants of the LOFSEP genes will show what functions the genes control in a non-redundant way. They will also show what morphological changes these mutants have in common between rice and barley and thus what functions LOFSEP genes may have in common among the grasses. Additionally, the differences in morphology between mutants of homologous LOFSEP genes in rice and barley can show whether they are involved in the contrasting differences in inflorescence development between these two grass species.

3.3 Results

Barley transformation efficiency reached as high as 70%

Binary CRISPR/Cas9 vectors targeting the LOFSEP SEPALLATA genes *HvMADS1*, *HvMADS5* and *HvMADS34* as well as the single related gene *HvMADS6* were constructed. Using a CRISPR system with a plant-optimised Cas9 and proven success in monocots (Ma et al., 2015) two guideRNAs were inserted into the vectors targeting *HvMADS1* and *HvMADS34*, while the *HvMADS5* gene was targeted using a single guide-RNA. GP was transformed with all vectors, WI4330 with vectors targeting only *HvMADS1*, *HvMADS5* and *HvMADS34* (Table 1).

Barley was transformed using *Agrobacterium* mediated immature embryo transformation and subsequent plant regeneration from callus. Some defects due to callus regeneration were found in the T0 population, such as doubled leaves and disturbed tiller phylotaxy, however no such defects were found in subsequent generations. The transformation efficiency was highest for GP, with transformation efficiencies up to 70% and for WI up to 14%, resulting in at least 40 T0 plants for each construct (Table 1). Transformation efficiency is defined here as the number of plants successfully established in soil compared to the number of immature embryos infected with *Agrobacterium*. The system established is highly efficient for CRISPR/Cas9.

Golden Promise

Target gene	# Explant	# T0 plants	Transf. Efficiency	WT	Hetero-zygous	Homo-zygous	Bi-allelic	Editing Efficiency
mads1 [N]	82	16	20%	1	2	7	6	94%
mads1 [G]	69	47	68%	4	7	8	28	91%
mads5 [N]	65	12	18%	0	0	6	6	100%
mads5 [G]	70	42	60%	2	9	14	17	95%
mads34 [N]	70	16	23%	0	6	6	4	100%
mads34 [G]	75	53	71%	0	13	18	22	100%
mads6 [N]	114	29	25%	29	0	0	0	0%

WI4330

mads1 [N]	84	12	14%	1	0	3	7	91%
mads5 [R]	442	25	6%	0	2	5	12	100%
mads34 [N]	122	9	7%	0	0	0	9	100%
mads34 [R]	517	24	5%	0	3	3	3	100%

Table 1: Transformation efficiency and CRISPR/Cas9 editing outcomes for all targeted genes in two barley varieties. The number of explants is taken at the start of co-cultivation and T0 plants are counted when established on soil. Letters in square brackets indicate who transformed that line; Transformation and editing efficiency data kindly provided by Dr. Gang Li [G] and Dr. Rohan Singh [R]; [N] for Nico Kuijer. For editing efficiency every non wild-type genotype is counted. Some [N] transformation efficiencies are comparatively low because they include early trials during the establishment of our barley transformation system, therefore [G] line transformation efficiencies are more representative for the efficiency of the system used.

Editing rates up to 90% result in knockout mutants for all LOFSEP target genes

CRISPR/Cas9 introduces mutations over time by cutting the target site repeatedly until the target sequence is changed by error prone repair mechanisms. This can lead to homozygous plants, where the mutation is the same for both alleles, heterozygous plants, or biallelic plants where each allele has a different mutation (Table 1). Additionally the genotype of different cells in one sample can be divergent, resulting in more than two genotypes being present in the sequencing results which is a chimeric genotype. Since only two alleles can be passed on to the next generation, this anomaly is of little consequence. Finally, a chimeric plant could have a mutant genotype in the leaf sample, but not in the germline cells and thus produce wild type progeny. However, this difference between leaf sample and progeny was not observed in our barley lines. Here, editing introduced deletions, substitutions and insertions, all originating 3 bp before the PAM, or 6 bp from the end of the target site (Figure 2). This is

consistent with the reported cleavage site for this Cas9 (Lawrenson et al., 2015; Ma et al., 2015). Genotyping of T0 plants shows editing rates over 90%, where any deviation from wild type is counted, and includes knockout mutants for all LOFSEP genes (Table 1, Figure 1). In the *hvmads1* mutants the gene with the most homology to *HvMADS1*, *HvMADS5*, was also sequenced, but no off-target mutations were found.

At least three independent homozygous T0 plants were selected for each gene for further propagation by self-pollination, and the resulting T1 plants were sequenced and found to all be homozygous for the mutations as well. Since a frame shift is introduced within 7 (HvMADS1), 4 (HvMADS5) or 8 (HvMADS34) amino acids and no phenotypical differences between the lines were observed, they are all considered equivalent knockout mutants. T2 and T3 seeds were planted in a controlled environment for phenotypic analysis.

Figure 1: Sequencing results showing the insertion and deletion mutants for *HvMADS1*, *HvMADS5* and *HvMADS34*. The mutations are in close proximity to the start codons (underlined) and thus the resulting frameshift changes the protein sequences only a few amino acids into the protein (right column), so the mutants are effective knockout alleles.

The *hvmads1* short awn is the only inflorescence phenotype amongst all LOFSEP mutant lines

Among the *hvmads1* T0 plants, homozygous mutants were already observed to have a short awn phenotype, this phenotype was unchanged in subsequent generations. In T2 and T3 plants, the GP wild-type awns were 8.3±0.2 cm long at maturity, while the *hvmads1* mutant awns only grew to 1.6±0.2 cm (Figure 2). Additionally, the *hvmads1* spikelet is slightly

slimmer than the wild-type (Figure 2B). The *hvmads5* and *hvmads34* mutants have no spike- or spikelet phenotype (Figure 2). With an awn length of 8.2±0.2 cm for *hvmads5* and 8.1±0.2 cm for *hvmads34* there is no significant difference from the wild-type (Figure 2C). No changes to the lodicules, stamens, carpels and floral determinacy were found in the LOFSEP mutants (data not shown).

The general inflorescence phenotype is the same in WI, where the only change from wild-type is the shorter awn in *hvmads1*. This shows the *hvmads1* phenotype, and the lack of a phenotype in *hvmads5* and *hvmads34* is not specific to the Golden Promise cultivar, but linked to the LOFSEP genes in barley. However, due to a lack of growing space, the WI plants were grown in the same growth room as the GP, at the ideal temperature for GP, which is 15°C days and 10°C nights. This is too cold for WI, where nearly all plants developed signs of cold stress, such as yellow spots on the leaves, and sometimes limited outgrowth of lateral spikelet lemmas on the inflorescence. Therefore no statistical analysis or further detailed phenotyping of the WI *hvmads1* mutant is included here, as it would be influenced by significant cold stress.

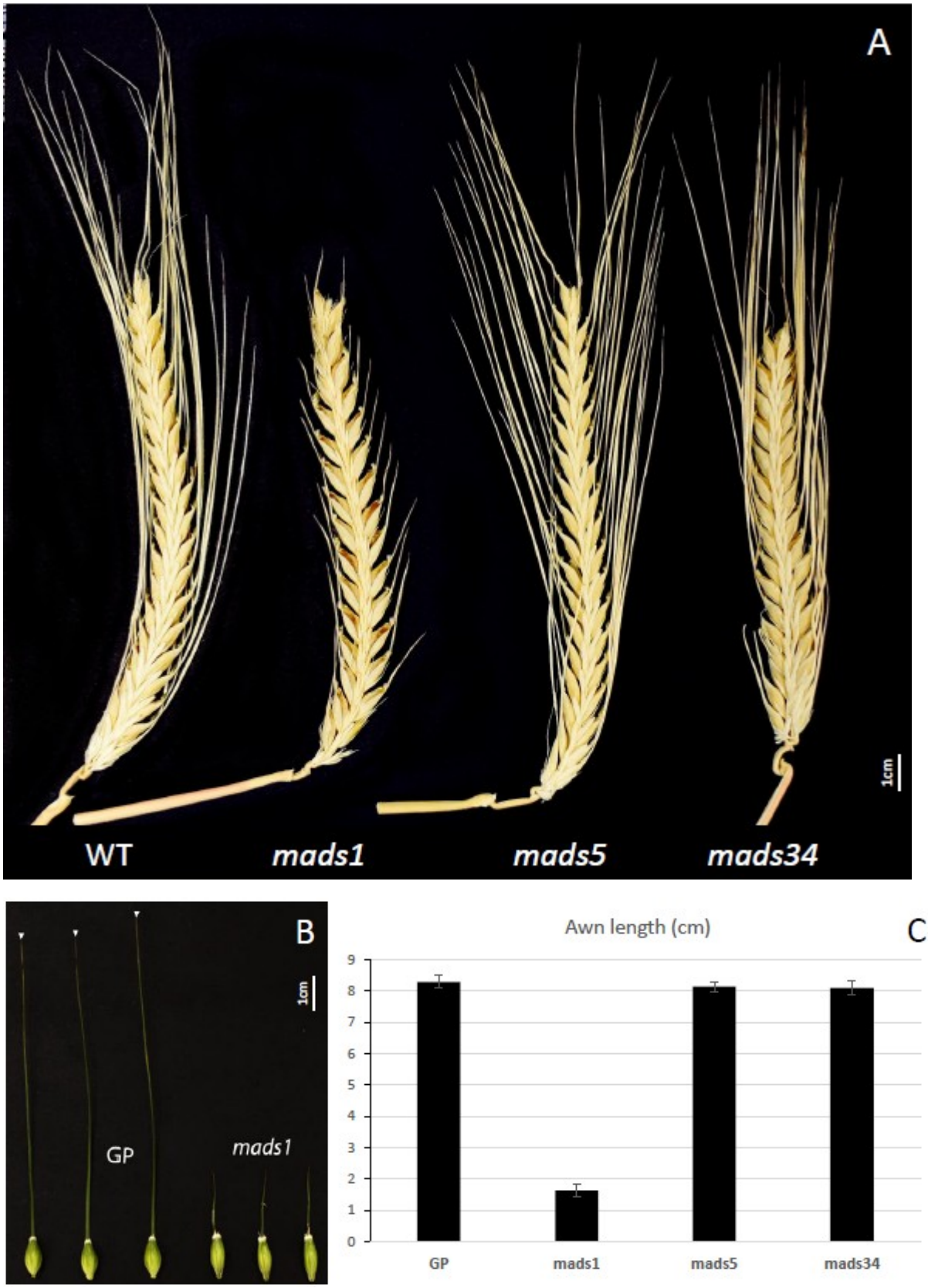

Figure 2: A) Spike phenotype of GP LOFSEP mutants. The *hvmads1* phenotype of shorter awns is the only morphological change. B) The awns of *mads1* spikelets are shorter, and the spikelets are slightly slimmer. C) Summary of the awn lengths for all LOFSEP mutants. Error bars, s.d.

The *hvmads1* mutant grows additional tillers, but yield is not increased

In addition to the shorter awns, *hvmads1* mutant plants also grow more tillers than wild-type (Figure 3F). The average number of fertile tillers for GP was 7.1±1.0, with 14.5±5.3 for *mads1* (Figure 3E). In addition to a number of additional fertile tillers, the *mads1* mutant continues to produce new tillers that do not reach maturity. The highly variable total number of tillers can reach a total of over 40 and may be influenced by the available light and water. Some variance in tiller number was observed depending on plant position in the growth room, where *hvmads1* mutant plants on the corner of a tray, or next to an empty pot, grew more tillers.

The total grain weight produced per plant was 5.1±1.1 g for GP and 4.2±1.2 for the *mads1* mutant (Figure 3C). The total number of filled grains produced per plant was not significantly different between GP (207±49) and *mads1* (197±58) (Figure 3D), but on average fewer filled grains per spike were found in the mutant plants (Figure 3G). The total filled grain number does appear to be very sensitive to growth circumstances, as *mads1* mutants grown for different purposes seem to have fewer fertility issues (for example Figure 2A), so this particular metric should be retested in further experiments. The fertility of spikelets in the *mads1* mutant was reduced in both GP and WI, as well as the average weight of the grains produced (Figure 3A, B). So while *mads1* mutants produce more tillers, the total plant yield is lower than GP, because of a reduced fertility rate and lower average grain weight.

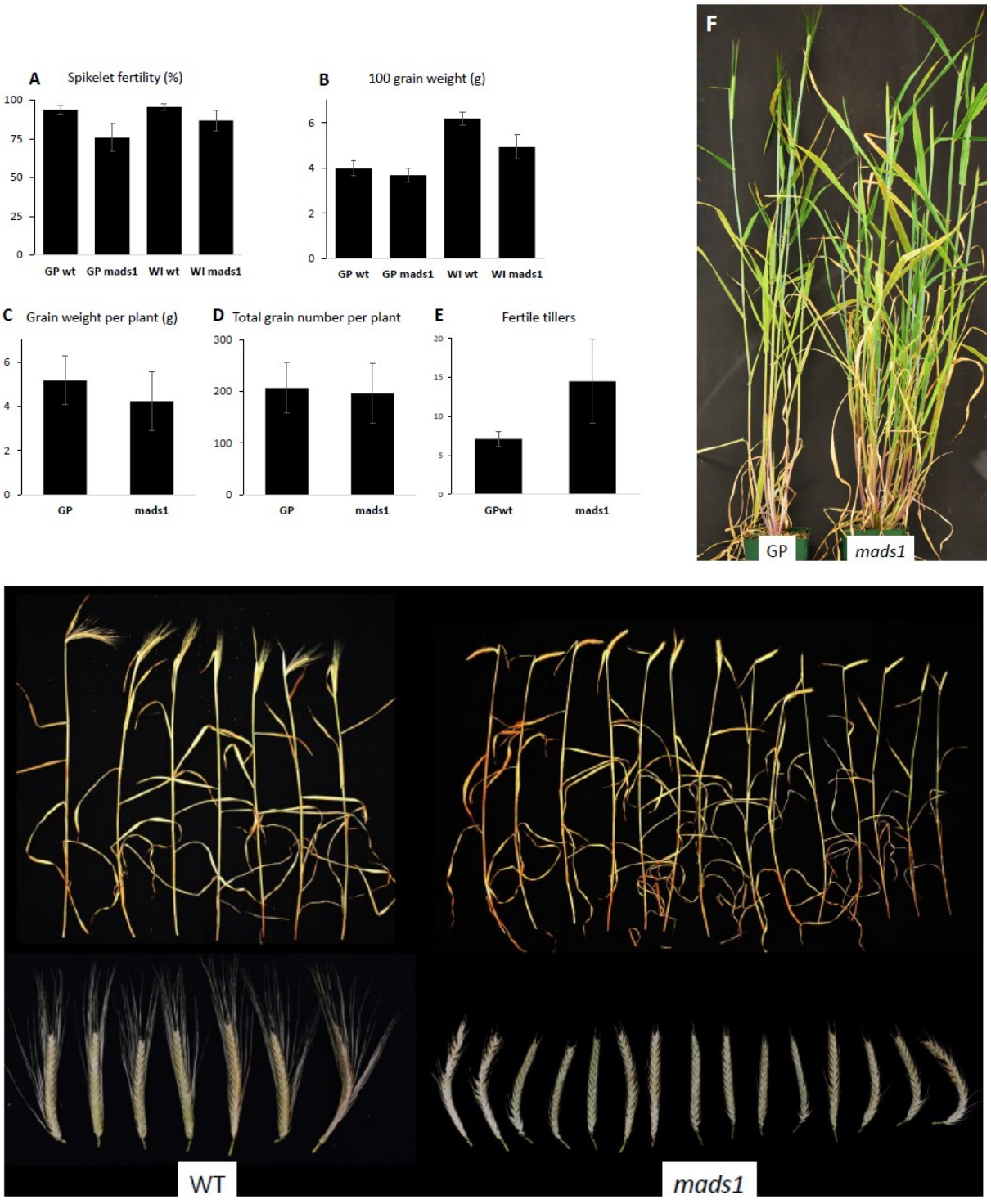

Figure 3: A) Spikelet fertility of wild type and *mads1* in GP (WT N=1638, *mads1* N=1894) and WI (WT N=839, *mads1* N=1443); B) 100 grain weight of wild type and *mads1* in GP (WT N=1536, *mads1* N=1467) and WI (WT N=802, *mads1* N=1259); C) Total filled grain weight per plant (GP N=5, *mads1* N=7); D) Total filled grain number per plant (GP N=5, *mads1* N=7); E) Number of fertile tillers per plant in GP wild type and *hvmads1* (GP N=9, *mads1* N=7). Error bars indicate one standard deviation. F) GP and *mads1* plants of the same age showing the mutant has many more tillers, though not all are fertile. G) Spread of the fertile tillers and spikes of typical GP and *hvmads1* plants. Bars indicate mean values, error bars, s.d.

3.4 Discussion

The short awn phenotype is the only morphological change in the *mads1* mutant spike

The shorter awn phenotype of *hvmads1* can be linked to the lack of expression of *HvMADS1* in the lemma of barley. The rice varieties used for *osmads* mutant studies have no awns, so a direct comparison of the phenotype is not possible. However, an elongated lemma, and a more leaf-like character in the *osmads1* mutant, suggests that a similar shift towards a leaf like organ may result in a shorter awn in barley. Since no further clear leaf-like characteristics were found in the *hvmads1* lemma, the identity of the body of the lemma is likely to be redundantly regulated by the LOFSEP genes in barley.

The barley awn

The awn is an elongated triangular green organ with three vascular bundles and a thick epidermis that can provide significant photosynthetic activity within the spike (Blum, 1985; Abebe et al., 2009). Considering the position of the spike, and especially the awn, at the top of the canopy, it can capture a lot of the incoming radiation. For wheat, awned spikes can intercept between 18 and 45% of the incident radiation, depending on the variety (López-Castañeda et al., 2014). Photosynthesis in the spike is an important factor in grain filling, but the exact amount differs vastly by variety and report (Blum, 1985; Bort et al., 1994). In an experiment where the spike was darkened to isolate its photosynthetic contribution, the yield of an awned genotype was reduced by 37.4%, while an awnless genotype lost only 14.8% yield (Bort et al., 1994). Clipping the awns from Morex spikes reduced grain width by 4.7% and grain weight by 16.1% (Liller et al., 2017). In wheat the awns have been shown to have a dominant photosynthetic contribution during the grain filling stage (Li et al., 2006).

Several QTLs that affect awn length have been identified (Liller et al., 2017). Some are linked to defects in brassinosteroid biosynthesis and signalling, and are accompanied by other morphological changes in the spike, stem and leaves (Dockter et al., 2014). The *SHORT AWN2* (*LKS2*) gene, a SHI-family transcription factor, has been linked to awn length. The *hvlks2* mutant has 50% shorter awns, probably due to reduced cell division (Yuo et al., 2012). The complete abolishment of the awn can be found in the *hooded* mutation, which causes a

new floret to form on top of the lemma. This dominant allele represents a duplication in an intron of the homeobox gene *KNOX3* (Müller et al., 1995).

Among the QTLs found for barley awn length the closest peak to *HvMADS1* on chromosome H4, 'AL4.1', is located at 59.6cM on the POPSEQ map, while at the position of *HvMADS1* at 61.69cM the peak has no significant correlation to awn length (Cantalapiedra et al., 2015; Liller et al., 2017). The lack of natural variation in *HvMADS1* (Chapter 2) may explain why it was not found in QTL assays, even including wild barley cultivars. Therefore the effect of an *hvmads1* mutation strongly reducing the awn length is a new finding.

The reduction of awn length in *hvmads1* appears without dwarfism, shortened spikes or irregular rachis internode lengths and other signs of disturbed brassinosteroid regulation (Dockter et al., 2014). While this points to *HvMADS1* not modifying awn length through interaction with the brassinosteroid pathway, there could still be a derailing of brassinosteroid signalling localised only to the lemma and awn, possibly resulting in reduced cell elongation in the awn.

The awn length regulator *HvLKS2* (Yuo et al., 2012)(HORVU7Hr1G095030), is not significantly differently expressed in *hvmads1* at W2 and W3.5 (Chapter 4). Additionally, the altered pistil morphology associated with *HvLKS2* (Yuo et al., 2012) is not observed in *hvmads1*, so the reduction in awn length in *hvmads1* is likely to be independent of *HvLKS2*.

The contrast between the severity of LOFSEP mutants in the rice and barley spikelet suggests additional redundancy between the LOFSEP genes in barley

The near complete redundancy among the LOFSEP genes in barley is a new finding in stark contrast to the complex phenotypes reported for LOFSEP mutants in rice (Gao et al., 2010; Kobayashi et al., 2010; Wu et al., 2018). The *osmads1* mutant in rice has floral organ defects, and reduced floral determinacy that do not appear in *hvmads1* spikelets. The complete lack of phenotype for the *hvmads34* mutant in barley is also in stark contrast to the phenotypes observed in rice. The *osmads34* mutant has reduced bract suppression, which leads to the outgrowth of the sterile lemmas and to a lesser extent the rudimentary glumes, while in *hvmads34* the glumes are unaffected. This striking difference between rice and barley is not simply a change in the expression profile of *HvMADS1*, *HvMADS5* and *HvMADS34*, as their expression pattern in the wild-type is very similar in early inflorescence development ((Digel

et al., 2015; Harrop et al., 2016); Figure 4). Therefore the E-class role in the spikelet- and floret meristems, as well as in the lemma and palea is likely to be covered redundantly by other E-class genes. The SEP3-like SEPs, *HvMADS7* and *HvMADS8*, are expressed too late to account for this early redundancy. So likely more spikelet and floret phenotypes will appear in double and triple LOFSEP mutants in barley.

The closest relative to the SEPALLATA *HvMADS6*, the only member of the AGL6 class in barley, may also add to the redundancy of the E-class role. *HvMADS6* is expressed at the right time, and has an expression profile similar to *HvMADS1*. *HvMADS6* is also strongly expressed in the palea, but unlike *HvMADS1*, absent in the lemma (Chapter 1), possibly explaining the awn phenotype. Additionally, *MADS6* performing an E-class function has been reported in rice and maize (Dreni and Zhang, 2016), while in rice the *Osmads1/6* double mutant has a more severe spikelet phenotype than the single mutants, also indicating redundancy (Ohmori et al., 2009). An *hvmads1/6* double mutant may thus be the best choice to further investigate the surprisingly mild phenotype of barley LOFSEP mutants after LOFSEP double and triple mutants.

The HvMADS34 expression peak in early inflorescence development may be vestigial

In rice the *osmads34* mutant has a strong effect on inflorescence architecture, and is the main E-class gene involved in inflorescence branching (Gao et al., 2010; Kobayashi et al., 2010). The *hvmads34* mutant has no inflorescence architecture phenotype, but *HvMADS34* expression is very similar to *OsMADS34* expression in early inflorescence development (Figure 4). Any function *HvMADS34* may have in early barley inflorescence development cannot be taken over by other E-class genes, or indeed the related *HvMADS6*, as they are not expressed as early, at W2 (Figure 4). *HvMADS34* has a redundant function with *HvMADS1* and *HvMADS5* in spikelet development, but the earlier expression may be vestigial. This would be in line with the idea that grass inflorescence evolution happened mainly reductively for barley, starting from a branched panicle (Vegetti and Anton, 1995). While the barley inflorescence does not branch, some of the regulatory genes required for branching may still be expressed at the right time.

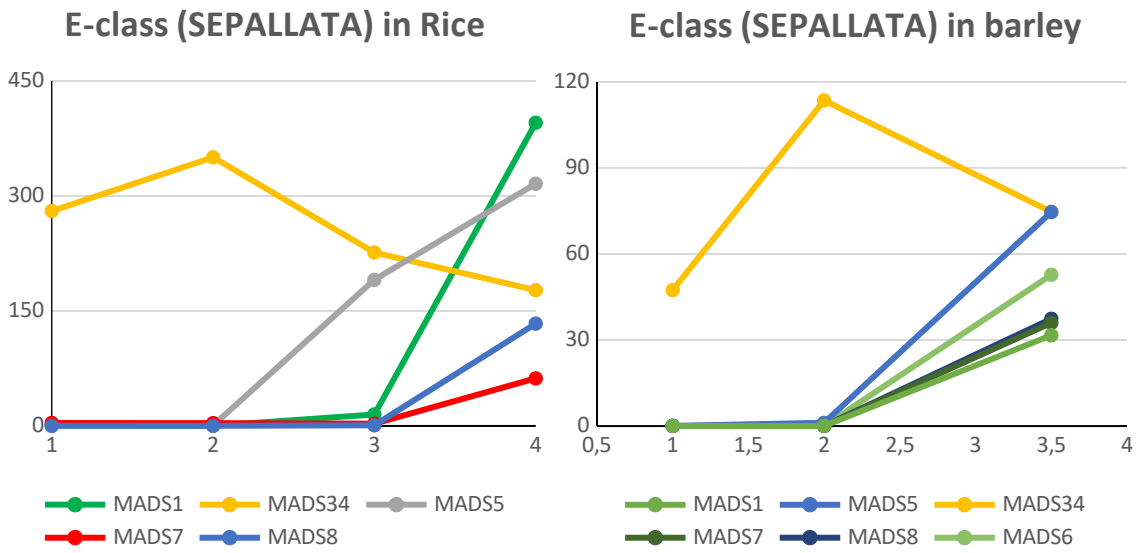

Figure 4: Expression of SEPALLATA in early inflorescence development of rice and barley. For rice 1: rachis meristem, 2: primary branch meristem, 3: branch meristem with axillary meristems, 4: spikelet meristem (Harrop et al. 2016). For barley early expression by Waddington stage (Digel et al. 2015).

The reduced yield in the *mads1* mutant may have several causes

Even though the *hvmads1* mutant produces more tillers, the yield is not improved. The two direct causes are a reduced number of filled grains per spike and a reduced average grain weight.

Part of the reason the *hvmads1* mutant has fewer grains per spike could be that HvMADS1 is important for spikelet fertility, although there are no morphological changes visible in the inner floral organs, and *HvMADS1* is not expressed in the stamens. There is some expression of *HvMADS1* in the carpel (Chapter 2), but this is likely to be related to the remnant of the floret meristem in the carpel samples, and is thus more likely important for floral determinacy than fertility.

A reason for the lower grain weight could be that the awn is an important source of photosynthetic activity, and the reduced awn in the *mads1* mutant is insufficient to do its part in filling the developing grain to the same degree as the GP wild type. Reduction in grain weight has been reported for awnless barley (by 26%) and wheat with the awns clipped off (by 5%), especially in water limited conditions (Bort et al., 1994; Rebetzke et al., 2016).

Finally, competition for plant resources by the additional tillers could limit the available energy to fill each grain properly in the *hvmads1* mutant. Not only are there more spikelets

competing, but unlike in the wild type, new tillers keep developing throughout the grain filling phase. Lower carbon availability could lead to smaller grains, and even prompt the abortion of a number of them. A similar reduction in grain number per panicle and grain weight has been found for rice mutants with increased tillering, where increased competition is considered the likely cause as well (Wang et al., 2007).

Tillers develop from lateral meristems of the shoot apical meristem in the axils of the lower leaves. These secondary tillers can then produce more lateral meristems, resulting in tertiary tillers and so on. Barley produces more tillers than wheat, and generally two-row barley makes more tillers than six-row barley (Alzueta et al., 2012). This inverse relationship between grains per tiller and tiller number again points to the distribution of nutrients as a limiting factor.

Outgrowth of tiller buds in barley continues until the stem elongation begins, and/or the canopy changes the ratio between red and far red light sufficiently (Alzueta et al., 2012). Tiller buds not yet developed at this time will stop vegetative growth and possess some characteristics of an early inflorescence apex. Underdeveloped tillers at this point will die, and much of their carbon is reabsorbed (Palta et al., 2007; Alzueta et al., 2012). In the *hvmads1* mutant the tillers do not die off, and new tillers are produced throughout the stages of inflorescence development. The observation of more tiller outgrowth on the mutant plants with less surrounding canopy indicates that the pathway responding to the ratio between red and far red light is likely still active. Therefore the signal from the developmental switch towards stem elongation and flowering, and stopping tillering is disrupted in the *hvmads1* mutant. One candidate for the mediation of a tillering signal is abscisic acid (ABA). Barley modified by RNAi to accumulate more ABA showed increased tillering, and a reduction in a natural strigolactone compound, 5-deoxystrigol (Wang et al., 2018). To study the tillering phenotype further, it may be useful to look at ABA and strigolactone concentrations and pathways.

One way to test whether the reduced yield in *hvmads1* stems from a source-sink imbalance would be to grow GP and *hvmads1* in conditions of overabundance, where each plant has more soil, space and light than in the standard growth conditions that were used here. While *hvmads1* may then surpass the wild type in yield per plant, the yield per square meter could still be better for wild-type GP since they can be planted closer together without competing for resources and no energy is wasted on heads with reduced fertility. Another interesting

outcome of this experiment would be to see how long an *hvmads1* plant could keep producing more tillers and grains. Under the current growth conditions the soil quantity and light availability may eventually limit the development of the newest tillers, but the *hvmads1* barley does not seem to have an internal signal to stop making new tillers.

CRISPR/Cas9 is successful in barley

The current methods of barley transformation are time consuming and finicky. It is a process that takes months, and requires extensive practice to do efficiently. When transformation efficiency and editing rate are low this becomes a severe bottleneck to functional research using CRISPR/Cas9 in barley.

We demonstrate that with the CRISPR/Cas9 system used here (Ma et al. 2015) the editing rate in barley can reach over 90% routinely in T0, even with multiple targets at the same time (not shown here). This effectively eliminates the need for testing guideRNA efficacy prior to use. Additionally, no off-target editing was detected in the sequence most closely resembling the *HvMADS1* target, the equivalent piece in *HvMADS5*. This CRISPR/Cas9 system is therefore highly recommended for the generation of mutants in barley.

A recent report on the use of a CRISPR/Cas9 system, with a Cas9 gene codon-optimised for monocot expression, found similar editing efficiencies in barley, where mutations were detected in up to 88% of the T0 plants (Gasparis et al., 2018). An earlier study found 10% and 23% editing rate in T0, using a Cas9 without plant codon optimisation (Lawrenson et al., 2015). This indicates that a Cas9 optimised for expression in plants, or specifically in monocots, is a key factor in obtaining high editing rates with CRISPR/Cas9 in barley, and possibly in other grasses as well.

Another important factor for high editing rates in barley could be the GC contents of the target site. The reported editing rates between *HvCKX1* and *HvCKX3* are very different at 68% and 18%, and may be linked to the GC content of 65% and 55% respectively (Gasparis et al., 2018). In rice a test of CRISPR/Cas9 efficiency on 11 genes found an average editing rate of 44%, with a minimum of 21% and a maximum of 67%, with a strong correlation to GC content of the target sites (Zhang et al., 2014). The positive influence of GC content of the target site on editing rate has also been suggested in human cells (Wang et al., 2014), making it a widespread characteristic of CRISPR/Cas9. The target sites used here have a GC

content of 55% to 75% (Table 2), which may have contributed to the high editing rates. GC-content is generally high in the beginning of open reading frames of *Gramineae* genes (Wong et al., 2002), so when selecting CRISPR/Cas9 target sites to create knockout mutants by introducing a frameshift mutation early in the genes, the naturally higher GC content will be beneficial in finding target sites with a high expected editing efficiency.

The use of T0 mutants (and even T1) for phenotypic characterisation is not advisable, since the effects of regeneration from callus can severely distort plant development. However in retrospect, the short awn phenotype for *hvmads1* was clearly present in T0 homozygous and bi-allelic mutants and was not visibly different from the T2 and T3 mutants used for phenotyping. CRISPR/Cas9 induced mutations in the *nud* gene also resulted in the formation of naked caryopses on the T0 generation (Gasparis et al., 2018). Together this shows that with a high editing rate, T0 phenotypes in the barley spike may be reasonably stable when comparing multiple independent mutants.

Transformation efficiency is low in barley

The transformation efficiency is still an open challenge. While we managed to regenerate plants from up to 71% of the initial scutella, the success rate was only this high in Golden Promise. This transformation efficiency is higher than the efficiency of up to 58% for GP reported in a study on transformation amenability in barley (Hisano et al., 2017) and the 8-12% reported for *Agrobacterium* mediated transformation with CRISPR/Cas9 constructs in GP (Gasparis et al., 2018). Working in barley varieties that are more closely related to commercial barley would open up avenues of cooperation with breeding companies, but currently the low transformation efficiencies are prohibitive. Even for fundamental research purposes Golden Promise is far from ideal because of its longer generation time of about three months, and for example as a spring barley GP is difficult to use for vernalisation research. Recently progress has been made towards identifying transformation amenability loci through crosses between GP and more recalcitrant barley cultivars, but the ease of transformation has not reached the level of GP yet (Hisano et al., 2017).

3.5 Materials and methods

Constructs

A CRISPR/Cas9 system for monocot and dicot plants with a plant codon optimized Cas9 was used to construct the vectors (Ma et al., 2015). We opted to use the pYLCRISPR/Cas9P$_{ubi}$-H version, in which Cas9 is driven by the ubiquitin promoter and Hygromycin is used as the selectable agent (Figure 5). This system was used to target *HvMADS1* and *HvMADS34* with two guide RNAs each and *HvMADS5* with one guide RNA.

Target	Sequence	GC content
HvMADS1T1	GTGGGAAGGTGGAGATGAGGCGG	60%
HvMADS1T2	GTCGCCCTCATCATCTTCTCCGG	55%
HvMADS5T1	CAGGATGGGGCGCGGGAAGGTGG	75%
HvMADS34T1	GAGGCAAGGTGGTGCTGCAGCGG	65%
HvMADS34T2	CTCGTCCTCTTCTCCCACGCCGG	65%

Table 2: Selected target sequences. PAM sites are indicated in red.

Target sequences were selected to be unique using BLAST in Geneious 8.1.3 (Biomatters Ltd) and close to the start of the genes, in the conserved MADS domain (Table 2). Primers containing the target sequence (without the PAM-site) were used to amplify the guideRNA backbone and the reverse complement of the target sequence for the U6a, U6b or U3 promoter sequence from intermediate vectors pYLgRNA-OsU6a-LacZ and pYLgRNA-OsU6a/b or –OsU3 (Figure 5A; Supplemental table 1). The resulting PCR products were fused by overlap extension PCR using the overlap of the 20bp target site. The individual cassettes were re-amplified using internal primers containing *Bsa*I restriction sites (a restriction enzyme that cuts outside its own recognition site) positioned in such a way that a unique 4-bp overhang is left after digestion. The re-amplified PCR products were then ligated into the destination vector in a combined restriction-ligation reaction, using the Golden Gate system (Engler and Marillonnet, 2014; Ma et al., 2015)(Figure 5A). Constructs were transformed into *E. coli* (DH5α), and subsequently isolated and transformed into *Agrobacterium* (AGL2).

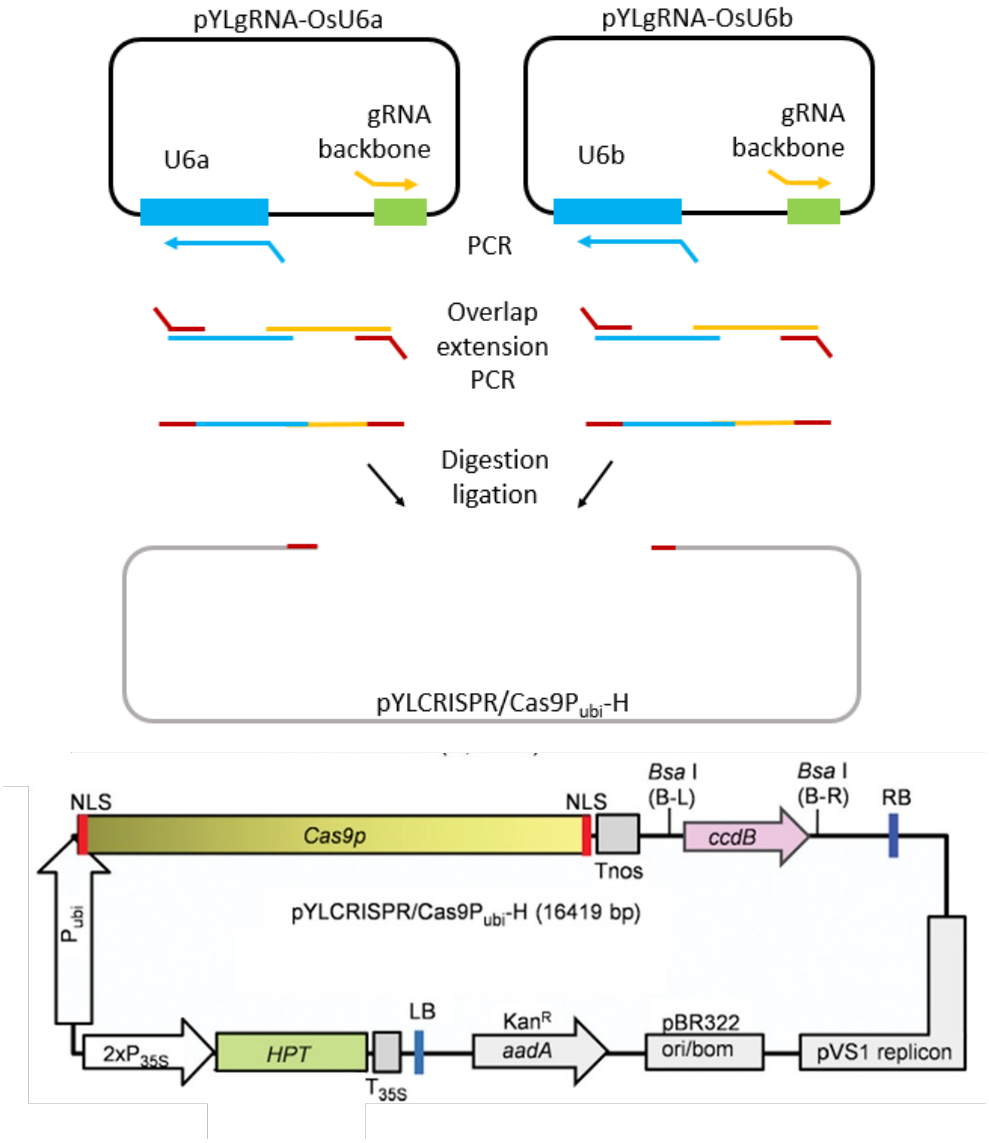

Figure 5: A) Schematic overview of the construction of a two-target CRISPR/Cas9 vector. The targeting cassettes are made separately and with different promoters and ligated together into the destination vector in one digestion/ligation reaction. B) Structure of the pYLCRISPR/Cas9P$_{ubi}$-H vector. One or more guideRNA cassettes were introduced between the *Bsa*I sites. P$_{ubi}$: maize ubiquitin promoter, NLS: nuclear localization signal, Cas9p: plant codon optimized Cas9, BsaI(B-L)/(B-R): BsaI sites left and right for insertion of targeting cassettes, ccdB: toxic gene (negative selection marker), LB/RB: left border and right border used by *Agrobacterium*, HPT: hygromycin B phosphotransferase, P35s: cauliflower mosaic virus 35S promoter.

Plant material

The starting material for barley transformation was harvested from Golden Promise (GP) and WI4330 (WI) plants grown in greenhouses (at least 16h light, no temperature control), growth rooms (16h light at 15°C, 8h dark at 10°C) and the field (Adelaide, May-October). Only barley not sprayed with any pest control agent for at least 3 weeks before collecting the

immature embryos was used. Immature embryos were harvested 11-14 days after pollination, when the immature embryos are 1-2 mm in diameter. Development of immature embryos was assessed by eye, and spikes only selected for transformation if the scutellum was still partly translucent or just turned opaque.

All plants used for phenotyping were grown in sterilised 'coco-peat' soil in 16h days at 15°C and 8h nights at 10°C with a humidity of 70%. A midday light maximum of 500 µmole photons m^{-2} s^{-1} was used.

Barley transformation

The *Agrobacterium*-mediated immature embryo barley transformation was performed according to a published method (Harwood, 2014), except for the following adjustments. Stocks and media were autoclaved instead of filter sterilized (excluding the antibiotics). Seeds were sterilized using a 0.8% sodium hypochlorite solution with 0.1% Tween 20 for 15 minutes, in addition to the ethanol washing steps. *Agrobacterium* was grown to an optical density of 0.8–1 absorbance at 600nm, before co-cultivation. Scutella were kept cut side up during co-cultivation and cut side down on selection media.

Regenerated plants were grown in a greenhouse with limited temperature control (estimated up to 30°C on some days) at a minimum 16h light cycle throughout the year.

Genotyping of transgenic plants

Leaf discs of 5mm diameter were taken from young leaves and used, without a DNA extraction step, as template for PCR amplification using the Phire Plant Direct PCR kit (Thermo Scientific) according to the manufacturer's instructions. Amplified fragments containing the target were sequenced using a commercial sequencing service (Australian Genome Research Facility (AGRF), Adelaide branch). Where necessary heterozygous and multiallelic obtained sequences were analysed with TIDE (tide.nki.nl; (Brinkman et al., 2014)), and further processing was done in Geneious 8.1.3 (Biomatters Ltd). The number of explants is taken at the start of co-cultivation and T0 plants are counted when established in soil. For editing efficiency every non wild-type genotype is counted.

Early inflorescence SEPALLATA expression data

Expression data for SEPALLATA genes during the early stages of barley and rice inflorescence development was collected from the supplementary data provided by Digel et al. (2015) and Harrop et al. (2016) respectively.

References

Abebe T, Wise R, W. Skadsen R (2009) Comparative Transcriptional Profiling Established the Awn as the Major Photosynthetic Organ of the Barley Spike While the Lemma and the Palea Primarily Protect the Seed. The Plant Genome Journal **2**

Agrawal G, Abe K, Yamazaki M, Miyao A, Hirochika H (2005) Conservation of the E-function for floral organ identity in rice revealed by the analysis of tissue culture-induced loss-of-function mutants of the OsMADS1 gene. Plant Molecular Biology **59:** 125-135

Alzueta I, Abeledo LG, Mignone CM, Miralles DJ (2012) Differences between wheat and barley in leaf and tillering coordination under contrasting nitrogen and sulfur conditions. European Journal of Agronomy **41:** 92-102

Angenent GC, Franken J, Busscher M, Vandijken A, Vanwent JL, Dons HJM, Vantunen AJ (1995) A NOVEL CLASS OF MADS BOX GENES IS INVOLVED IN OVULE DEVELOPMENT IN PETUNIA. Plant Cell **7:** 1569-1582

Blum A (1985) Photosynthesis and Transpiration in Leaves and Ears of Wheat and Barley Varieties. Journal of Experimental Botany **36:** 432-440

Bort J, Febrero A, Amaro T, Araus JL (1994) Role of awns in ear water-use efficiency and grain weight in barley. Agronomie **14:** 133-139

Brinkman EK, Chen T, Amendola M, van Steensel B (2014) Easy quantitative assessment of genome editing by sequence trace decomposition. Nucleic acids research **42:** e168-e168

Callens C, Tucker MR, Zhang D, Wilson ZA (2018) Dissecting the role of MADS-box genes in monocot floral development and diversity. J Exp Bot **69:** 2435-2459

Cantalapiedra CP, Boudiar R, Casas AMR, Igartua E, Contreras-Moreira B (2015) BARLEYMAP: physical and genetic mapping of nucleotide sequences and annotation of surrounding loci in barley. Molecular Breeding **35:** 1-11

Christensen AR, Malcomber ST (2012) Duplication and diversification of the LEAFY HULL STERILE1 and Oryza sativa MADS5 SEPALLATA lineages in graminoid Poales. Evodevo **3**

Ciaffi M, Paolacci AR, Tanzarella OA, Porceddu E (2011) Molecular aspects of flower development in grasses. Sexual Plant Reproduction **24:** 247-282

Coen ES, Meyerowitz EM (1991) THE WAR OF THE WHORLS - GENETIC INTERACTIONS CONTROLLING FLOWER DEVELOPMENT. Nature **353:** 31-37

Cui R, Han J, Zhao S, Su K, Wu F, Du X, Xu Q, Chong K, Theissen G, Meng Z (2010) Functional conservation and diversification of class E floral homeotic genes in rice (Oryza sativa). Plant J **61:** 767-781

Digel B, Pankin A, von Korff M (2015) Global Transcriptome Profiling of Developing Leaf and Shoot Apices Reveals Distinct Genetic and Environmental Control of Floral Transition and Inflorescence Development in Barley. Plant Cell **27:** 2318-2334

Dockter C, Gruszka D, Braumann I, Druka A, Druka I, Franckowiak J, Gough SP, Janeczko A, Kurowska M, Lundqvist J, Lundqvist U, Marzec M, Matyszczak I, Müller AH, Oklestkova J, Schulz B, Zakhrabekova S, Hansson M (2014) Induced Variations in Brassinosteroid Genes Define Barley Height and Sturdiness, and Expand the Green Revolution Genetic Toolkit. Plant Physiology **166:** 1912

Dreni L, Zhang D (2016) Flower development: the evolutionary history and functions of the AGL6 subfamily MADS-box genes. Journal of Experimental Botany **67:** 1625-1638

Engler C, Marillonnet S (2014) Golden Gate cloning. Methods Mol Biol **1116:** 119-131

Gao X, Liang W, Yin C, Ji S, Wang H, Su X, Guo C, Kong H, Xue H, Zhang D (2010) The SEPALLATA-like gene OsMADS34 is required for rice inflorescence and spikelet development. Plant Physiol **153:** 728-740

Gasparis S, Kala M, Przyborowski M, Lyznik LA, Orczyk W, Nadolska-Orczyk A (2018) A simple and efficient CRISPR/Cas9 platform for induction of single and multiple, heritable mutations in barley (Hordeum vulgare L.). Plant Methods **14:** 111

Harrop TW, Ud Din I, Gregis V, Osnato M, Jouannic S, Adam H, Kater MM (2016) Gene expression profiling of reproductive meristem types in early rice inflorescences by laser microdissection. Plant J **86:** 75-88

Harwood WA (2014) A protocol for high-throughput Agrobacterium-mediated barley transformation. Methods Mol Biol **1099:** 251-260

Hisano H, Meints B, Moscou MJ, Cistue L, Echavarri B, Sato K, Hayes PM (2017) Selection of transformation-efficient barley genotypes based on TFA (transformation amenability) haplotype and higher resolution mapping of the TFA loci. Plant Cell Rep **36:** 611-620

Khanday I, Yadav SR, Vijayraghavan U (2013) Rice LHS1/OsMADS1 Controls Floret Meristem Specification by Coordinated Regulation of Transcription Factors and Hormone Signaling Pathways. Plant Physiology **161:** 1970-1983

Kobayashi K, Maekawa M, Miyao A, Hirochika H, Kyozuka J (2010) PANICLE PHYTOMER2 (PAP2), encoding a SEPALLATA subfamily MADS-box protein, positively controls spikelet meristem identity in rice. Plant Cell Physiol **51:** 47-57

Koppolu R, Anwar N, Sakuma S, Tagiri A, Lundqvist U, Pourkheirandish M, Rutten T, Seiler C, Himmelbach A, Ariyadasa R, Youssef HM, Stein N, Sreenivasulu N, Komatsuda T, Schnurbusch T (2013) Six-rowed spike4 (Vrs4) controls spikelet determinacy and row-type in barley. Proc Natl Acad Sci U S A **110:** 13198-13203

Lawrenson T, Shorinola O, Stacey N, Li C, Ostergaard L, Patron N, Uauy C, Harwood W (2015) Induction of targeted, heritable mutations in barley and Brassica oleracea using RNA-guided Cas9 nuclease. Genome Biol **16:** 258

Li X, Wang H, Li H, Zhang L, Teng N, Lin Q, Wang J, Kuang T, Li Z, Li B, Zhang A, Lin J (2006) Awns play a dominant role in carbohydrate production during the grain-filling stages in wheat (Triticum aestivum). Physiologia Plantarum **127:** 701-709

Liller CB, Walla A, Boer MP, Hedley P, Macaulay M, Effgen S, von Korff M, van Esse GW, Koornneef M (2017) Fine mapping of a major QTL for awn length in barley using a multiparent mapping population. Theor Appl Genet **130:** 269-281

Lim WL, Collins HM, Singh RR, Kibble NAJ, Yap K, Taylor J, Fincher GB, Burton RA (2018) Method for hull-less barley transformation and manipulation of grain mixed-linkage beta-glucan. Journal of Integrative Plant Biology **60:** 382-396

López-Castañeda C, Molero G, Reynolds M (2014) Genotypic variation in light interception and radiation use efficiency: A comparison of two different planting systems,

Ma X, Zhang Q, Zhu Q, Liu W, Chen Y, Qiu R, Wang B, Yang Z, Li H, Lin Y, Xie Y, Shen R, Chen S, Wang Z, Chen Y, Guo J, Chen L, Zhao X, Dong Z, Liu YG (2015) A Robust CRISPR/Cas9 System for Convenient, High-Efficiency Multiplex Genome Editing in Monocot and Dicot Plants. Mol Plant **8:** 1274-1284

Ma XL, Zhang QY, Zhu QL, Liu W, Chen Y, Qiu R, Wang B, Yang ZF, Li HY, Lin YR, Xie YY, Shen RX, Chen SF, Wang Z, Chen YL, Guo JX, Chen LT, Zhao XC, Dong ZC, Liu YG (2015) A Robust CRISPR/Cas9 System for Convenient, High-Efficiency Multiplex Genome Editing in Monocot and Dicot Plants. Molecular Plant **8:** 1274-1284

Malcomber ST, Kellogg EA (2005) SEPALLATA gene diversification: brave new whorls. Trends in Plant Science **10:** 427-435

Müller KJ, Romano N, Gerstner O, Garcia-Marotot F, Pozzi C, Salamini F, Rohde W (1995) The barley Hooded mutation caused by a duplication in a homeobox gene intron. Nature **374:** 727-730

Murai K (2013) Homeotic Genes and the ABCDE Model for Floral Organ Formation in Wheat. Plants-Basel **2:** 379-395

Ohmori S, Kimizu M, Sugita M, Miyao A, Hirochika H, Uchida E, Nagato Y, Yoshida H (2009) MOSAIC FLORAL ORGANS1, an AGL6-like MADS box gene, regulates floral organ identity and meristem fate in rice. Plant Cell **21:** 3008-3025

Palta JA, Fillery IRP, Rebetzke GJ (2007) Restricted-tillering wheat does not lead to greater investment in roots and early nitrogen uptake. Field Crops Research **104:** 52-59

Pelaz S, Ditta GS, Baumann E, Wisman E, Yanofsky MF (2000) B and C floral organ identity functions require SEPALLATA MADS-box genes. Nature **405:** 200-203

Prasad K, Parameswaran S, Vijayraghavan U (2005) OsMADS1, a rice MADS-box factor, controls differentiation of specific cell types in the lemma and palea and is an early-acting regulator of inner floral organs. Plant Journal **43:** 915-928

Rebetzke GJ, Bonnett DG, Reynolds MP (2016) Awns reduce grain number to increase grain size and harvestable yield in irrigated and rainfed spring wheat. Journal of Experimental Botany **67:** 2573-2586

Schmitz J, Franzen R, Ngyuen TH, Garcia-Maroto F, Pozzi C, Salamini F, Rohde W (2000) Cloning, mapping and expression analysis of barley MADS-box genes. Plant Mol Biol **42:** 899-913

Vegetti A, Anton AM (1995) SOME EVOLUTION TRENDS IN THE INFLORESCENCE OF POACEAE. Flora **190:** 225-228

Waddington SR, Cartwright PM, Wall PC (1983) A Quantitative Scale of Spike Initial and Pistil Development in Barley and Wheat. Annals of Botany **51:** 119-130

Wang F, Cheng F-m, Zhang G-p (2007) Difference in Grain Yield and Quality among Tillers in Rice Genotypes Differing in Tillering Capacity. Rice Science **14:** 135-140

Wang H, Chen W, Eggert K, Charnikhova T, Bouwmeester H, Schweizer P, Hajirezaei MR, Seiler C, Sreenivasulu N, von Wirén N, Kuhlmann M (2018) Abscisic acid influences tillering by modulation of strigolactones in barley. Journal of experimental botany **69:** 3883-3898

Wang KJ, Tang D, Hong LL, Xu WY, Huang J, Li M, Gu MH, Xue YB, Cheng ZK (2010) DEP and AFO Regulate Reproductive Habit in Rice. Plos Genetics **6**

Wang T, Wei JJ, Sabatini DM, Lander ES (2014) Genetic screens in human cells using the CRISPR-Cas9 system. Science **343:** 80-84

Wong GK, Wang J, Tao L, Tan J, Zhang J, Passey DA, Yu J (2002) Compositional gradients in Gramineae genes. Genome Res **12:** 851-856

Wu D, Liang W, Zhu W, Chen M, Ferrandiz C, Burton RA, Dreni L, Zhang D (2018) Loss of LOFSEP Transcription Factor Function Converts Spikelet to Leaf-Like Structures in Rice. Plant Physiol **176:** 1646-1664

Yuo T, Yamashita Y, Kanamori H, Matsumoto T, Lundqvist U, Sato K, Ichii M, Jobling SA, Taketa S (2012) A SHORT INTERNODES (SHI) family transcription factor gene regulates awn elongation and pistil morphology in barley. J Exp Bot **63:** 5223-5232

Zahn LM, King HZ, Leebens-Mack JH, Kim S, Soltis PS, Landherr LL, Soltis DE, dePamphilis CW, Ma H (2005) The evolution of the SEPALLATA subfamily of MADS-Box genes: A preangiosperm origin with multiple duplications throughout angiosperm history. Genetics **169:** 2209-2223

Zhang H, Zhang J, Wei P, Zhang B, Gou F, Feng Z, Mao Y, Yang L, Zhang H, Xu N, Zhu JK (2014) The CRISPR/Cas9 system produces specific and homozygous targeted gene editing in rice in one generation. Plant Biotechnol J **12:** 797-807

Supplemental data

Supplemental table 1: primers used

CRISPR/Cas9 mutant generation			
target gene	Gene ID	Primer name	Primer sequence (5' to 3')
MADS1	HORVU4Hr1G067680	N01OsU6aSEP1T1	CCTCATCTCCACCTTCCCACGGCAGCCAAGCCAGCA
		N02gRSEP1T1	GTGGGAAGGTGGAGATGAGGGTTTTAGAGCTAGAAA T
		N03OsU6bSEP1T2	GAGAAGATGATGAGGGCGACAACACAAGCGGCAGC
		N04gRSEP1T2	GTCGCCCTCATCATCTTCTCGTTTTAGAGCTAGAAAT
MADS5	HORVU7Hr1G025700	N35OsU6bSEP2	CCTTCCCGCGCCCCATCCTGCAACACAAGCGGCAGC
		N36gRSEP2	CAGGATGGGGCGCGGGAAGGGTTTTAGAGCTAGAAA T
MADS34	HORVU5Hr1G095710	N05OsU6aSEP3T1	CTGCAGCACCACCTTGCCTCGGCAGCCAAGCCAGCA
		N06gRSEP3T1	GAGGCAAGGTGGTGCTGCAGGTTTTAGAGCTAGAAAT
		N07OsU6bSEP3T2	GCGTGGGAGAAGAGGACGACAACACAAGCGGCAGC
		N08gRSEP3T2	GTCGTCCTCTTCTCCCACGCGTTTTAGAGCTAGAAAT
MADS6	HORVU6Hr1G066140	N361M6CRISPROsU6b	GTTGATCTTGTTCTCGATGCAACACAAGCGGCAGC
		N362M6CRISPRgRT2	GCATCGAGAACAAGATCAACGTTTTAGAGCTAGAAAT
Generic CRISPR primers (Ma et al., 2015):			
Internal amplification		Pps-GGL	TTCAGAggtctcTctcgACTAGTATGGAATCGGCAGCAAAG G
		Pgs-GG2	AGCGTGggtctcGtcagggTCCATCCACTCCAAAGCTC
		Pps-GG2	TTCAGAggtctcTctgacacTGGAATCGGCAGCAAAGG
		Pgs-GGR	AGCGTGggtctcGaccgACGCGTATCCATCCACTCCAAGCT C
Genotyping			
target gene	Gene ID	Primer name	Primer sequence (5' to 3')
MADS1	HORVU4Hr1G067680	N54IDAA400SEP1F	GATCAGACATCGCTCTGCTGGC
		N48IDAA400SEP1R	CATGAAGGAAAGCTGCGGCAG
MADS5	HORVU7Hr1G025700	N71IDAA400SEP2F	GCTAGCGCTATCCGATCCGAG
		N70IDAA1kSEP2R	GGACACAGCAATCAAATCTTTCCCC
MADS34	HORVU5Hr1G095710	N55IDAA400SEP3F	CATGCCATCCTAGCTCGCCC
		N50IDAA400SEP3R	GATCCACGCCGCAAAATCAGAAAG
MADS6	HORVU6Hr1G066140	N52IDAA400AGL6R	GGAACAGCGGAGAAGCTAGGC
		N56IDAA400AGL6F	GTGTTAGTAGGTGGCACCGCC

Chapter 4: The *hvmads1* mutant has a branched inflorescence when grown at high ambient temperature

4.1 Abstract

The *hvmads1* mutant spike phenotypes of reduced awn length, fertility changes and reduced seed weight becomes more complex when grown at high ambient temperature. The mutant spike develops some branch like structures in the lower half of the spike, changing the inflorescence morphology so it more closely resembles rice or maize panicles, partially reverting to the presumed ancestral branching inflorescence morphology. Branches form in place of the central spikelets and often produce an axillary spikelet that resembles the wild type spikelet, suggesting that the branch meristem may be present as a short-lived intermediary in wild type barley as well.

Expression analysis by RNAseq shows that the increased ambient temperature is the cause of the differential expression of most differentially expressed genes (DEGs). The increased number of DEGs in *hvmads1* at high temperature compared to the number of DEGs related to the mutation and those related to the temperature increase combined, shows interaction between *HvMADS1* and the temperature response pathway. The expression of several genes shows significant correlation with the branching phenotype. Reduced expression of C-class genes *HvMADS3* and *HvMADS58* indicate a delay in floret formation. Increased expression of heat shock factors, but not heat shock proteins, suggests the mutant may be sensitised to higher temperatures. The increased expression of *HvODDSOC* may be involved in the delay of spikelet initiation, since this MADS-box gene has been previously associated with outgrowth of axillary meristems in early inflorescence development in barley.

4.2 Introduction

Inflorescence branching

The agriculturally important *Triticeae*, such as wheat and barley, have an unbranching spike style of inflorescence architecture, but the ancestral shape is a branching inflorescence (Vegetti and Anton, 1995; Kellogg et al., 2013; Remizowa et al., 2013), which implies it may be possible to revert a spike to a panicle with few adaptations. While a branching

inflorescence mutant may be of interest for breeding higher yielding new varieties (Sreenivasulu and Schnurbusch, 2012), very few have been reported (Echeverry-Solarte et al., 2014; Poursarebani et al., 2015), suggesting multiple mutations may be needed to achieve full reversion. Supernumerary spikelets, the collective term including very weak variants, is more common, and has been reported, but sometimes also requires multiple mutations (Sun et al., 2009; Boden et al., 2015).

Rice and the maize tassel have a branching inflorescence, called a panicle, and may provide insight into the morphology and regulation of a hypothetical barley panicle. Grass inflorescences develop from a series of specialised inflorescence axillary meristem types. The most relevant developmental difference between the panicle of rice and maize and the barley spike is the absence of a branch meristem in the developing barley inflorescence (Bommert et al., 2005; Ciaffi et al., 2011; Tanaka et al., 2013). Several genes reported as important for inflorescence architecture act on the initiation of axillary meristems in the inflorescence, such as the AUX/IAA-like *BARREN INFLORESCENCE* genes that are involved in the auxin signalling required for branch initiation in the maize inflorescence (Galli et al., 2015). However, the barley inflorescence does generate axillary meristems, so definition of the genes governing the *identity* of the branch meristem are more likely to illuminate the molecular differences underlying the altered inflorescence morphology. Laser dissection of inflorescence meristem types in rice followed by RNA sequencing has provided a wealth of expression data for the branch meristem. This large repository of differentially expressed genes shows that the branch meristem can be distinguished from the shoot apical meristem (SAM) it emerges from and the spikelet meristems it produces. Several gene families alter expression significantly through development: transcript level of the AUX-IAA-like family declines upon the transition from the SAM to the branch meristem, while the expression of the PHD-like family, a family with diverse functions named after a motif found in plant homeodomain proteins, strongly increases (Harrop et al., 2016). Individual genes are enriched in the branch meristem as well, such as *OsMADS34*, which has a role in inflorescence architecture, as demonstrated by the alterations in panicle branching in *osmads34* mutants (Gao et al., 2010; Kobayashi et al., 2010; Meng et al., 2017).

Responses to high ambient temperature

Plants are unable to relocate and have to adjust to fluctuating environmental temperatures. When the temperature surpasses a heat threshold, protective heat stress responses are activated. The temperature range above the optimal temperature, but below the point of heat stress is considered to be high ambient temperature. High ambient temperature has many regulatory effects in plants, such as altered prevalence of histone variants, DNA methylation, alternative splicing, protein degradation and protein localisation. These primary responses can lead to secondary responses such as changes to the circadian clock and hormone signalling (Susila et al., 2018)

High ambient temperature results in early flowering in barley under long day conditions (Aspinall, 1969; Ejaz and von Korff, 2017). While *FLOWERING LOCUS T* (*FT*) mediates acceleration of flowering by high ambient temperature under long day conditions in *Arabidopsis* (Blázquez et al., 2003), the FT-like genes in barley are not likely to be involved in high temperature responses because FT-like genes are not upregulated in high temperature growth conditions and artificially high expression of FT-like genes does not accelerate flowering in barley (Hemming et al., 2012). Instead, the vernalisation related genes *HvMADS14* (*HvVRN1*) and *HvODDSOC2* (*HvOS2*) have been implicated in the high temperature response of flowering time in barley (Hemming et al., 2012). The MADS-box gene *HvOS2* belongs to a cereal specific clade within the type-I MADS-box genes, together with its homolog *OsMADS51* (Greenup et al., 2009; Kapazoglou et al., 2012). Plants overexpressing *HvOS2* showed reduced expression of *FLOWERING PROMOTING FACTOR1* (*FPF1*), a gene that promotes floral development and enhances cell elongation (Greenup et al., 2010).

Heat stress responses

Heat stress responses in eukaryotes are mediated by heat stress factors (Hsfs) that are transcription factors that activate heat responses through binding to heat shock elements in the promoters of effector genes. One of the upregulated families are the heat shock proteins (Hsps), which assist in maintaining protein folding to stabilise other proteins, among other roles, thereby mitigating the denaturing effect of heat. While vertebrates have only 3 Hsfs, plants have 20 or more, which can be divided into A-, B-, and C-class Hsfs. *HsfA1* is a master regulator of heat response in tomato, responsible for transcription of *HsfA2* and *HsfB1*. *HsfB1*

acts as an enhancer for *HsfA1* and *HsfA2* and is involved with keeping housekeeping genes expressed properly during heat stress and recovery. *HsfA2* acts as a cumulative response to heat stress by accumulating in cytoplasmic complexes, and migrating to the nucleus by hetero-oligomerisation with *HsfA1*, or activation by *Hsp17* (Baniwal et al., 2004). Hsf and Hsp expression levels have been linked to differences in heat tolerance in rice cultivars (Chandel et al., 2012).

High temperature affects the *hvmads1* phenotype

The *hvmads1* mutant has increased tillering and reduced awn growth at the optimal growth temperature of 15°C for Golden Promise (Chapter 3). However, when the first *hvmads1* generation was grown in less controlled and warmer greenhouse conditions, additional spikelets were occasionally observed, wedged within the row of central spikelets, suggesting that a high ambient temperature may trigger additional morphological changes. Temperature dependant changes in the affinity of MADS-box transcription factors for their CArG box recognition sites have been reported in *Arabidopsis* (Muino et al., 2014), so in barley HvMADS1 affinity for promoter sequences may be directly influenced by ambient temperature, or *HvMADS1* may interact with other pathways induced by high ambient temperature. To test the effects of a high ambient temperature on the *hvmads1* phenotype, these plants were grown under hotter conditions and plant responses monitored.

4.3 Results

The *hvmads1* mutant spike shows branching at high ambient temperature

When grown at 15°C the only spike phenotype of the *hvmads1* mutant compared to the Golden Promise (GP) wild type is the shorter awns (Figure 1A). However, when grown at a high ambient temperature of 28°C during early inflorescence development the *hvmads1* mutant spike shows a branching phenotype, while the wild-type shows no change in spike morphology apart from an occasional slight colouring of the spikelets (Figure 1B). The apparent branching of the mutant spike is more pronounced at the base of the spike, where the branches are longer and bending of the rachis can be seen, and gradually decreases towards the top, where no branches are observed. The branching is only observed in the positions of the central spikelet and does not seem to affect the fertility and outgrowth of the lateral spikelets.

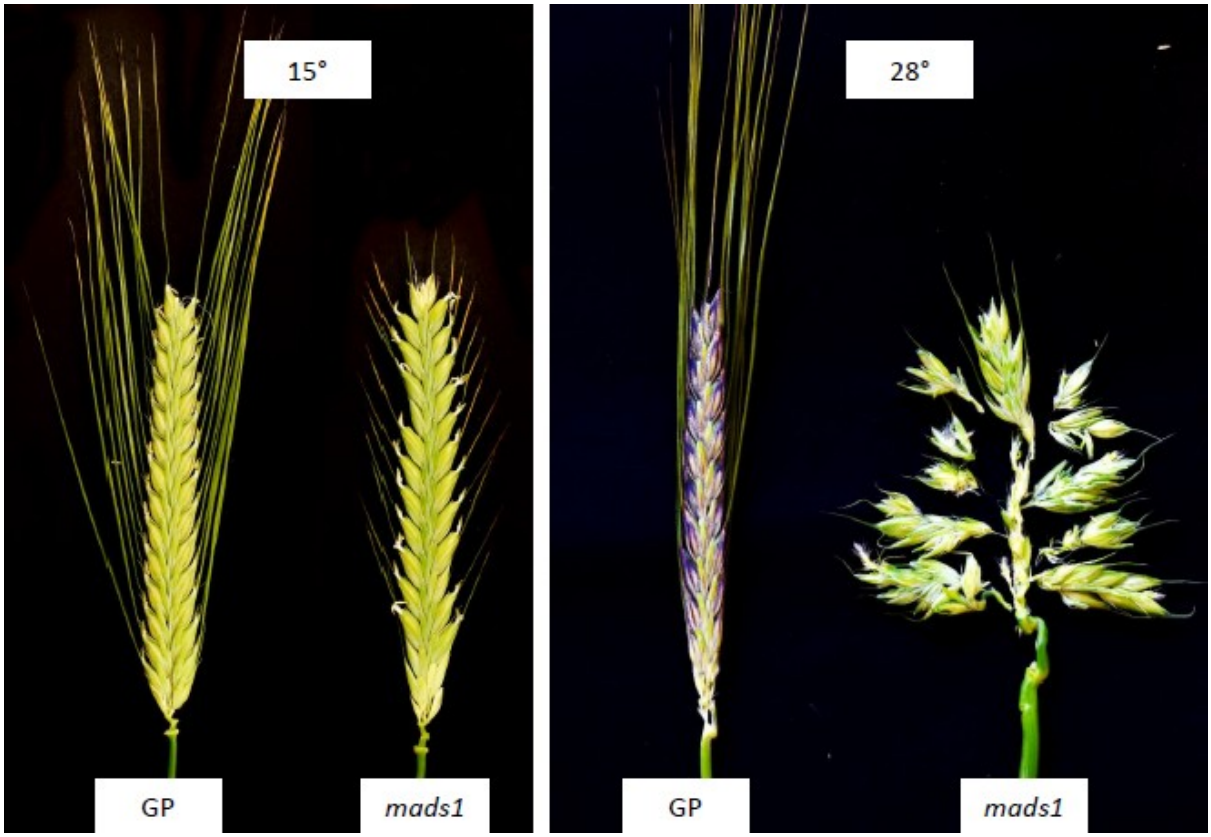

Figure 1: Spike phenotype of GP and *mads1* at 15°C and 28°C. A) Short awn phenotype of the *hvmads1* mutant at 15°C compared to the GP wild type. B) Kindly provided by Dr. Gang Li. Branching spike phenotype of the *hvmads1* mutant grown at 28°C during early inflorescence development (up to W7) compared to the wild type grown at high temperature.

To get a clear mature phenotype the plants were transferred from 28°C to 15°C after the inflorescence architecture had been established. Some central spikelets were removed to highlight the branching structure.

The morphology of many *hvmads1* HT spikelets is aberrant

The spikelets of the GP wild type and *hvmads1* at 15°C develop normally, as do the spikelets of GP grown at 28°C during early inflorescence development (figure 2A-D). In the *hvmads1* mutant, grown at high ambient temperature during early inflorescence development (W1-W7), the spikelets are often replaced by a small branch like structure which supports multiple spikelets (Figure 2E-H). These branch like structures can contain multiple fertile spikelets that develop normally, but often have several spikelets that develop only partially, or with aberrant morphology. Some of these spikelets have outgrowths from within the floret, indicating floret determinacy may be compromised. The aberrant morphology may be partially due to the limited space available for the developing inflorescence in barley as the physical constraint of the sheath does not account for a branching inflorescence. Therefore a more structured view of the nature of these branch-like structures may be obtained earlier in development.

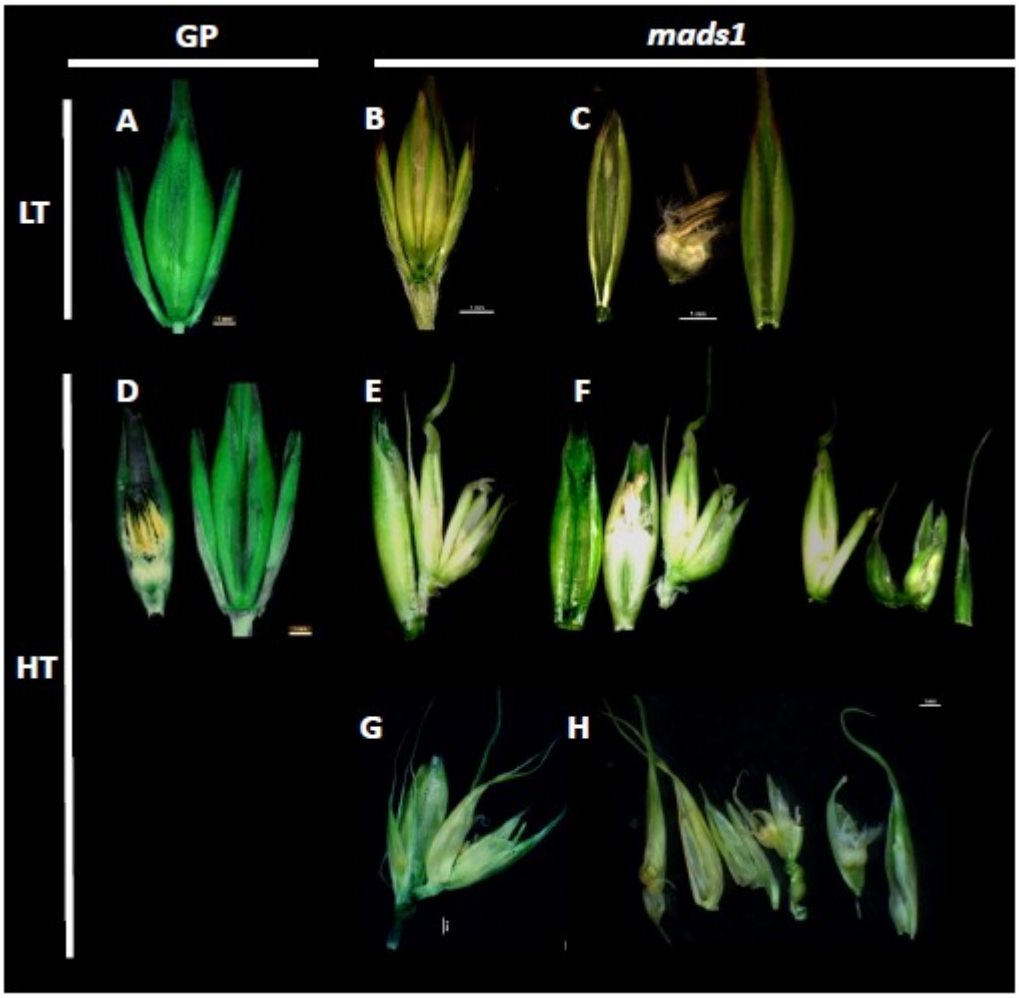

Figure 2: Spikelet phenotypes of GP and *hvmads1* grown at low and high ambient temperatures. A) GP grown at low temperature. B, C) *hvmads1* at low temperature, opened floret in C showing floral organs. D) GP at high temperature, opened to show floral organs. E,F,G,H) *hvmads1* at high temperature showing a branch like structure in E,G and these structures opened up in F and H respectively. Pictures G and H were kindly provided by Dr. Gang Li.

Branches form at the position of the central spikelets, but do not always develop fully

The earliest observable mutant phenotype of *hvmads1* at HT is an elongation of the central 'spikelet' meristem after W2.5, where the wild type would progress to the floret meristem and lemma primordium at W3 (Figure 3-I). Not all of these outgrowing meristems develop into branches bearing more than one spikelet. Some cease growth and are later dwarfed by the accompanying spikelet, visible only as an extra meristem within the file of central spikelets at W4 (Figure 3-II, 3-III). At 28°C GP spikes develop normally, except for the rare (arrested) additional meristem on some inflorescence meristems (Figure 3-III D, E). At W2

(double ridge stage) there is no difference between the GP and *hvmads1* meristem (Figure 3-III A, G), and at W2.5, when the central spikelet meristem starts to grow at about one third from the bottom of the spike, GP and *hvmads1* still look almost identical (Figure 3-III B, H). At W3 the floret meristem and lemma primordium have formed in GP, but in the *hvmads1* mutant the central meristem grows out instead of differentiating (Figure 3-III C, I, J). The branch like outgrowths produce lateral meristems that develop into spikelets in some of the mutant inflorescences (Figure 3-III K, L), occasionally with additional meristems between the spikelets, possibly indicating underdeveloped secondary branches. In other *hvmads1* mutant spikes however, the outgrowths do not fully develop into branch-like structures and are only visible as additional meristems between the main row spikelets (Figure 3-III M, N). When grown at 15°C neither GP nor *hvmads1* inflorescence meristems have any additional meristems developing between the spikelets (Figure 3-III P, R).

Cell division is an early sign of additional meristem development

5-ethynyl-2'-deoxyuridine (EdU) staining is a way to visualise dividing cells within a tissue sample. EdU is added to living tissue, and will be incorporated into newly synthesised DNA. After fixing the sample, a fluorescent label that can attach to the EdU is added, and labelled DNA can be observed by excitation of the fluorophore. Applying this to inflorescence meristems grown at high ambient temperature shows that the most actively dividing tissues within the GP inflorescence meristem are the developing spikelets (Figure 4A GP; Supplemental figure 3). The same can be observed in the *hvmads1* mutant, with additional cell division visible in tissue between the spikelets (Figure 4A arrow heads). The PI stained red cells show this additional dividing tissue is attached to the spikelets, especially in the righthand image, where only the optical layers including the additional tissue are shown (Figure 4A).

3-I **3-II**

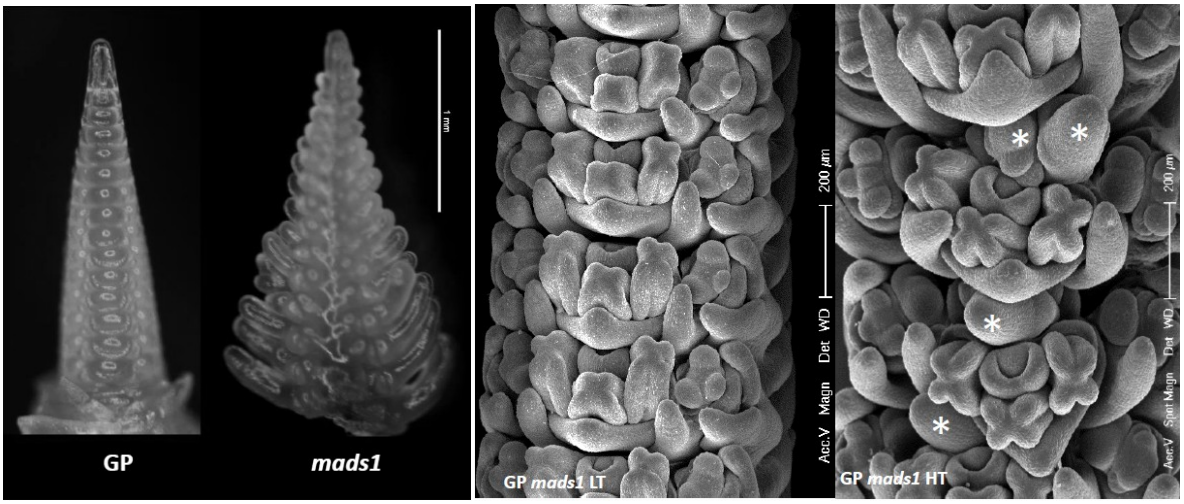

3-III

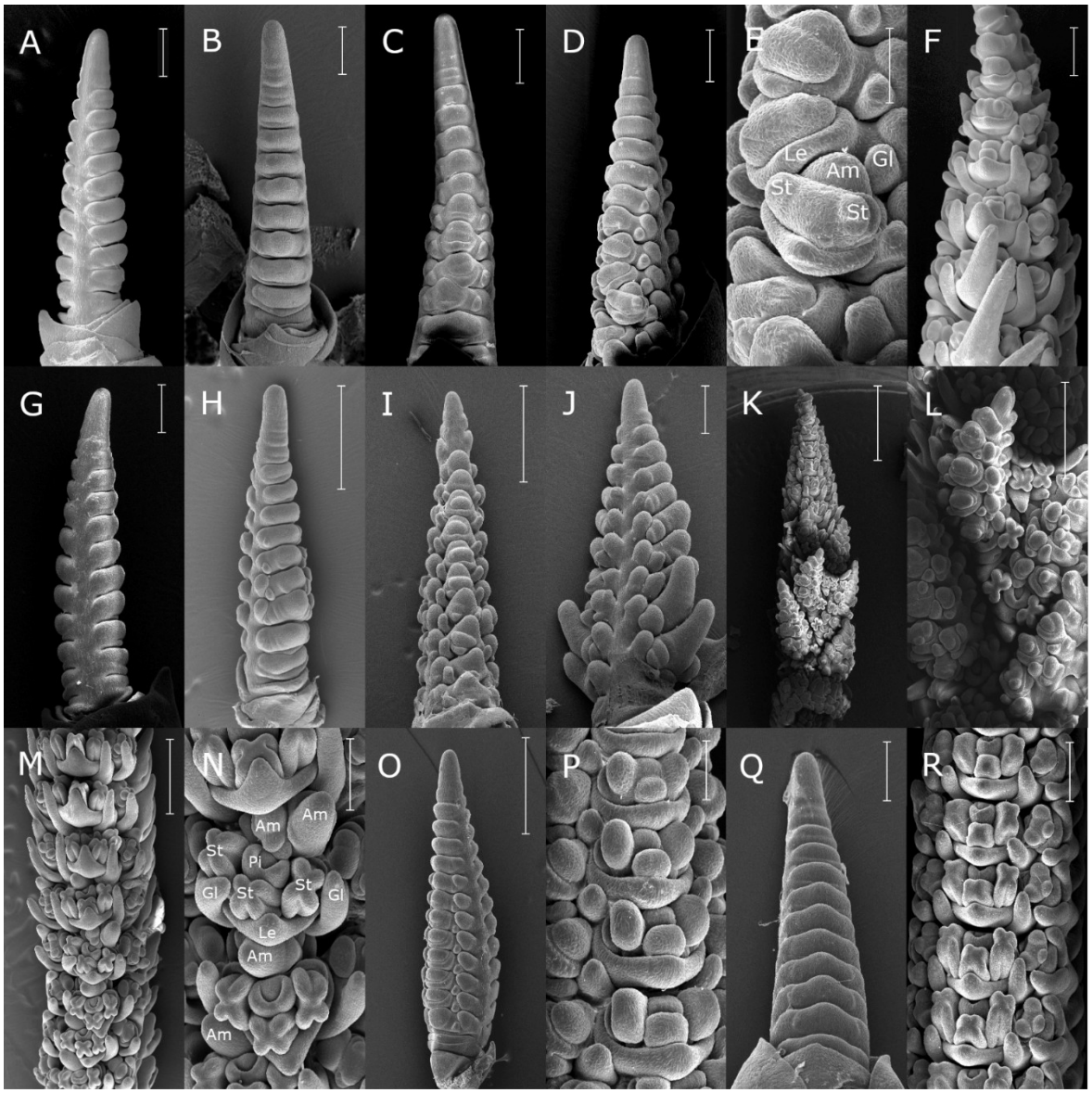

Figure 3: Early branching inflorescence meristem phenotypes of *hvmads1* as compared to GP wild-type. **I**) In wild-type GP the central axillary meristem turns into a floret meristem at

Waddington stage 3, and forms the lemma primordium. The *hvmads1* mutant grown at high ambient temperature produces outgrowing meristematic tissue instead and only later develops spikelets and florets. **II**) The branch-like outgrowths are often overtaken by spikelets later (here shown at W4), leaving them as undifferentiated growths (indicated with stars) within the files of central spikelets. **III**A-F) young GP inflorescence meristems grown at 28°C. 3G-N) Young *mads1* inflorescence meristems grown at 28°C. 3O-R) Young GP and *mads1* inflorescence meristems grown at low ambient temperature. Am = additional meristem, Gl = glume primordium, Le = lemma, Pi = pistil, St = stamen. White scale bars are 200 µm, except H,I,L,M,O are 500 µm, E and P bars are 100 µm and K is 1mm.

HvMADS1 is weakly expressed in the spikelet primordium, but more strongly in older spikelets

HvMADS1 expression in the developing barley inflorescence starts after W2, and increases up to W9.5 (Chapter 2). RNA *in situ* hybridisation shows that *HvMADS1* is expressed in the spikelet primordia at W2.5 (Figure 4F, G), the same stage where the *hvmads1* phenotype first diverges from GP. *HvMADS1* expression at W3.5 is stronger, and still confined to the developing spikelets (Figure 4H). When the floral organs mature *HvMADS1* is expressed mostly in the lemma and palea, and weakly in the carpel (Chapter 2).

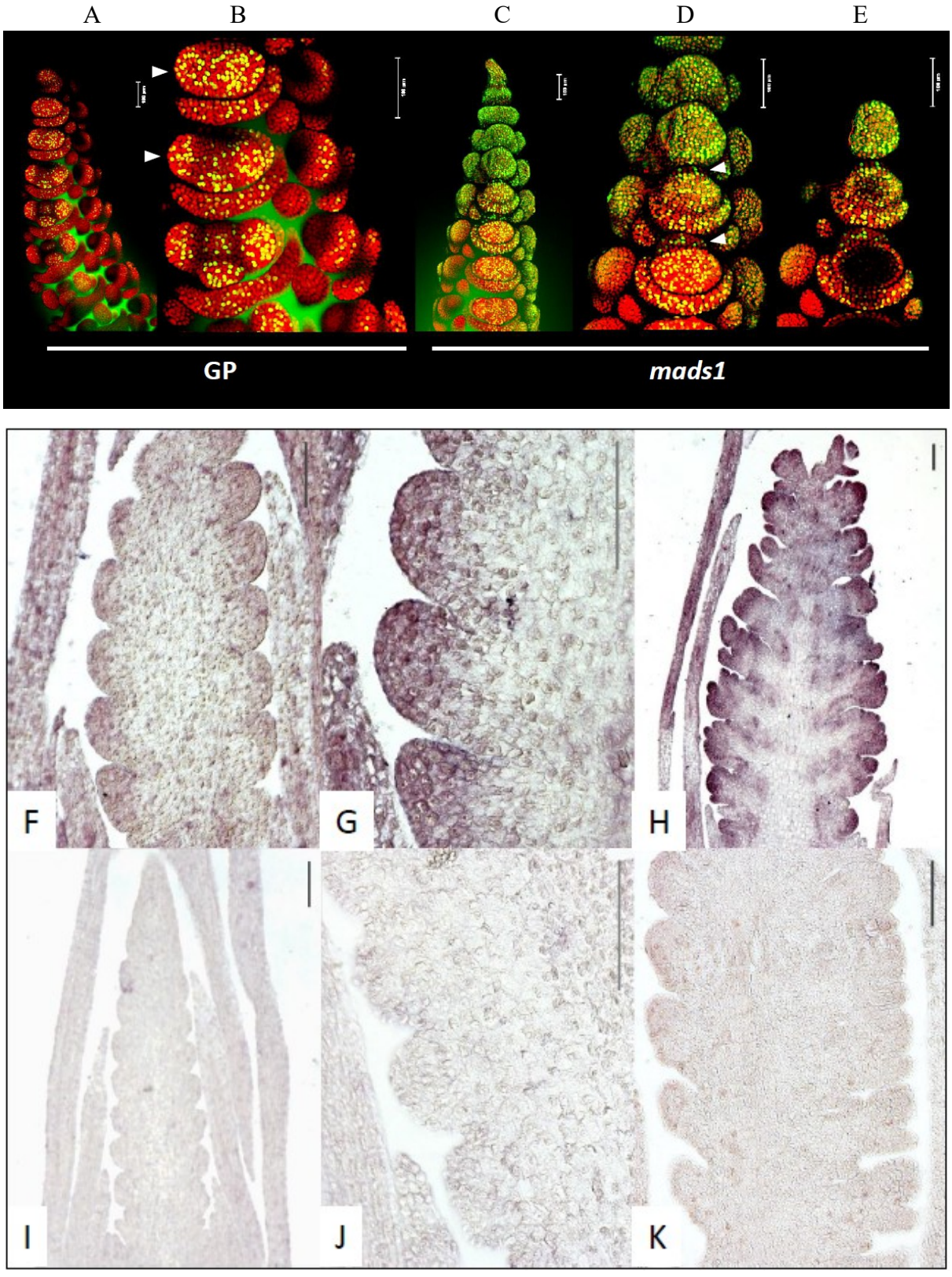

Figure 4: A-E) Young inflorescence meristems labelled with an EdU fluorescent marker for cell division. Fluorescence is mostly localised in the developing spikelets and the tip of the inflorescence meristem. In GP (A, B), fluorescence is visible in the spikelets (arrowheads), with no additional tissue between the spikelets. In the *hvmads1* mutant (C-E) PI staining (red) shows a growth between the spikelets, and the fluorescence indicates this tissue is dividing

(arrowheads). Picture E is a stack of just the optical layers that include the extra dividing tissue, showing that the dividing tissue is attached at the base of the spikelet. F-K) *HvMADS1 in situ* hybridisation in developing inflorescence meristems. At W2.5 (F,G, sense probe I,J) *HvMADS1* expression is weak and localised in the lateral meristems of the inflorescence. At W3.5 (H, sense probe K) *HvMADS1* expression is stronger but still confined mostly to the developing spikelet and floret. Scale bars = 100µm.

Transcript analysis by RNA sequencing

With the phenotype described from its first appearance, the next questions are "What is the nature of this branch-like outgrowth?", "What type of meristem is formed?" and "What triggers this deviation from normal barley inflorescence development?" To get more detailed information, transcript patterns were examined. GP wild type and *hvmads1* mutant barley was grown at 15°C (LT) and 25°C (HT) and whole inflorescence meristem samples collected at W2.5, when the phenotype probably starts, and W3.5, when there is an appreciable amount of the branch-like tissue present. From the resulting 8 samples (collected in triplicate) RNA was extracted and sequenced. Clean reads averaged 46 million per biological replicate and of the clean reads 90-92% was mapped to exons. The comparisons of the biological replicates used were all over a Pearson coefficient squared R^2>0.96. A Pearson correlation analysis between the 8 samples shows that correlation between all samples is high (0.92), with temperature responsible for most of the differential expression. The second most influential factor is the phenotype (0.96), which sets the mutant grown at high temperature to W3.5 (MUHT35) apart, and finally the *hvmads1* mutation and the developmental stage correlate with fewer DEGs, especially at low ambient temperature (Figure 6A).

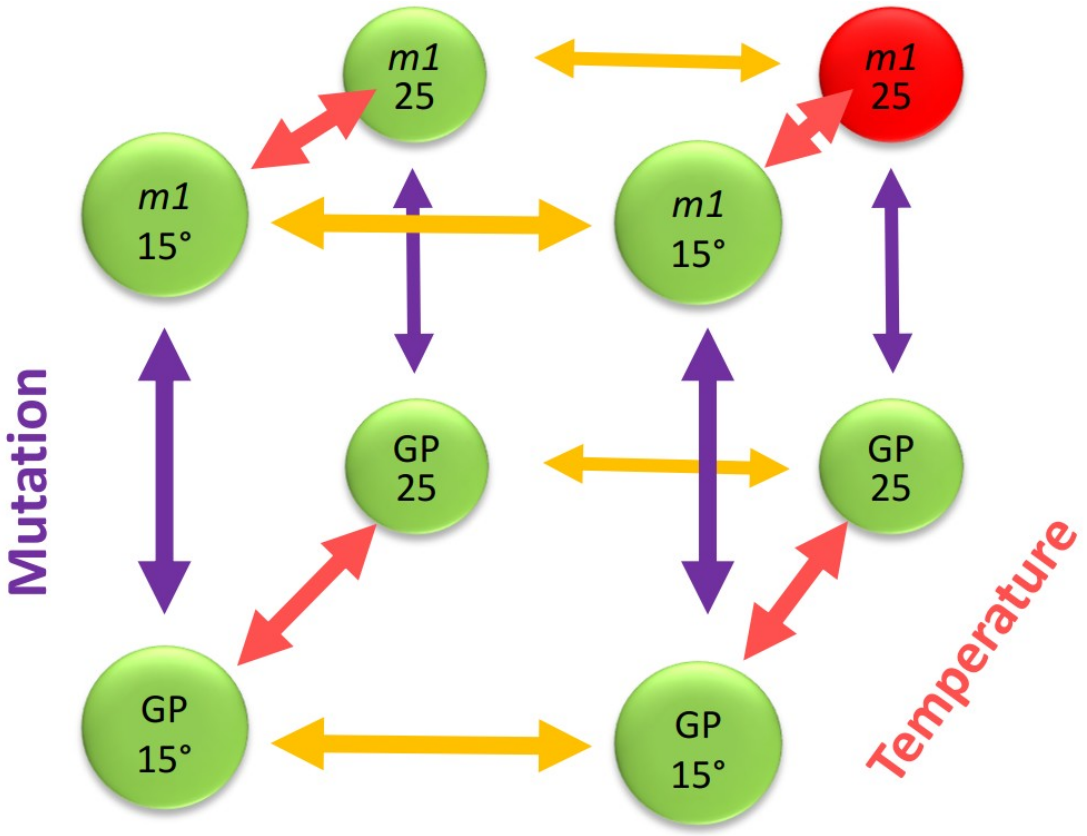

Figure 5: RNA-seq setup overview. Gene expression from 8 samples from GP and the *hvmads1* mutant at two temperatures (15°C and 25°C) and two developmental stages (Waddington stage 2.5 and 3.5) was analysed, depicted as eight globes in the figure. The red globe (*m1*-25°C-3.5) represents the only incidence of the branching phenotype. While changing only one variable at a time, these datasets can be compared pairwise in 12 ways, shown as arrows in the figure. The four purple arrows represent DEGs correlated to the *mads1* mutation, orange arrows for DEGs correlated with progression through developmental stages, and red arrows indicate DEGs correlated to heightened ambient temperature.

DEGs can be organised by three variables: *hvmads1* mutation, temperature and developmental stage

The 8 samples cover three variables which are mutant vs no mutant (MU vs GP), stage (W2.5 vs W3.5) and temperature (LT vs HT). Only one of the 8 samples contains the branching phenotype (MUHT35) and one may provide regulatory clues for the initiation of the branch like meristem (MUHT25). To distinguish the gene expression related to the phenotype from the effects of just one of the variables, like heat, it is important to see DEGs associated with HT in general. While changing only one variable at a time, the expression datasets from the 8 samples can be compared pairwise in 12 ways (Figure 5). This results in four DEG lists where temperature is the only variable, under different circumstances, and similarly four

DEG lists where the only variable is the *hvmads1* mutation. The last four lists of DEGs are related to the change in developmental stage from W2.5 to W3.5.

Global comparison of DEGs shows temperature is the most influential parameter

One way to visualise the DEG lists is in a Venn diagram, although this format is not suitable to show all 12 DEG lists simultaneously. A comparison of DEGs (p_{adj}<0.01) for all combinations of mutation and temperature at stage W2.5 shows that high amounts of DEGs correlate with changes in temperature (GP and MU 602 DEGs (green and yellow overlap)), and this is even more prominent in the mutant alone (MU 2599 DEGs (yellow alone); Figure 6B). The same pattern can be observed at W3.5 where a change in temperature correlates with many DEGs (yellow and green overlap, 2147 DEGs). The number of DEGs related to the branching inflorescence phenotype (red and yellow), but not the *hvmads1* mutation at LT (blue), or the temperature change in GP (green) is 476. These 476 differentially expressed genes may be associated with the branching tissue and/or the possible branch meristem. However, some of these DEGs may still be associated with developmental stage. Additionally there is no indication of the direction of change, which should be the same in order to qualify as a candidate for a potential branch meristem-associated gene.

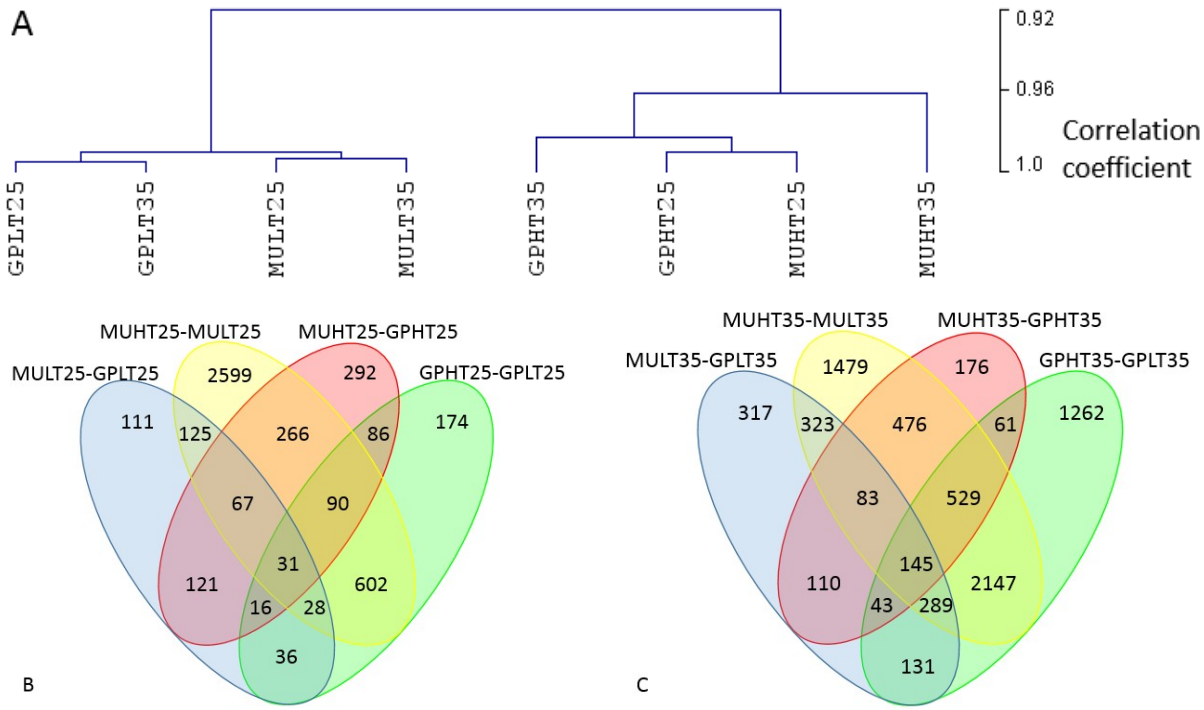

Figure 6: Overview of RNA-seq outcomes. A) Correlation analysis for all samples. Correlation between all samples is high (0.92), with temperature responsible for most of the differential expression. The second most influential factor is the phenotype (0.96), which sets MUHT35 apart, and finally the *mads1* mutation and the developmental stage correlate with fewer DEGs, especially at low ambient temperature. B) Venn diagram of all DEGs (p_{adj}<0.01) at Waddington stage 2.5. High amounts of DEGs correlate with changes in temperature (yellow and green overlap), and this is even more prominent in the mutant (yellow alone). C) Venn diagram of all DEGs (p_{adj}<0.01) at Waddington stage 3.5. The same pattern as at W2.5 can be observed where a change in temperature correlates with many DEGs (yellow and green overlap). The number of DEGs related to the branching inflorescence phenotype (red and yellow), but not the *mads1* mutation at LT (blue), or the temperature change in GP (green) is 476.

MADS-box gene expression is generally correlated with developmental stage

The MADS-box gene family is strongly associated with inflorescence development, as described in the previous chapters, so it would make sense to examine the differential expression of MADS-box genes (Table 1). The expression of most MADS-box genes increases with the progression of inflorescence development from W2.5 to W3.5 (middle four columns, orange label) except the SVP-like genes *HvMADS22/47/55* that go down, which matches the results for the RT-qPCR experiment reported in chapter 1. The SOC1-like *HvMADS56* expression pattern shows a small negative correlation with temperature. The

strong expression level drop in *HvMADS6/7/8* that is not reflected in neighbouring DEGs, are all associated with the GPLT25 sample. Because these three genes are very strongly dependant on the exact developmental stage, the GPLT25 sample may have been collected at slightly too late a stage and skewed these numbers. A smaller effect of the same origin can be seen for C-class genes *HvMADS3/58*, *HvMADS16* and *HvMADS32*, lowering their numbers in the GPLT35-GPLT25 column.

HvMADS22, *HvMADS3* and *HvMADS58* negatively correlate with the branching phenotype

Correlation is assigned based on three or four expression changes in the same direction associated with the same trait, while the other expression changes were of lesser magnitude, or a clear additive effect is present in the case of multiple correlations. Judging by the boxed columns, *HvMADS22*, *HvMADS3*, *HvMADS58* and possibly *HvMADS7* are negatively associated with the branching phenotype (Table 1). *HvMADS22* expression is lower in MUHT35 compared to GP (Column 4), compared to W2.5 (Column 8) and compared to low temperature (Column 12). Incidental other expression changes are of lesser magnitude than the phenotype-associated changes. *HvMADS3* and *HvMADS58* expression is lower, or less increased going from W2.5 to W3.5 (middle four columns), with the phenotype. *HvMADS7* may be negatively correlated to the branching phenotype, but does not strictly fulfil the criteria because of the GPLT25 sample related noise. *HvMADS34* expression has a negative correlation with temperature, but additionally a positive correlation with stage at high temperature. All temperature comparisons are negative, but the W3.5 ones less so, and the stage columns for HT show increasing expression. The temperature correlation is roughly -1.2 log2 (foldchange) (2.3 times lower) and the stage-at-HT correlation is roughly 0.5 (1.4 times higher).

	mutation				stage				Temperature			
	MULT25-GPLT25	MULT35-GPLT35	MUHT25-GPHT25	MUHT35-GPHT35	GPLT35-GPLT25	GPHT35-GPHT25	MULT35-MULT25	MUHT35-MUHT25	GPHT25-GPLT25	GPHT35-GPLT35	MUHT25-MULT25	MUHT35-MULT35
MADS22				-0.92		-1.2		-1.72	0.69	-0.44		-1.11
MADS47			-1.4		-1.56	-2.96	-1.26	-1.42	1.14			
MADS55					-0.67	-1.75		-1.59	0.86			-0.79
MADS14				0.4			0.52	0.68				
MADS15					0.73	1.13	1.31	1.45			-0.52	
MADS18						0.72	0.67	1.01	-0.89	-0.47	-0.8	-0.49
MADS2												
MADS4												
MADS16				-0.94	3.35	5.05	4.36	3.58				
MADS3				-1.11		8.13	6.68	3.71				-1.29
MADS58		0.84		-0.99	2.64	4.12	4.23	1.51				-1.45
MADS1	-1.2	-0.39			0.57	2.95	1.38		-2.3		-0.74	
MADS5					0.99	3.23	1.95	3.07	-2.43		-1.93	-0.83
MADS34						0.69		0.44	-1.17	-0.71	-1.25	-0.96
MADS7	-6.88			-1.26	3.86	10.53	10.9	4.94	-6.76			-1.52
MADS8	-4.18				2.91	8.65	7.31	6.05	-5.78			-0.81
MADS6	-4.15			-0.74	1.78	7.92	5.79	5.24	-6.67	-0.5		-1.14
MADS32					0.53	1.75	1.11	1.21	-1.24		-0.44	-0.37
MADS56						0.37			-0.62	-0.4	-0.37	-0.88

Table 1: MADS-box DEGs (P_{adj}<0.01), sorted by mutation, stage and temperature change and denoted in log2 fold change of transcription. The boxed columns indicate DEGs that correlate to the branching inflorescence phenotype (arrows pointing at the red sphere in Figure 5). Generally the MADS-box genes show a strong increase in expression level with developmental stage, except for MADS22/47/55, that are the SVP-like floral repressors. Some MADS-box genes react to increased ambient temperature, and there is little difference in expression levels caused by the *hvmads1* mutation.

Auxin related gene expression shows correlation with ambient temperature and branching phenotype

Outgrowth of lateral organs often involves auxin signalling (Zhao et al., 2010; Galli et al., 2015), and many auxin related genes are differentially expressed between the collected meristem samples (table 2; supplemental table 1). Expression of auxin response factors and some auxin transporters is negatively correlated with temperature, while an auxin repressed gene (HORVU4Hr1G011740) is upregulated. A correlation to the branching phenotype is observed for HORVU4Hr1G011740 (auxin repressed), HORVU1Hr1G025670 (*IAA15*), HORVU5Hr1G062510 (dormancy/auxin related) and HORVU7Hr1G096880 (SAUR-like auxin-responsive).

	mutation				stage				temperature				
Horvu	MULT25-GPLT25	MULT35-GPLT35	MUHT25-GPHT25	MUHT35-GPHT35	GPLT35-GPLT25	GPHT35-GPHT25	MULT35-MULT25	MUHT35-MUHT25	GPHT25-GPLT25	GPHT35-GPLT35	MUHT25-MULT25	MUHT35-MULT35	Gene name
HORVU4Hr1G026680	0.42						-0.44	-0.41	-0.49	-0.31	-0.89	-0.89	Aux efflux carrier fam.
HORVU1Hr1G076690										-0.23	-0.36	-0.35	Aux response factor 14
HORVU1Hr1G087460			0.28				-0.45	-0.50	-0.57	-0.50	-0.45	-0.52	Aux response factor 15
HORVU3Hr1G096410										-0.32	-0.48	-0.38	aux response factor 2
HORVU3Hr1G072340									-0.45	-0.23	-0.42	-0.47	Aux response factor 3
HORVU5Hr1G009650					0.52	0.52			-0.55	-0.53	-0.49		aux response factor 6
HORVU7Hr1G106280					0.65	0.77			-0.70	-0.56	-0.54	-0.85	aux response factor 6
HORVU3Hr1G084750					0.40	1.52	0.59	1.48	-0.78	0.36	-0.42	0.46	Aux transporter-like 1
HORVU4Hr1G063650				-0.43				-0.40	-0.77	-0.50	-0.65	-1.04	Aux transporter-like 2
HORVU1Hr1G016700						0.29			-0.53	-0.49	-0.65	-1.08	Aux transporter-like 3
HORVU4Hr1G011740	-1.51			1.04		0.98		1.76		0.91	1.23	2.96	Aux-repressed 12kDa pro
HORVU3Hr1G074230	0.94				-1.01	-2.18	-1.70	-1.32	1.07				Aux-responsive GH3 fam
HORVU1Hr1G025670			0.41	0.77				0.58		0.42		0.83	Aux-responsive IAA15
HORVU3Hr1G031460							0.42			-0.49	-0.41	-0.74	Aux-responsive IAA17
HORVU4Hr1G047240	-0.73			0.68				0.98	0.54	0.69	1.20	1.74	Dormancy/aux associatec
HORVU5Hr1G062510	-0.68	0.77		1.65	-0.44			1.32		0.92	1.47	2.92	Dormancy/aux associatec
HORVU5Hr1G086080										1.66	1.73	1.76	SAUR-like aux-responsive
HORVU7Hr1G096880				-1.18				-1.60				-1.64	SAUR-like aux-responsive
HORVU7Hr1G107340						-1.11	-0.80	-1.05					SAUR-like aux-responsive

Table 2: Auxin related DEGs (P_{adj}<0.01), by mutation, stage and temperature change and denoted in log2 fold change of transcription. The boxed columns indicate DEGs correlate to the branching inflorescence phenotype (arrows pointing at the red sphere in figure 5). Colouring on the gene number indicates the correlation: red for temperature, orange for stage and yellow for phenotype. Several auxin related genes are downregulated with increased ambient temperature, while some show a clear correlation to the phenotype.

Several heat stress factors are strongly correlated to the branching phenotype, but not to ambient temperature

Since high ambient temperature is an important factor in inducing the branching phenotype, the expression of heat shock proteins and heat stress factors may provide insight. Some heat shock proteins are upregulated by high ambient temperature, while others show reduced expression levels (Table 3; Supplemental table 1). Several Hsfs show a strong positive correlation with the branching phenotype, but no correlation with high ambient temperature. HORVU5Hr1G094380 (*HvHSF A-2a*) has the strongest correlation with the phenotype with an average 24.3 fold increase in expression, while HORVU2Hr1G014590 (*HvHSF A-2b*) HORVU3Hr1G069590 (*HvHSF C-1b*) and HORVU4Hr1G090090 (*HvHSF C-2a*) all have an over 4 fold average increase.

	mutation				stage				temperature				
Horvu	MULT25-GPLT25	MULT35-GPLT35	MUHT25-GPHT25	MUHT35-GPHT35	GPLT35-GPLT25	GPHT35-GPHT25	MULT35-MULT25	MUHT35-MUHT25	GPHT25-GPLT25	GPHT35-GPLT35	MUHT25-MULT25	MUHT35-MULT35	Gene name
HORVU1Hr1G027420									-0.54	-0.60	-0.67	-0.82	Hsp 15
HORVU5Hr1G113180				-0.49				-0.40		-0.18		-0.52	Hsp 3
HORVU6Hr1G081460				0.49		0.32		0.75	0.61	0.72	0.61	1.12	Hsp 3
HORVU6Hr1G008880			-0.33	-0.44		-0.44		-0.56		-0.66	-0.46	-0.97	Hsp C
HORVU7Hr1G036470										-1.07	-1.21	-1.87	Hsp 21
HORVU7Hr1G036540										-1.10	-1.69	-1.82	Hsp 21
HORVU5Hr1G072420						0.41		0.63	0.48	0.94	0.59	1.14	Hsp 81.4
HORVU5Hr1G123770				0.65				0.73		0.59	0.61	1.21	Hsf A2
HORVU5Hr1G094380				3.48				3.55				6.78	Hsf A-2a
HORVU2Hr1G014590				1.12				2.18		1.00		3.12	Hsf A-2b
HORVU3Hr1G069590			1.21	1.99		1.15		1.93			1.25	3.30	Hsf C-1b
HORVU4Hr1G090090				2.67				2.23				2.70	Hsf C-2a

Table 2B: Selected heat shock proteins and heat stress factors. Some heat shock proteins genes are upregulated with increased ambient temperature while others are downregulated. Several heat stress transcription factors show a strong positive correlation with the phenotype.

	mutation				stage				temperature				
Horvu	MULT25-GPLT25	MULT35-GPLT35	MUHT25-GPHT25	MUHT35-GPHT35	GPLT35-GPLT25	GPHT35-GPHT25	MULT35-MULT25	MUHT35-MUHT25	GPHT25-GPLT25	GPHT35-GPLT35	MUHT25-MULT25	MUHT35-MULT35	Gene name
HORVU3Hr1G027590		0.55			1.61	2.70	1.90	1.69	-2.32	-1.21	-1.66	-1.89	FT2
HORVU1Hr1G076430													FT3/PPDH1
HORVU3Hr1G097810													FPF1
HORVU2Hr1G007350	-0.88	-0.95		-1.17	0.89	3.40	0.82						FPF1-like
HORVU7Hr1G108970	0.73					-1.44	-0.92	-1.18	1.21				APO1
HORVU0Hr1G022670						0.66		0.63		0.37	-0.42	0.48	CLV
HORVU5Hr1G049190								-1.10					WUS
HORVU3Hr1G095240				0.60		0.89		1.51		1.38		1.78	OS2

Table 2C: Other development related genes of interest. Of these only HORVU3Hr1G095240 (HvOS2) is correlated to the branching inflorescence phenotype.

Further development related genes

Inflorescence architecture can be influenced by meristem size, in which the CLV-WUS feedback loop is central (Ha et al., 2010; Ta et al., 2017). Meristem maintenance genes *HvCLV-LIKE* and *HvWUS-LIKE* show no link to the branching phenotype (Table 2C).

HvODDSOC2 (HvOS2) expression is linked to the branching phenotype, but also has a slightly heightened expression in GP at W3.5 in HT (Table 2C, Figure 7). However the expression of the *HvFPF* gene, possibly regulated by *HvODDSOC* (Greenup et al., 2010), shows no correlation to the phenotype.

HvFT2 expression goes up between W2.5 and W3.5, but is downregulated with high ambient temperature (Table 2C).

ABERRENT PANICLE ORGANISATION1 (OsAPO1), encoding an F-box protein, is important in rice panicle architecture (Ikeda et al., 2007). *HvAPO1* shows no correlation with the branching phenotype (Table 2C).

4.4 Discussion

Branch-like structures point to a possible reversion to an ancestral panicle inflorescence morphology

When grown at high ambient temperature (HT) during early inflorescence development, the *hvmads1* inflorescence produces some branch-like structures in the lower half of the spike (Figure 1, 2). The phenotype is first apparent at W2.5, where the wild type would form the central spikelet meristem (Figure 3-III B,C; (Waddington et al., 1983)), while in the *hvmads1* mutant at HT the meristem at the spikelet position elongates before forming one or more spikelets on its side (Figure 3-III H,I,J). Some of these branch-like structures are then outgrown by the spikelet, and appear as additional meristems between the central spikelets (Figure 3-III M,N), while others develop into full branches (Figure 3-III K,L).

While the closely related wheat has spikelets that produce multiple grains, which may look like stunted branches, these are contained within the spikelet structure itself, delimited by the glumes. In contrast, the branch-like structures observed in the *hvmads1* mutant at HT can produce multiple spikelets, including glumes (Figure 3-III L) (Forster et al., 2007). Therefore the absence of *HvMADS1* via the application of CRISPR/Cas9 technology at HT has altered barley inflorescence morphology from a spike towards a more panicle-like inflorescence architecture.

Barley spikes may produce transient branch meristems

In rice the panicle branches are formed from specialised branch meristems, which have a gene expression profile that is distinct from both the shoot apical meristem and the spikelet meristem (Harrop et al., 2016). No inflorescence branch meristem has been described in barley, but since the spike evolved reductively there may be a transient branch meristem identity present around the W2.5 stage. In the wild type this branch meristem would immediately transition to spikelet formation, but in the *hvmads1* mutant grown at high ambient temperature the lifetime and size of the branch meristem may be increased, resulting in the formation of small branches.

In rice the branch meristem terminates by conversion into a terminal spikelet meristem (Ikeda et al., 2007). At first glance it might be tempting to designate the central spikelets in barley as a terminal spikelet, thereby assuming the transient branch meristem terminates by changing its identity into a spikelet meristem. However, observing the branching inflorescence early phenotype in detail, the spikelet meristem forms on the side of the branch (Figure 3-III I) resulting in the branch- and spikelet meristem being present simultaneously. The row of central spikelets can then develop as in the wild type, with the exception of some additional (branch-) meristems (Figure 3-III M,N). Also, in rice *ABERRANT PANICLE ORGANISATION* (*OsAPO1*) prevents the premature conversion of branch meristems into terminal spikelets (Ikeda et al., 2007), but the expression of the barley homolog *HvAPO1* is not correlated with the branching phenotype (Table 2C). Therefore it is likely that in barley the central spikelet is actually the first spikelet to form on the branch meristem as a lateral meristem, while the branch meristem itself then quickly diminishes.

Expression of *HvMADS1* at W2.5 in the right position for the transition from branch to spikelet

Early *HvMADS1* expression is visible from W2.5 onwards, in the tips of the emerging spikelet primordia (Figure 4B). This is the exact stage where the phenotype of the *hvmads1* mutant at HT starts to diverge, and just after the expression maximum of *HvMADS34* (Chapter 1). The timing and location of the *HvMADS1* expression fits well with the transient branch meristem hypothesis, where *HvMADS1* is important for the transition to spikelets. To put this to the test it would be interesting to see where genes expressed in the spikelet/floret meristem would locate in a young inflorescence with the mutant phenotype. If spikelet/floret meristem markers are expressed only in the axillary meristems of the branch-like organs, that would further confirm the branch identity of the outgrowths in the *hvmads1* young inflorescence.

Increased number of differentially expressed genes indicates interaction between *HvMADS1* and the high temperature response pathway

Since all samples are a complete early inflorescence meristem, it is not surprising to find a high level of correlation between the samples, with a minimum correlation coefficient of

0.92. Gene expression is generally very similar and DEGs are the exception, rather than the rule. Of the differentially expressed genes most are related to a change in temperature, which is to be expected since temperature affects nearly all processes in the plant and to maintain homeostasis the expression level of many genes has to adapt. While the mutant displays relatively few DEGs at LT, this is increased significantly in HT, at both W2.5 and W3.5. The same pattern can be observed for a change in temperature, where the number of DEGs is higher in the mutant (Figure 6B). Together this indicates that the combination of *hvmads1* and HT has more impact than the sum of *hvmads1* and HT individually. Or in other words, there is interaction between *HvMADS1* and the high temperature response, such that in the absence of HvMADS1 the effects of high temperature on gene expression are more extensive.

Comparison to the *HvFT3* overexpression phenotype, the 'opposite' of branching

HvFT3 overexpression accelerates spikelet initiation in early barley inflorescence development (Mulki et al., 2018), an effect opposite to the *hvmads1* mutant at HT, which delays spikelet initiation in favour of the branch meristem. A similar acceleration in spikelet initiation and reduction in branching can be observed in rice when *OsMADS1* is ectopically overexpressed (Wang et al., 2016), strengthening the idea that these phenotypes are opposites. Accordingly *HvMADS1* expression in the *HvFT3* overexpression line is increased between W2 and W3 compared to the wild type (Mulki et al., 2018), suggesting that HvFT3 may act through upregulation of *HvMADS1* in early inflorescence development. Additionally there are some DEGs acting oppositely between the *HvFT3* overexpression line and the *hvmads1* mutant at HT (described below). However, important flowering time genes *HvFT3*/ *Ppd-H1* and *HvFPF1* are expressed predominantly in the leaves, and no significant expression was detected in the inflorescence (Table 2C).

Expression of several MADS-box genes correlates to the branching phenotype

HvMADS22, *HvMADS3* and *HvMADS58* negatively correlate with the branching phenotype. The C-class genes *MADS3* and *MADS58* are first to be expressed in the floret meristem, so a delay in the formation of florets in the branching inflorescence can explain the lower expression at W3.5 in *hvmads1* at HT. The opposite can be observed in the *HvFT3*

overexpression line, where florets are formed earlier and many floral homeotic genes are upregulated (Mulki et al., 2018).

The expression of SVP-like floral repressor *HvMADS22* declines from a peak early in inflorescence development to a nadir at W2, and then starts increasing again up to pollination, mostly in the stamen (Chapter 2). While *HvMADS22* is known as a floral repressor (Trevaskis et al., 2007), its function in stamen development is unknown. The *hvmads1* branching phenotype changes *HvMADS22* expression at W3.5, which is when expression is in its second phase, and presumably concentrated in the stamens. So in this second unknown function *HvMADS22* expression is lower in *hvmads1* at HT, and might also be explained by a delay in the formation of the stamens.

In rice, *OsMADS34* is expressed highest in the branch meristem (Harrop et al 2016) and associated with the regulation of panicle branching (Gao et al., 2010; Kobayashi et al., 2010). Thus *HvMADS34* would be expected to be upregulated in the branch meristem of barley, but *HvMADS34* is not significantly correlated to the branching phenotype. There is a small correlation to stage at HT, but a stronger negative correlation with temperature, so it seems *HvMADS34* is surprisingly not linked to the observed branching inflorescence phenotype (Table 1; Figure 7). Perhaps the small and irregular branches observed in *hvmads1* at HT would grow to a more complete panicle with increased *HvMADS34* expression, making this partial panicle morphology comparable to the *osmads34* mutant phenotype.

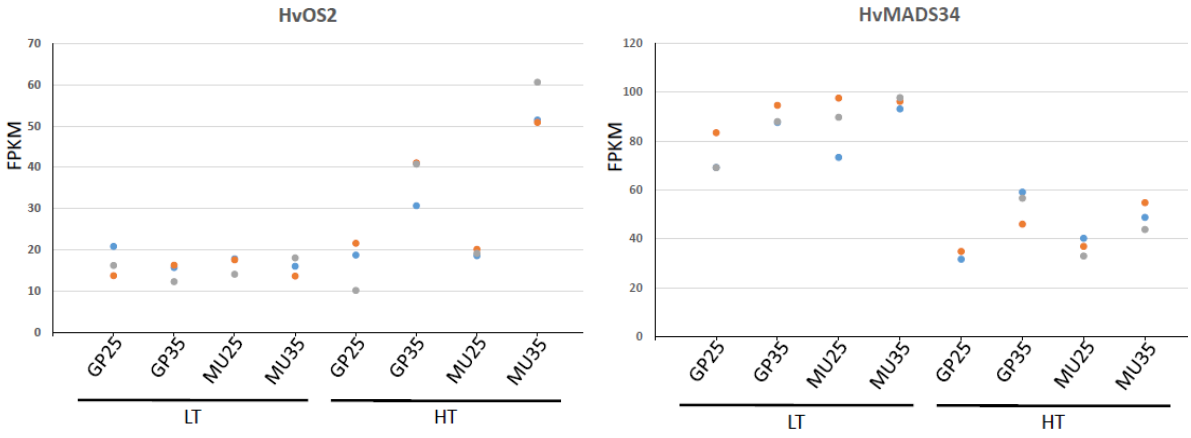

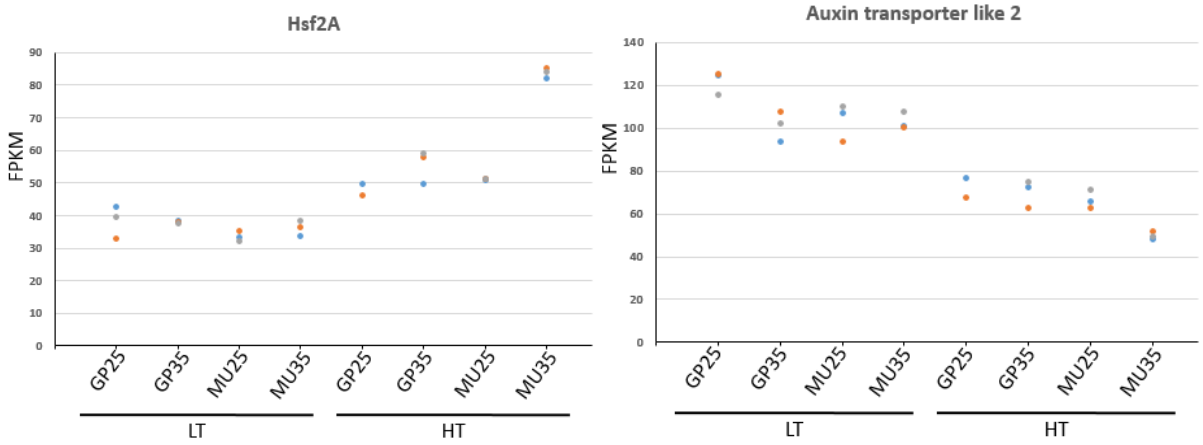

Figure 7: Absolute expression in fragments per kilobase per million reads (FPKM) of selected genes from all samples. The dots represent the three biological replicates for each sample.

HvOS2 is likely to be a regulator of progression in early inflorescence development

Under short day conditions at 25°C 'expanding spikelet primordia' have been described in barley (Hemming et al., 2012). These expanding primordia appear at W2.5 and look similar to the potential early branch meristems observed in the *hvmads1* mutant at HT (Figure 3). This suggests that increased *HvOS2* expression may be involved in the slowdown of developmental progression in early inflorescence development (Hemming et al., 2012). Similarly there is a correlation between the branching phenotype and *HvOS2* expression in the *hvmads1* mutant at HT (Table 2C; Figure 7), making it a prime candidate for further scrutiny. Since *HvOS2* is part of a cereal specific clade within the type-1 MADS-box genes, no direct homolog in *Arabidopsis* can provide clues to its function (Greenup et al., 2010). The *HvOS2* promoter is bound by *VERNALISATION1* (*HvVRN1*) also known as *HvMADS14* and downregulated (Deng et al., 2015). OsMADS1 and OsMADS14 can interact, so it is likely HvMADS1 and HvMADS14 can interact as well, especially now that they are both implicated in downregulating *HvOS2*. Both *HvMADS1* and *HvMADS14* are expressed at W2.5, when *HvOS2* is likely downregulated in wild type barley. An *HvOS2* overexpression line in barley, or an *OS2* mutant in a panicoid grass species like rice or maize, could show the extent of *ODDSOC2* influence on inflorescence architecture in grasses.

Auxin-related gene expression shows mixed patterns

While most auxin response factors and auxin transporters seem to be mildly down regulated by increased ambient temperature, this effect is not universal. Both ambient temperature and auxin are associated with many plant processes and without more specific data on the individual function of these auxin related genes in barley, not much can be gleaned from this data. Small auxin up RNAs (SAURs) are a family of auxin responsive genes only found in plants. SAURs are involved in integration of temperature and hormonal signals, cell elongation and many other processes (Ren and Gray, 2015). A SAUR gene (HORVU7Hr1G096880) has a strong and clear link to the phenotype (Table 2). Visualising local auxin concentrations through a reporter and comparing the concentration in lateral meristems of the inflorescence in GP and *hvmads1* may show whether a change in local auxin concentration accompanies the outgrowth of the branch-like organs. Meanwhile, a topical application of auxin in GP inflorescences at W2.5 could determine whether hormone treatment alone is sufficient to induce outgrowth of branch-like organs. While it is important to test for changes in auxin concentrations, the mixed changes in the expression of auxin related genes shown here indicates a more specific change in reaction to existing auxin levels is more likely. Therefore, an overexpression mutant for the SAUR gene HORVU7Hr1G096880 could prove insightful.

hvmads1 may sensitise the inflorescence to heat

The expression of some Hsps correlates with temperature, but while some may be slightly upregulated (*Hsp81*, *Hsp3*), others Hsps are clearly and more strongly downregulated, such as *Hsp21* and *Hsp15* (Table 2B; Supplemental table 1). The mixed or reduced expression of Hsps indicates that for GP, growth in 25°C does not constitute heat stress, but merely high ambient temperature. This is in accord with reported heat stress for barley commencing above 30°C (Abiko et al., 2005). The expression of *HsfA2* genes is correlated with the phenotype, and while the expression of some is still very low, HORVU5Hr1G123770 (*HsfA2*) expression is 84 FPKM (Figure 7). Since *HsfA2* by itself probably resides in the cytoplasm, the lack of Hsp expression can be explained. Accumulation of *HsfA2* is normally a sign of repeated heat stress, but since it is not observed in GP plants grown in the same growth space, it is not caused by temperature spikes in the growth environment. Somehow the lack of *HvMADS1* is increasing *HsfA2* expression at HT and thereby effectively sensitising the inflorescence to

heat stress. The severity of the branching phenotype increases with temperatures between 20°C and 28°C (results not shown), and at 28°C some extra meristem tissue can be observed even in GP (Figure 3-III D,E). This may be a mechanism where formation of sensitive tissues like the spikelet/floret is delayed when the plant is under heat stress, but when development has started, marked by *HvMADS1* expression, development has to continue, and thus this checkpoint is over-ridden. Here the plants are not experiencing heat stress, but perhaps the lack of HvMADS1 to supress *HsfA2* expression triggers a partial response regardless. This response is however not visible in the Hsps expression. Testing what potential branch-like phenotype develops in GP at temperatures above 28°C may be hampered by deleterious heat stress responses that swamp it (Abiko et al., 2005).

Future directions: linking HvMADS1 and temperature effects

Plants do not have specific receptors for high ambient temperature like they do for light, or certain hormones. Instead high ambient temperature affects many processes directly, such as membrane fluidity, chromatin state, RNA processing and protein translation and stability. These primary responses can lead to secondary responses such as changes to the circadian clock and hormone signalling (Susila et al., 2018). Finally these lead to developmental outcomes such as flowering time and hypocotyl length and can modulate plant defence pathways (Wigge, 2013; Susila et al., 2018). This makes approaching the interaction between *HvMADS1* and high ambient temperature from the temperature side a daunting task: there are many, often subtle, changes that can lead to a temperature response. This is further illustrated by the majority of DEGs found being related to the ambient temperature change (Figure 6).

Analysis of gene expression in the *hvmads1* mutant at HT has revealed several genes that are correlated to appearance of the branching phenotype at W3.5, and thus provide evidence that the branch-like growths come from ectopic or altered branch meristems. However, these effects are consequences of a developmental change, and leave the important question of how high ambient temperature and *HvMADS1* interact to trigger this change unsolved. Unfortunately the DEGs involved are likely to be confined to very small primordia, and are therefore unlikely to be detectable in whole shoot apical meristem samples. Additionally, correlation alone is not enough, and more specific experiments are needed to identify the regulatory network surrounding *HvMADS1*, and its link to high ambient temperature responses.

Firstly, testing the affinity of HvMADS1 for variations of the CArG-box at different temperatures will show whether HvMADS1 itself can function as a temperature sensor. If HvMADS1 binds to promoter elements more strongly at higher temperatures, that would imply that HvMADS1 is responsible for activating genes needed for normal inflorescence development at higher temperatures. Instead a potential partly redundant gene could activate these downstream genes at low temperatures, which would explain the lack of similar branching phenotype in the *hvmads1* mutant at LT.

Chromatin immunoprecipitation followed by sequencing (ChIP-seq) could be used to isolate promoter sequences that HvMADS1 can bind *in vivo*. The resulting list of direct targets can then be compared to the RNA-seq DEGs at W2.5 to narrow down the candidates that link *HvMADS1* to the outgrowth of the branching phenotype.

4.5 Materials and methods

Plant growth

T2 *hvmads1* mutant grains from three sequenced homozygous independent T1 mutants were grown in a controlled environment at 15°C day, 10°C night (low temperature, LT), 25°/20°C and 28°/23°C (high temperature, HT) in 16 hour days. Grains for growth at HT were first geminated at LT, because germination rate is better at LT and then transferred to HT at W1. Since inflorescence development is severely hampered at HT, some plants were transferred to LT after W7 to finalise spikelet and floret growth and observe the phenotype in the mature spike without some of the later deleterious effects of HT conditions.

Scanning electron microscopy (SEM)

GP and *mads1* mutant barley plants were grown at LT and HT as described above. Inflorescence meristem samples were taken between W2 and W4, and treated according to Bomblies et al. (2008). Samples were fixed in FAA (3.7% v/v formaldehyde, 50% ethanol, 5% acetic acid), vacuum infiltrated until no longer buoyant by syringe in a small flask with rubber stopper and stored at 4°C. Fixed samples were dehydrated in ethanol and dried in a critical point dryer (Leica EM CPD300) using ethanol as a solvent. Dried samples were attached to an SEM pin with adhesive and coated in platinum (Cressington 208 HR Sputter Coater). Imaging was performed on a Phillips XL20 scanning electron microscope.

RNA *in situ* hybridisation

Meristem samples were taken from the main stem and examined under a dissecting microscope. Meristems exactly matching the desired Waddington stage were immediately collected in fixative solution FAA (3.7% v/v formaldehyde, 50% ethanol, 5% acetic acid), vacuum infiltrated until no longer buoyant by syringe in a small flask with rubber stopper and stored at 4°C. Samples were dehydrated in an ethanol series which was subsequently swapped for D-lemonene (HistoChoice, Sigma), and finally paraffin wax (Paramat pastillated, Gurr) at 60°C. Embedded samples were cut into 6-8µm sections on a Leica RM2265 microtome and placed on lysine coated slides in water and dried first with sterile filter paper and further at 37°C.

Dioxigenin labelled probes were made, in sense and antisense configuration, using the DIG labelling kit (Roche Diagnostics), following the manufacturer's instructions.
Antisense probe primers:
F: AGATACCGCACCTGCAACTC
R: TAATACGACTCACTATAGGGGGTGTCTTGCAGCTTCTTCC
Sense probe primers:
F: TAATACGACTCACTATAGGGAGATACCGCACCTGCAACTC
R: GGTGTCTTGCAGCTTCTTCC

Slides were dewaxed in D-lemonene and rehydrated in an ethanol series (2x 100%, 95% ethanol and 85% & 75% ethanol with 0.85% NaCl). The following steps were performed with an InsituPro robot (Invatis): Finalise rehydration, proteinase K digestion, re-dehydration. Re-dehydration was finalised with a reverse of the rehydration steps above, and the slides dried at 37°C. The following steps were performed with the InsituPro robot again: Hybridisation, stringent washes, RNAse digestion, immunolabelling (1:1000 AntiDIG-APconjugate, Roche) and washing. Substrate (NBT/BCIP, Roche) was added according to the manufacturer's instructions and incubated overnight in the dark. Slides were fixed with ImmunoHistoMount (Sigma-Aldrich). Stained slides were photographed with a Nikon Ni-E microscope, and processed for colour, brightness and contrast in GIMP2.10.2 (www.gimp.org).

5-ethynyl-2'-deoxyuridine (EdU) staining

EdU staining is a way to visualise dividing cells within a tissue sample. 5-Ethynyl-2'-deoxyuridine (EdU) is added to living tissue, and will be incorporated into newly synthesised DNA. After fixing the sample, a fluorescent label that can attach to the EdU is added, and labelled DNA can be observed by excitation of the fluorophore. The EdU protocol has been adapted from the manufacturers' instructions and Kotogány et al., (2010) for application in the barley inflorescence meristem as follows;

GP and *mads1* barley plants were grown to Waddington stage 3.5 at 28°C. The inflorescence meristem was exposed by cutting away the leaves, without damaging the soft meristem, nor compromising its attachment to the stem (Supplemental figure 1.2). A piece of a pipet tip was cut to size and placed on the shoot surface surrounding the meristem in a water-tight fashion.

The basin was filled with fresh 10µM EdU working solution, submerging the meristem for 1 hour (Supplemental figure 1.4). Where necessary bubbles were removed with a syringe and the basin was refilled to keep the meristem submerged to ensure the staining is distributed evenly. The meristems were harvested into 2ml tubes with 0.5 mL fixative (100% ethanol + 0.1% triton x-100) and incubated for 30 min at room temperature. The samples were washed 2x in PBS and incubated in 250µL fresh Click-iT reaction solution with Alexa Fluor azide, prepared according to the manufacturer's instructions (Click-iT EdU kit, Thermo-Fisher) for 30 min at room temperature in the dark. Samples were then washed in PBS once followed by PBS with 10 µg/mL PI and incubated for 30 min at room temperature in the dark. After another wash in PBS the samples were stored in fresh PBS until imaging under a Nikon A1R laser scanning confocal microscope. GFP wavelength settings of 488nm excitation and 510nm emission were used.

RNA-sequencing

Whole inflorescence meristem samples were taken from GP and *mads1* plants grown in 15°C and 25°C at Waddington stage W2.5 and W3.5 in three biological replicates and immediately frozen in liquid nitrogen. Since some related genes may be expressed on a circadian rhythm, all samples were collected 2-4 hours into the daylight time. RNA extraction was performed using TRIzol (Life Technologies), DNA removed by RNase-free kit (Ambion), and the RNA checked for degradation by agarose gel electrophoresis, and the concentration and purity checked by nanodrop. RNA samples were kept in -80°C and dried with an RNAstable tube kit (Biomatrica) for transport. RNA integrity was measured with a 2100 Bioanalyser (Agilent), RNA was enriched for mRNA using oligo(dT) beads, fragmented and reverse-transcribed into cDNA using random hexamers, the resulting cDNA was then made double-stranded, purified and an A-tail and sequencing adaptors were attached, and after size selection and PCR enrichment the resulting libraries were quantified using a Qubit 2.0 fluorometer (Life Technologies) and rechecked for insert size on an Agilent 2100 and requantified by qPCR and then finally sequenced on Illumina sequencing machines and taken through primary analysis, all with a commercial RNA-sequencing service (Novogene Bioinformatics Technology). They also performed quality control of the raw data with Illumina CASAVA v1.8 and A/T/G/C distribution. After disqualifying reads with adaptor related sequences, N-contamination and low quality sequences, 95-98% of reads was classified as a clean read. Clean reads average 46 million per biological replicate, with

GPHT25_2 the lowest at 36 million clean reads. Of the clean reads 90-92% was mapped to exons in the barley genome sequence (Mascher et al., 2017) using the HISAT algorithm (Pertea et al., 2016). The comparison of the biological replicates was all over a Pearson coefficient squared R^2>0.96, except for the pairwise comparisons including the GPHT25_3 sample, where the R^2 dropped to 0.8 (Supplemental figure 2). To remove this relatively bad replicate, expression data was re-analysed without the GPHT25_3 sample by Huiran Liu. Expression data was further processed by Huiran Liu, normalising read counts to fragments per kilobase per million (FPKM) and generating 12 lists with P_{adj}<0.01 DEGs only using DESeq2 (Love et al., 2014).

The average expression per gene per sample was used to calculate the correlation between the samples using the Pearson correlation function in MeV4.9 (http://mev.tm4.org). The presence of each DEG with P_{adj}<0.01 in sample comparisons was tabulated using Microsoft excel 2013 and represented in a Venn diagram.

Likely candidate genes and gene families were selected either from functional studies or expression changes in rice inflorescence branching meristems (Harrop et al., 2016). DEGs with P_{adj}<0.01 of selected families were collated into tables and each gene assigned one or more correlations, if applicable. Correlation was assigned based on 3 or 4 expression changes in the same direction associated with the same trait, while the other expression changes were of lesser magnitude, or a clear additive effect was present in the case of multiple correlations.

References

Abiko M, Akibayashi K, Sakata T, Kimura M, Kihara M, Kazutoshi Itoh K, Asamizu E, Sato S, Takahashi H, Higashitani A (2005) High-temperature induction of male sterility during barley (Hordeum vulgare L.) anther development is mediated by transcriptional inhibition. Sexual Plant Reproduction **18:** 91-100

Aspinall D (1969) The Effects of Day Length and Light Intensity on Tile Growth of Barley. Australian Journal of Biological Sciences **22:** 53-68

Baniwal SK, Bharti K, Chan KY, Fauth M, Ganguli A, Kotak S, Mishra SK, Nover L, Port M, Scharf KD, Tripp J, Weber C, Zielinski D, von Koskull-Doring P (2004) Heat stress response in plants: a complex game with chaperones and more than twenty heat stress transcription factors. J Biosci **29:** 471-487

Blázquez MA, Ahn JH, Weigel D (2003) A thermosensory pathway controlling flowering time in Arabidopsis thaliana. Nature Genetics **33:** 168-171

Boden SA, Cavanagh C, Cullis BR, Ramm K, Greenwood J, Jean Finnegan E, Trevaskis B, Swain SM (2015) Ppd-1 is a key regulator of inflorescence architecture and paired spikelet development in wheat. Nat Plants **1:** 14016

Bommert P, Satoh-Nagasawa N, Jackson D, Hirano H-Y (2005) Genetics and Evolution of Inflorescence and Flower Development in Grasses. Plant and Cell Physiology **46:** 69-78

Chandel G, Dubey M, Meena R (2012) Differential expression of heat shock proteins and heat stress transcription factor genes in rice exposed to different levels of heat stress. Journal of Plant Biochemistry and Biotechnology **22:** 277-285

Ciaffi M, Paolacci AR, Tanzarella OA, Porceddu E (2011) Molecular aspects of flower development in grasses. Sex Plant Reprod **24:** 247-282

Deng W, Casao MC, Wang P, Sato K, Hayes PM, Finnegan EJ, Trevaskis B (2015) Direct links between the vernalization response and other key traits of cereal crops. Nat Commun **6:** 5882

Echeverry-Solarte M, Kumar A, Kianian S, Mantovani E, Simsek S, Alamri S, Mergoum M, Echeverry-Solarte M, Kumar A, Kianian S, E Mantovani E, Simsek S, S Alamri M (2014) Genome-Wide Genetic Dissection of Supernumerary Spikelet and Related Traits in Common Wheat. The Plant Genome **0**

Ejaz M, von Korff M (2017) The Genetic Control of Reproductive Development under High Ambient Temperature. Plant Physiol **173:** 294-306

Forster BP, Franckowiak JD, Lundqvist U, Lyon J, Pitkethly I, Thomas WT (2007) The barley phytomer. Ann Bot **100:** 725-733

Galli M, Liu Q, Moss BL, Malcomber S, Li W, Gaines C, Federici S, Roshkovan J, Meeley R, Nemhauser JL, Gallavotti A (2015) Auxin signaling modules regulate maize inflorescence architecture. Proceedings of the National Academy of Sciences of the United States of America **112:** 13372-13377

Gao X, Liang W, Yin C, Ji S, Wang H, Su X, Guo C, Kong H, Xue H, Zhang D (2010) The SEPALLATA-like gene OsMADS34 is required for rice inflorescence and spikelet development. Plant Physiol **153:** 728-740

Greenup A, Peacock WJ, Dennis ES, Trevaskis B (2009) The molecular biology of seasonal flowering-responses in Arabidopsis and the cereals. Ann Bot **103:** 1165-1172

Greenup AG, Sasani S, Oliver SN, Talbot MJ, Dennis ES, Hemming MN, Trevaskis B (2010) ODDSOC2 is a MADS box floral repressor that is down-regulated by vernalization in temperate cereals. Plant Physiol **153:** 1062-1073

Ha CM, Jun JH, Fletcher JC (2010) Shoot apical meristem form and function. Curr Top Dev Biol **91:** 103-140

Harrop TW, Ud Din I, Gregis V, Osnato M, Jouannic S, Adam H, Kater MM (2016) Gene expression profiling of reproductive meristem types in early rice inflorescences by laser microdissection. Plant J **86:** 75-88

Hemming MN, Walford SA, Fieg S, Dennis ES, Trevaskis B (2012) Identification of high-temperature-responsive genes in cereals. Plant Physiol **158:** 1439-1450

Ikeda K, Ito M, Nagasawa N, Kyozuka J, Nagato Y (2007) Rice ABERRANT PANICLE ORGANIZATION 1, encoding an F-box protein, regulates meristem fate. Plant J **51:** 1030-1040

Kapazoglou A, Engineer C, Drosou V, Kalloniati C, Tani E, Tsaballa A, Kouri ED, Ganopoulos I, Flemetakis E, Tsaftaris AS (2012) The study of two barley type I-like MADS-box genes as potential targets of epigenetic regulation during seed development. BMC Plant Biol **12:** 166

Kellogg EA, Camara PE, Rudall PJ, Ladd P, Malcomber ST, Whipple CJ, Doust AN (2013) Early inflorescence development in the grasses (Poaceae). Front Plant Sci **4:** 250

Kobayashi K, Maekawa M, Miyao A, Hirochika H, Kyozuka J (2010) PANICLE PHYTOMER2 (PAP2), encoding a SEPALLATA subfamily MADS-box protein, positively controls spikelet meristem identity in rice. Plant Cell Physiol **51:** 47-57

Kotogány E, Dudits D, Horváth G, Ayaydin F (2010) A rapid and robust assay for detection of S-phase cell cycle progression in plant cells and tissues by using ethynyl deoxyuridine. Plant methods **6:** 5

Mascher M, Gundlach H, Himmelbach A, Beier S, Twardziok SO, Wicker T, Radchuk V, Dockter C, Hedley PE, Russell J, Bayer M, Ramsay L, Liu H, Haberer G, Zhang XQ, Zhang Q, Barrero RA, Li L, Taudien S, Groth M, Felder M, Hastie A, Simkova H, Stankova H, Vrana J, Chan S, Munoz-Amatriain M, Ounit R, Wanamaker S, Bolser D, Colmsee C, Schmutzer T, Aliyeva-Schnorr L, Grasso S, Tanskanen J, Chailyan A, Sampath D, Heavens D, Clissold L, Cao S, Chapman B, Dai F, Han Y, Li H, Li X, Lin C, McCooke JK, Tan C, Wang P, Wang S, Yin S, Zhou G, Poland JA, Bellgard MI, Borisjuk L, Houben A, Dolezel J, Ayling S, Lonardi S, Kersey P, Langridge P, Muehlbauer GJ, Clark MD, Caccamo M, Schulman AH, Mayer KFX, Platzer M, Close TJ, Scholz U, Hansson M, Zhang G, Braumann I, Spannagl M, Li C, Waugh R, Stein N (2017) A chromosome conformation capture ordered sequence of the barley genome. Nature **544:** 427-433

Meng Q, Li X, Zhu W, Yang L, Liang W, Dreni L, Zhang D (2017) Regulatory network and genetic interactions established by OsMADS34 in rice inflorescence and spikelet morphogenesis. J Integr Plant Biol **59:** 693-707

Muino JM, Smaczniak C, Angenent GC, Kaufmann K, van Dijk AD (2014) Structural determinants of DNA recognition by plant MADS-domain transcription factors. Nucleic Acids Res **42:** 2138-2146

Mulki MA, Bi X, von Korff M (2018) FLOWERING LOCUS T3 Controls Spikelet Initiation But Not Floral Development. Plant Physiol **178:** 1170-1186

Poursarebani N, Seidensticker T, Koppolu R, Trautewig C, Gawronski P, Bini F, Govind G, Rutten T, Sakuma S, Tagiri A, Wolde GM, Youssef HM, Battal A, Ciannamea S, Fusca T, Nussbaumer T, Pozzi C, Borner A, Lundqvist U, Komatsuda T, Salvi S, Tuberosa R, Uauy C, Sreenivasulu N, Rossini L, Schnurbusch T (2015) The Genetic Basis of Composite Spike Form in Barley and 'Miracle-Wheat'. Genetics **201:** 155-165

Remizowa MV, Rudall PJ, Choob VV, Sokoloff DD (2013) Racemose inflorescences of monocots: structural and morphogenetic interaction at the flower/inflorescence level. Ann Bot **112:** 1553-1566

Ren H, Gray WM (2015) SAUR Proteins as Effectors of Hormonal and Environmental Signals in Plant Growth. Mol Plant **8:** 1153-1164

Sreenivasulu N, Schnurbusch T (2012) A genetic playground for enhancing grain number in cereals. Trends Plant Sci **17:** 91-101

Sun D, Fang J, Sun G (2009) Inheritance of genes controlling supernumerary spikelet in wheat line 51885. Euphytica **167:** 173-179

Susila H, Nasim Z, Ahn JH (2018) Ambient Temperature-Responsive Mechanisms Coordinate Regulation of Flowering Time. International journal of molecular sciences **19:** 3196

Ta KN, Adam H, Staedler YM, Schonenberger J, Harrop T, Tregear J, Do NV, Gantet P, Ghesquiere A, Jouannic S (2017) Differences in meristem size and expression of branching genes are associated with variation in panicle phenotype in wild and domesticated African rice. Evodevo **8:** 2

Tanaka W, Pautler M, Jackson D, Hirano HY (2013) Grass meristems II: inflorescence architecture, flower development and meristem fate. Plant Cell Physiol **54:** 313-324
Trevaskis B, Tadege M, Hemming MN, Peacock WJ, Dennis ES, Sheldon C (2007) Short vegetative phase-like MADS-box genes inhibit floral meristem identity in barley. Plant Physiol **143:** 225-235
Vegetti A, Anton AM (1995) Some evolution trends in the inflorescence of Poaceae. Flora **190:** 225-228
Waddington SR, Cartwright PM, Wall PC (1983) A Quantitative Scale of Spike Initial and Pistil Development in Barley and Wheat. Annals of Botany **51:** 119-130
Wang L, Zeng X-Q, Zhuang H, Shen Y-L, Chen H, Wang Z-W, Long J-C, Ling Y-H, He G-H, Li Y-F (2016) Ectopic expression of OsMADS1 caused dwarfism and spikelet alteration in rice. Plant Growth Regulation **81:** 433-442
Wigge PA (2013) Ambient temperature signalling in plants. Current Opinion in Plant Biology **16:** 661-666
Zhao Z, Andersen SU, Ljung K, Dolezal K, Miotk A, Schultheiss SJ, Lohmann JU (2010) Hormonal control of the shoot stem-cell niche. Nature **465:** 1089-1092

Supplementary figures

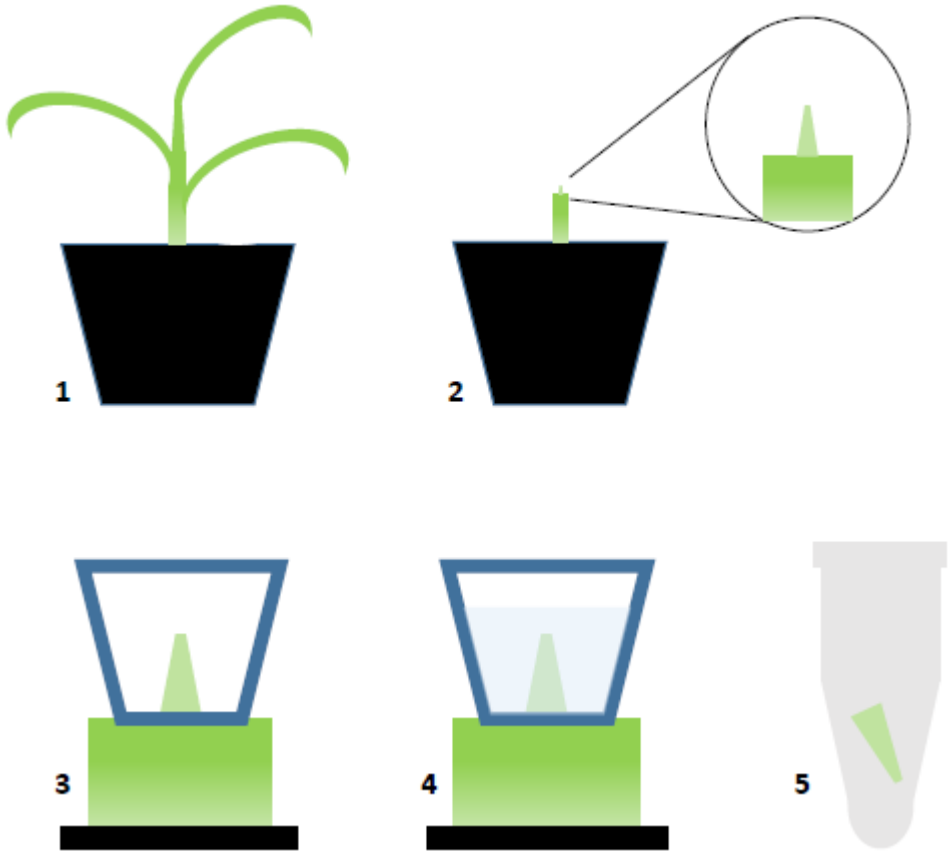

Supplemental figure 1: Schematic representation of the EdU experimental workflow. 1) Plants are grown in soil. 2) The inflorescence meristem is exposed by removing the leaves. 3) A piece of a pipet tip is cut to size and placed on the shoot surface surrounding the meristem. 4) The basin is filled with fresh 10µM EdU working solution, submerging the meristem for 1 hour. 5) The meristem is cut and put in a fixative solution, then the Click-it reaction solution and finally a PI solution and is then ready to observe under a confocal microscope.

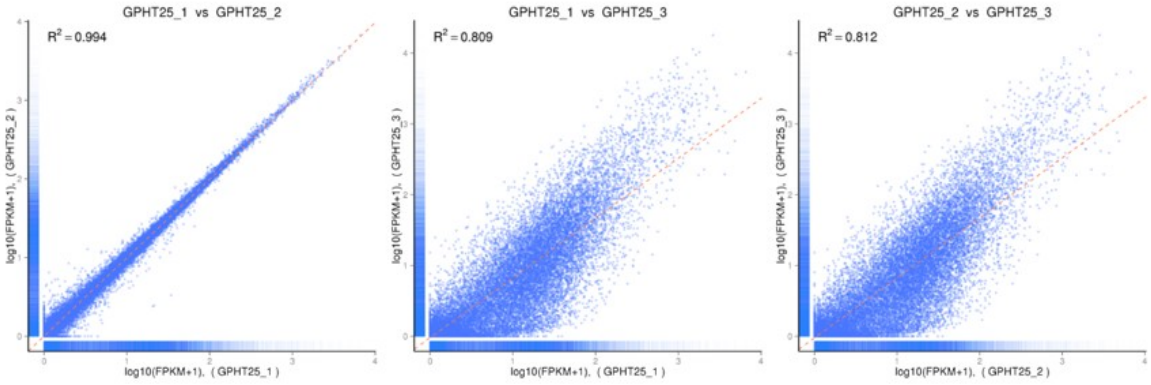

Supplemental figure 2: Pearson correlation between biological replicates of the GPHT25 sample. GPHT25_1 and GPHT25_2 show high correlation (R^2>0.99), while the correlations are much lower with GPHT25_3. Therefore GPHT25_3 is excluded from further analysis.

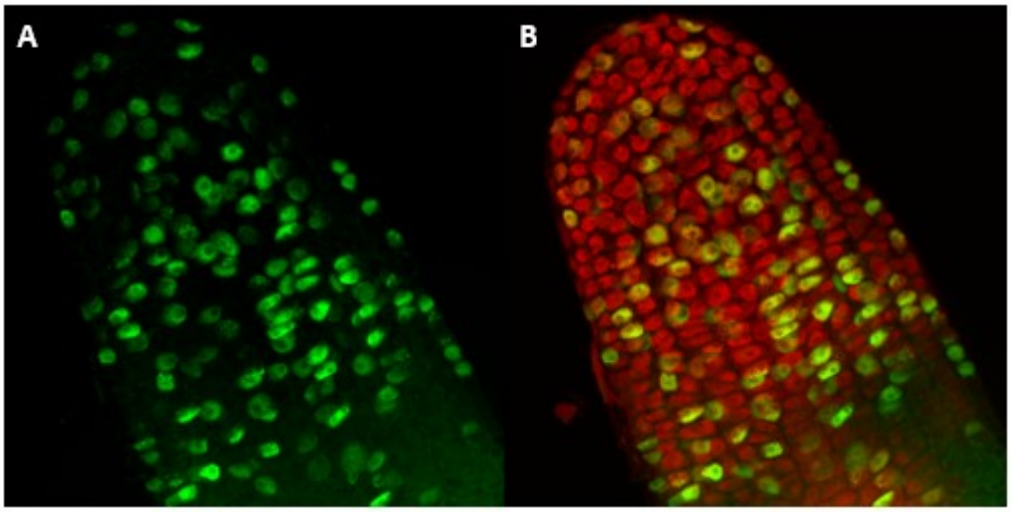

Supplemental figure 3: EdU staining in a young barley inflorescence meristem tip. Labelled cells are visible in green in A, and additional red PI staining of all cells is visible in B. The apical meristem itself is dividing, not only the lateral organs which are more prominently featured in figure 4. EdU labelled cells are often seen in pairs, indicating the two daughter cells of a recent division, and thereby showing the predominant direction of division. The direction of division is unclear in the tip of the meristem, but is predominantly vertical in the lower half of the picture.

Abridged EdU protocol for barley inflorescence meristem

Nico Kuijer, june 2018

Partially based on (Kotogány et al., 2010)

Stocks: PBS (pH7.4)
PBS with 20 µg/mL PI
100% ethanol + 0.1% triton x-100
EdU stock 10 mM in PBS
Alexa Fluor azide in DMSO
1x Click-it buffer from 10x
10x buffer additive
CuSO4 100 mM

Prep 10µM EdU working solution in water

Cut barley to just above the meristem and inject with plenty of EdU. The young leaves are water resistant, so make sure the liquid reaches the meristem.

Grow for 1-2 hours

Cut the meristem into 2ml tubes with 0.5 mL fixative (100% ethanol + 0.1% triton x-100)

Incubate 30 min at room temperature

Start preparing the Click-it reaction solution near the end of the incubation step: (fresh up to 15 min before use; order of adding ingredients is important)

Prep dilution of reaction buffer additive stock (fresh for 1 day) from 10x stock
860 µL 1x reaction buffer
40 µL CuSO4
2.5 µL Alexa Fluor azide
100 µL 1x reaction buffer additive
Makes 1 mL, for four 250 µL reactions

Wash 2x in PBS

Add 250 µL Click-it reaction solution; mix gently

Incubate 30 min at room temperature in the dark

Wash in PBS

Add PBS with 20 µg/mL PI

Incubate for 30 min at room temperature in the dark

Wash in PBS

Store in PBS

Check under confocal, excitation 495 nm, emission 519 nm (GFP settings work)

	mutation				stage				temperature				
	MULT25-GPLT25	MULT35-GPLT35	MUHT25-GPHT25	MUHT35-GPHT35	GPLT35-GPLT25	GPHT35-GPHT25	MULT35-MULT25	MUHT35-MUHT25	GPHT25-GPLT25	GPHT35-GPLT35	MUHT25-MULT25	MUHT35-MULT35	
HORVU3Hr1G057630								1.16			-1.42		Auxin efflux carrier
HORVU4Hr1G026680	0.42						-0.44	-0.41	-0.49	-0.31	-0.89	-0.89	Auxin efflux carrier
HORVU6Hr1G076110	0.58					-1.01	-0.89	-0.69	0.58	-0.29			Auxin efflux carrier
HORVU7Hr1G038700	0.50					-0.28	-0.54				-0.35		Auxin efflux carrier
HORVU2Hr1G109650						-0.34				-0.37	-0.41		ARF 11
HORVU1Hr1G076690										-0.23	-0.36	-0.35	ARF 14
HORVU1Hr1G087460			0.28				-0.45	-0.50	-0.57	-0.50	-0.45	-0.52	ARF 15
HORVU3Hr1G010140						-1.10			1.12		0.96		ARF 16
HORVU7Hr1G096460				0.44			-0.44					0.73	ARF 19
HORVU3Hr1G096410										-0.32	-0.48	-0.38	ARF 2
HORVU3Hr1G097200			0.29	0.33						0.21	0.37	0.62	ARF 2
HORVU3Hr1G072340									-0.45	-0.23	-0.42	-0.47	ARF 3
HORVU5Hr1G009650					0.52	0.52			-0.55	-0.53	-0.49		ARF 6
HORVU6Hr1G026730	0.96	0.79	0.91	0.54									ARF 6
HORVU7Hr1G106280					0.65	0.77			-0.70	-0.56	-0.54	-0.85	ARF 6
HORVU3Hr1G084750					0.40	1.52	0.59	1.48	-0.78	0.36	-0.42	0.46	Aux transporter-like 1
HORVU4Hr1G063650				-0.43				-0.40	-0.77	-0.50	-0.65	-1.04	Aux transporter-like 2
HORVU1Hr1G016700						0.29			-0.53	-0.49	-0.65	-1.08	Aux transporter-like 3
HORVU4Hr1G011740	-1.51			1.04		0.98		1.76		0.91	1.23	2.96	Aux-repressed 12.5 kDa
HORVU3Hr1G029670						1.27		0.97		0.69	0.71	1.06	Aux-responsive GH3
HORVU3Hr1G074230	0.94				-1.01	-2.18	-1.70	-1.32	1.07				Aux-responsive GH3
HORVU1Hr1G025670			0.41	0.77				0.58		0.42		0.83	IAA15
HORVU1Hr1G028170			-0.41	-0.44	-0.53	-1.16	-0.52	-1.20	0.84	0.41			IAA16
HORVU3Hr1G031460							0.42			-0.49	-0.41	-0.74	IAA17
HORVU3Hr1G019750						0.87		0.71		0.32			IAA2
HORVU0Hr1G021630						-0.30		-0.37			0.35		IAA21
HORVU5Hr1G014290						-1.04			1.27		0.75		IAA31
HORVU3Hr1G070620		-0.69				-1.05	-1.07	-0.52	0.70		0.61	1.13	IAA6
HORVU4Hr1G047240	-0.73			0.68				0.98	0.54	0.69	1.20	1.74	Dormancy/aux associated
HORVU5Hr1G062510	-0.68	0.77		1.65	-0.44			1.32		0.92	1.47	2.92	Dormancy/aux associated
HORVU2Hr1G092070								0.95		0.87	0.83	1.96	SAUR-like aux-responsive
HORVU4Hr1G002600		-0.55							0.97	0.91	1.11	1.88	SAUR-like aux-responsive
HORVU5Hr1G062720						-2.54		-2.49				-2.49	SAUR-like aux-responsive
HORVU5Hr1G086080										1.66	1.73	1.76	SAUR-like aux-responsive
HORVU7Hr1G096880				-1.18				-1.60				-1.64	SAUR-like aux-responsive
HORVU7Hr1G107340						-1.11	-0.80	-1.05					SAUR-like aux-responsive

Supplemental table 1: full list of auxin related genes with multiple DEG listings.

Chapter 5: Summary, speculation and future directions

5.1 Summary of important outcomes

The MIKCc MADS-box gene family is important for plant flowering and specifically the correct formation of the floral organs in eudicots and grasses alike. From mutant studies mostly in rice, and expression data from wheat, maize and other grasses it seems that the ABCDE model of floral organogenesis, developed in eudicots, can be used in grasses with some adaptations.

Chapter 2: Expression profiling

There are 34 MIKCc MADS-box genes in the barley genome and most genomic sequences of this family have remained extremely conserved during evolution/domestication. Combined expression analysis for various inflorescence developmental stages and individual floral organs by RT-qPCR shows that MADS-box genes are generally expressed at key developmental stages and in four whorls of floral organs in barley as predicted by the ABCDE model. However, expression patterns of MADS genes like *HvMADS58* and *HvMADS34* were deviate, placing them outside the scope of the classical ABCDE model of floral development. Co-expression in three sets shows that different members of the barley MADS-box gene family are likely to be involved in the associated developmental events of inflorescence meristem initiation, floral meristem identity and floral organ determination. A potential ABCDE working model in barley is proposed where the classic model is generally upheld, but with some notable deviations: the antagonism between A-class and C-class gene expression, a central tenet of the ABC model, is not present in barley.

Chapter 3: CRISPR/Cas9 and *hvmads1* phenotype

Mutants for *HvMADS1*, *HvMADS5* and *HvMADS34* were generated in barley by *Agrobacterium* mediated transformation of immature embryos with CRISPR/Cas9 constructs. No mutant phenotype was observed for *hvmads5* and *hvmads34*, and for *hvmads1* the phenotype is limited to shorter awns and increased tillering. The contrast between the severity of LOFSEP mutants in the rice and barley spikelet suggests there is additional redundancy between the LOFSEP genes in barley.

The shorter awns on *hvmads1* are likely to be independently regulated from the brassinosteroid pathway and *SHORT AWN2* (*LKS2*). The additional tillers do not result in higher yield, because fertility and grain weight are reduced. Reduced grain weight could be the result of the lower photosynthetic contribution from the shorter awns and competition for plant resources by additional tillers during the grain filling phase.

Chapter 4: the *hvmads1* inflorescence branches under high ambient temperature

Under high ambient temperatures, the *hvmads1* mutant spike develops some branch like structures in the lower half of the spike, changing the inflorescence morphology towards the rice or maize panicle and partially reverting to the presumed ancestral branching inflorescence morphology. Branches form in place of the central spikelets and often produce an axillary spikelet that resembles the wild type spikelet, suggesting the branch meristem may be present as a short-lived intermediary in wild type barley as well.

Expression analysis by RNAseq shows that the increased ambient temperature is responsible for most of the differentially expressed genes (DEGs). The increased amount of DEGs in *hvmads1* at high temperature over the DEGs from the mutation and the temperature increase separately, shows interaction between *HvMADS1* and the temperature response pathway. The expression of several genes shows significant correlation with the branching phenotype. Reduced expression of C-class genes *HvMADS3* and *HvMADS58* indicate a delay in floret formation. Increased expression of heat shock factors, but not heat shock proteins, suggests the mutant may be sensitised to high temperature. The increased expression of *HvODDSOC* may be involved in the delay of spikelet initiation, since this MADS-box gene has been associated with outgrowth of axillary meristems in early inflorescence development in barley previously.

5.2 Speculative explanations

5.2.1 Is the redundancy of MIKCc MADS-box genes stable?

Many MIKCc MADS-box genes are classified as redundant in function, but the extreme conservation is surprising from an evolutionary perspective. How could there be enough selection pressure to keep these genes conserved and redundant if they don't individually contribute to fitness?

The concept of redundant genes itself is at odds with evolution: if two genes perform the same function, then there is no selection pressure on the 'second' gene to keep it conserved. Yet redundancy between genes is often observed in plants and animals (Martin et al., 1997). Recent gene duplications can be a source of redundant genes and, if the mutation rates are similar, these can be stable for a long time (Martin et al., 1997). Another form of stable redundancy arises from functional overlap, where an independent function provides selection pressure to one or both of the genes sharing a redundant function. The redundant function here is maintained because a deleterious mutation is more likely to disrupt gene function altogether than just one of the functions while leaving the other intact (Martin et al., 1997). Finally, redundancy can be maintained if there is selection pressure arising from developmental error, where redundant genes in the germ line may not always make it to the developmental stage where their function is performed intact. Redundancy stabilisation by developmental error is most common in essential genes that are expressed in specific spatio-temporal patterns (Martin et al., 1997).

Many of the MIKCc MADS-box genes share at least partial redundancy within their class, and the genes within each class predominantly arose from recent duplications (Chapter 2). Although the MIKCc MADS-box genes share many functions, some have individual functions as well, such as a role in awn development for *HvMADS1* (Chapter 3). The importance of inflorescence development for fitness, and the specific expression time and place for MADS-box genes makes those genes likely candidates for redundancy stabilisation by developmental error. And indeed this has been observed in *Arabidopsis* for E-class genes *AtSEP1* and *AtSEP2* (Moore et al., 2004).

5.2.2 Redundancy among the SEPALLATA in barley

The SEPALLATA genes in barley have all the reasons listed above to be redundant in function: 1) recent duplications, which applies mostly for the *HvMADS1*/*HvMADS5* and *HvMADS7*/*HvMADS8* pairs; 2) redundant functions in addition to individual functions, like the role in awn development for *HvMADS1*; 3) redundancy stabilisation by developmental error.

Looking at the difference in redundancy between the *MADS1* and *MADS5* function in barley and rice from a perspective of evolutionary stability of redundant genes, a new hypothesis can be formulated. The presence and importance of the awn for fitness in barley (Chapter 3)

may have provided the selection pressure needed to keep *HvMADS1* from drifting, and if *HvMADS5* has a lower mutation rate this system can be stable. In rice the common absence of an awn provides no such selection pressure and therefore *OsMADS1* and *OsMADS5* may have lacked selection pressure, resulting in functional diversification to the point of incomplete redundancy in other aspects of floral development. In other words the *osmads1* single mutant necessarily has a floret phenotype.

The branching phenotype of *hvmads1* under high ambient temperature (Chapter 4) suggests a different form of redundancy is at work. When a seemingly redundant gene only provides a fitness advantage in specific environmental circumstances it is called 'generic redundancy' (Martin et al., 1997). The function of *HvMADS1* in supressing branching may be redundantly covered at normal growth conditions, but its unique function in high ambient temperature provides enough selective pressure to prevent further functional drift (Figure 1).

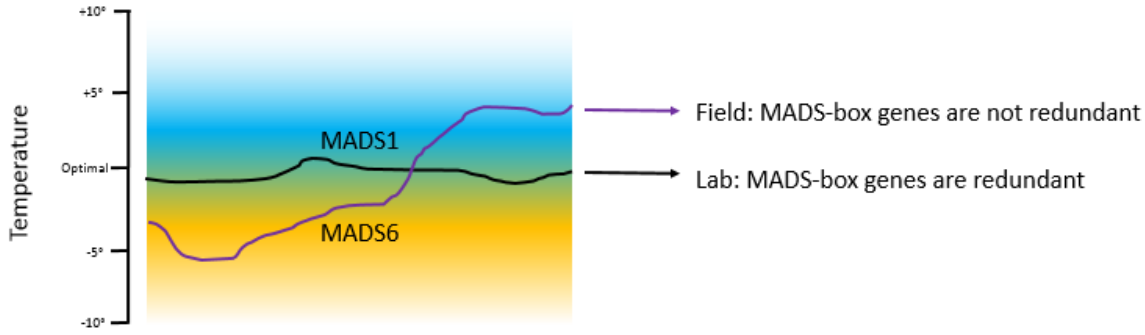

Figure 1: Genes that seem redundant under standard conditions often used in laboratory settings may seem redundant until their robustness is challenged with different environmental conditions. The hypothetical example used here has MADS1 and MADS6 act redundantly around the optimal growth temperature, and MADS1 covers the high temperature and MADS6 the low temperature. In a *mads1* single mutant no phenotype would present at laboratory conditions, and the gene would be labelled redundant. However, out in the field (high temperature variance) a phenotype would emerge if one were missing.

A similar mechanism could be in place for *HvMADS7* and *HvMADS8*, and growing mutants for these genes in various environmental circumstances may reveal phenotypes not present under standard conditions. Although alternatively stabilisation by developmental error could be sufficient, as suggested for the *SHATTERPROOF* genes *AtSHP1* and *AtSHP2* in *Arabidopsis* (Moore et al., 2004).

5.2.3 The function of *HvMADS34* early in barley inflorescence development is unknown

For *HvMADS34* some of the same basic reasons for redundancy with the other LOFSEP genes could apply, however the expression profile of *HvMADS34* is different to the other LOFSEP genes (Chapter 2). When compared to *OsMADS34*, which has important functions associated with its early expression, *HvMADS34* early expression has no apparent function (Chapter 3). So an argument can be made that *OsMADS34* redundancy in the E-function can be stabilised by an individual function earlier in inflorescence development providing selection pressure. Even though *HvMADS34* is expressed around W2, the *hvmads34* mutant does not seem to lose any fitness, so the same argument does not apply in barley as in rice. This leaves the stability of *HvMADS34* redundancy with the other LOFSEP genes an open question. By expression and comparison to rice it is likely that MADS34 is mostly of importance for the LOFSEP function in the lemma and palea (Chapter 2). In addition to double mutants, it could be insightful to challenge *hvmads34* plants with various environmental conditions, such as changes to temperature, light and water availability to detect generic redundancy.

Ultimately we have to realise that barley is a living organism, and the current state of *HvMADS34* is not necessarily at an equilibrium. Redundancy can be meta stable for many generations (Martin et al., 1997). The loss of a separate individual function for *HvMADS34* could be recent on an evolutionary scale and some amount of redundancy stabilisation by developmental error may have prevented functional drift for now.

5.2.4 Branch meristems are likely to be present in barley, possibly within a 'floral' quartet

Branching is the ancestral state, but blocked in more than one way in barley, because it is a rare and incomplete phenotype. The presence of a vestigial transient 'branch meristem' in barley was suggested based on the morphology of the *hvmads1* mutant at high temperature, combined with the rare and slight phenotype in the wild type a high temperature (Chapter 4). In combination with the co-expression of *HvMADS34* with *HvSOC1* and A-class genes around Waddington stage 2 (Chapter 2), the stage where the branch meristem would be present, I would hypothesise the possibility of a 'floral' quartet associated with the branch meristem. This quartet would normally quickly be stopped by *HvMADS1* triggering the

formation of the spikelet/floret meristem. Therefore, in the MADS1 mutant the branch meristem could remain active longer, but without outgrowth. Only the combination with high ambient temperature makes some of the branch meristems grow out, but the proximal nature of this second factor, be it a gene or a hormone, remains elusive for now.

5.3 Future directions

With the expression profiles of MIKCc MADS-box genes available, further research into barley inflorescence development has a useful reference. Of particular interest would be the apparent lack of A- and C-class antagonism, which is an important part of the ABCDE model for *Arabidopsis*. Further research into the mechanism of 2nd and 3rd whorl separation in *Triticeae* may yield far reaching results about the divergence of floral organogenesis between grasses and dicots. A promising start for such research would be functional analysis of *HvMADS6* and *HvMADS32*. Additionally, further research into the unlikely expression of a floral repressor, *HvMADS22*, in the stamen could refine the ABCDE model for barley, and perhaps other grasses, to different floral quartets acting at the tissue level within a developing floral organ.

The clear next step in LOFSEP functional research in barley is to generate and analyse double and triple mutants. The high efficiency results for CRISPR/Cas9 and transformation indicate it should be possible to create these *de novo* and prevent having to rely on crosses, saving a lot of time. Successfully targeting multiple genes in a family with a single construct has been shown in *Arabidopsis* with the same CRISPR/Cas9 system (Ma et al., 2015). It is likely that *HvMADS6* has at least partial redundancy with LOFSEP genes, so an *hvmads6* mutant and double mutants with LOFSEP genes may prove insightful. The reduced yield per spike of the *hvmads1* line can most likely be attributed to the shorter awn, and a direct comparison to wild type barley with clipped awns could test this. The role of *HvMADS1* in stopping additional tillers from developing shows it is involved in an inflorescence-to-tiller-bud signal, and cataloguing direct targets of *HvMADS1* by ChIP-seq may reveal more about the nature of this signal.

The branching barley inflorescence phenotype may have implications for research into the branching of grass inflorescences in general and its evolution. Unfortunately the data presented here are mostly descriptive pertaining to the nature of the branches and the genetic consequences of the morphological changes. The question of how the combination of the

hvmads1 mutant and high ambient temperature causes the branches to develop remains unanswered. Promoter affinity studies for HvMADS1 at different temperatures could show whether HvMADS1 itself changes in its effectiveness as a direct response to a change in ambient temperature, while a ChIP-seq experiment would identify direct targets of HvMADS1, which could provide candidates for the regulatory network for branching in the barley inflorescence. The ChIP-seq results could then be compared to the RNA-seq results correlating with temperature and phenotype.

Combined these results advance the pursuit of a generic toolbox for the adaptation of grass inflorescence morphology. Further research building on the branching barley presented here may lead to a higher yielding barley 'panicle', which may be translatable to the closely related wheat. Additionally, more research into the adaptations of the ABCDE model in grasses may provide both evolutionary insights and likely additions of complexes like the 'floral' quartets beyond the floral organs themselves, strengthening a grass specific model.

Ma X, Zhang Q, Zhu Q, Liu W, Chen Y, Qiu R, Wang B, Yang Z, Li H, Lin Y, Xie Y, Shen R, Chen S, Wang Z, Chen Y, Guo J, Chen L, Zhao X, Dong Z, Liu YG (2015) A Robust CRISPR/Cas9 System for Convenient, High-Efficiency Multiplex Genome Editing in Monocot and Dicot Plants. Mol Plant **8:** 1274-1284

Martin AN, Maarten CB, Jonathan C, John Maynard S (1997) Evolution of genetic redundancy. Nature **388:** 167

Moore RC, Grant SR, Purugganan MD (2004) Molecular Population Genetics of Redundant Floral-Regulatory Genes in Arabidopsis thaliana. Molecular Biology and Evolution **22:** 91-103

Abbreviations

ABCDE model	Model for floral organogenesis, first described in *Arabidopsis*
AP3/DEF	APETALA3/DEFICIENS, a subclade of B-class genes
bp	Base pair
cDNA	Complementary DNA
CRISPR/Cas9	Targeted DNA editing technique derived from bacterial defence mechanism
DEGs	Differentially expressed genes
DL	*DROOPING LEAF*
FAA	Formaldehyde Acetic Acid, a fixative solution
GP	Golden Promise, a barley cultivar
HT	High temperature
Kb	Kilo base
LOFSEP	Subclade within the SEPALLATA; consists of *HvMADS1*, *HvMADS5* and *HvMADS34* in barley
LT	Low temperature
MIKCc	MADS, Intervening, Keratin-like and C-terminal domain, Classic
MIKC*	MADS, Intervening, Keratin-like and C-terminal domain, Star
OS2	*ODDSOC2,* a MADS-box gene with a SOC-like domain
PAM	Protospacer adjacent motif, a part of CRISPR target sites
PI/GLO	PISTILLATA/GLOBOSA, a subclade of B-class genes
RT-qPCR	Reverse transcription quantitative polymerase chain reaction
SAM	Shoot apical meristem
SEPs	SPALLATA or E-class genes
SNPs	Single nucleotide polymorphisms
WI(4330)	A barley cultivar formerly used as breeding line
W1-W10	Waddington stages of inflorescence development in barley